POLITECNICO DI MILANO
DEPARTMENT OF MECHANICAL ENGINEERING
DOCTORAL PROGRAMME IN MECHANICAL ENGINEERING

AN INNOVATIVE APPROACH TO EVALUATE PEOPLE'S EFFECTS ON THE DYNAMIC BEHAVIOUR OF STRUCTURES

Doctoral dissertation of:
Anna Maria Chiara Cappellini

Supervisor:
Prof. Alfredo Cigada

Tutor:
Prof. Francesco Braghin

The Chair of the Doctoral Program:
Prof. Bianca Maria Colosimo

2015 – XVII CYCLE

To my husband and

my parents

Abstract: People acting on pedestrian structures behave as dynamical systems capable of modifying the dynamics of the structure itself as well as of introducing a load. At present the knowledge of this phenomenon, commonly referred to as Human-Structure Interaction, is still limited. Indeed, the determination of vibration amplitudes of structures occupied by people is a very complex task.

This work mainly focuses on the analysis of vertical vibrations of slender structures. As regards vertical vibrations, the experimental evidence suggests that people interacting with a structure are a source of added damping. For this reason, considering the dynamic properties of the empty structure to estimate the structural response can lead to a high overestimation of the vibration amplitudes. Thus, an innovative approach to include the effect of people's presence when simulating the dynamics of joint Human-Structure systems is proposed. By using the proposed approach, reliable predictions of the dynamic behaviour of joint Human-Structure systems could be obtained.

First, the work focused on the analysis of passive people's effect. To this purpose an appropriate model is proposed and validated. The proposed approach only requires the knowledge of the modal model of the empty structure and of the driving point Frequency Response Functions of each subject on the structure. No restriction on the structural degrees of freedom is required. The method was then extended with the purpose of quantifying the in-service vibration amplitudes. The idea behind such an extension is the identification of an equivalent dynamic model to represent the dynamic behaviour of the joint structure-moving people system. An appropriate active force is then applied to this equivalent model in order to get a prediction of vibration levels. Also in this case experiments and numerical simulations were performed to validate the proposed method.

The approach was also used to perform a theoretical analysis of Human-Structure Interaction. The differences between a complete model of Human-Structure systems and the use of the modal superposition method in case of Multi Degree of Freedom structures were investigated. Possible effects due to people in different postures and due to different directions of vibrations are also investigated.

At last, the proposed approach was applied to predict the dynamic behaviour of a stadium grandstand, to test it on a more complex case structure.

Aknowledgments

I would like to express my gratitude to my supervisor Prof. Alfredo Cigada. Special thanks to Prof. Stefano Manzoni and Prof. Marcello Vanali for their guidance and support along these years.

I'm also very grateful to all the colleagues (Matteo, Ambra, Marta, Simona, Giorgio, Andrea, Paolo, Lumpi, Alessandro, Giacomo, Marco, Diego, Stefano, Silvio, Liang Liang, Livio, Toni), students (Marco M., Andrea, Elia, Fabio, Davide, Marco A., Michele), friends (Lillo, Saul, Federica, Benni, Edoardo) and all the others who contributed at any degree to this work.

Many thanks to my son Lorenzo for having had a lot of patience in the last 18 months. Lastly, I'm very grateful to my parents and to my husband for their support in the past years.

Table of contents

Chapter 1

Introduction

This Chapter is intended to provide an overview of the problem investigated in this thesis. In the first part of the Chapter the topic of Human-Structure Interaction is introduced and the goal of the work is clarified. The second part of the Chapter summarises the thesis outline

1.1 Human- Structure interaction

In recent years, problems related to in-service vibrations have gained a growing attention. Recent reviews demonstrate the interest in the topic [1]-[5]. Since brand new structures have become more and more slender, an increasing number of problems related to unexpected vibration amplitudes have been recorded. Reported problems regard various kinds of structures such as footbridges [6],[7], football stadia [8],[9] and long-cantilevered structures [10]. Indeed, people acting on pedestrian structures, such as a footbridge or a staircase, behave as dynamical systems capable of modifying the dynamics of the structure itself as well as of introducing a load. This phenomenon is commonly known as Human-Structure Interaction (HSI). At present, however, the knowledge of HSI is still limited. Indeed, the determination of vibration amplitudes of structures occupied by people is a very complex phenomenon. Particularly, at least two main critical issues can be identified. The first aspect regards a correct characterization of the active forces induced by people on the structure. The majority of standards and codes suggest to model human-induced forces as harmonic forces [11]-[13]. However, this assumption is too simplistic and does not reflect the real trend of human-induced forces. This problem was addressed in many works and approaches to correctly identify such forces were proposed. Furthermore, the structural movement can influence the active forces exerted by humans to the structure itself. The second aspect regards the influence of people on the dynamic properties of the structure they occupy. Few attempts were made to include the effect of people other than the simple added mass or force models [14]-[20]. However, a model capable of providing an accurate prediction of the experimental evidence does not currently exist in literature.

Although the experimental evidence suggests that appropriate dynamic models of human occupants should be used in order to obtain an accurate model of Joint Human-Structure (H-S) systems, it is common practice to consider people interacting with a structure only as a force source. This approach, however, may lead to an erroneous estimation of the vibration levels at the design stage for the cases were the influence of people is not negligible.

In this context there is still ground for general methods able to account for people's presence. Thus, this work aims at improving the experience in this field, proposing a method to account for people's presence and to get reliable predictions of vibration amplitudes.

1.2 Thesis outline

This work mainly focuses on the analysis of vertical vibrations of a slender structure proposing an approach to predict such vibrations. As for vertical vibrations, the experimental evidence suggests that people interacting with a structure are a source of added damping. For this reason, considering the dynamic properties of the empty structure to estimate the structural response can lead to erroneous estimates of the vibration amplitudes.

At first an overview of the state of the art is proposed (Chapter 2).

The influence of passive people is then considered (Chapter 3). An appropriate analytical model is proposed to include the effect of people's presence on the dynamic behaviour of a slender structure. The proposed approach only requires the knowledge of the modal model of the empty structure and of the driving point Frequency Response Functions (FRFs) of each subject on the structure. Combining this information, an accurate prediction of the FRF of the joint H-S system can be achieved. The analytical model is used to simulate the dynamics of structures occupied by people. The results of the numerical simulations are compared to experimental tests to validate the proposed method.

The method is then extended with the purpose of accurately quantifying the in-service vibration amplitudes of a slender structure due to people's presence. The idea behind such an extension is the identification of an equivalent model to represent the dynamic behaviour of the joint structure-moving people system. An appropriate active force (i.e. the force exerted by people on the structure) is then applied to this equivalent model in order to get a prediction of vibration levels. To the purpose of validating the methodology, appropriate tests were carried out. Slender staircases were used to verify the results. Suitable test set-ups were used to measure the vibration levels and the forces induced by moving people. The effectiveness of the approach is verified through experimental tests performed under controlled conditions (Chapter 4). Then, the approach is used to predict the vibration amplitudes during normal operating conditions (Chapter 5).

Chapter 6 proposes a theoretical analysis of HSI. The study aims at exploring the properties of the HSI from a mathematical point of view. The matrix properties of joint H-S systems are investigated. Multi Degree of Freedom (MDOF) structures are considered and the differences between a complete model of H-S systems and the use of the modal superposition method are investigated. Then, a criterion to evaluate the influence of people based on the direct analysis of apparent mass curves is proposed. In addition, an analysis of the effects of subjects in different postures is proposed. The analysis is performed using various apparent mass curves representative of different postures and related to various vibration directions.

Chapter 7 proposes a field case, i.e. an analysis of a grandstand of the San Siro Stadium. The effects of the presence of people during some football matches are evaluated. These effects are analysed in terms of changes in modal parameters and vibrations amplitudes, proposing an extension of the model proposed in Chapter 3 to a different and more complex case. The impact of the number of people on the structure on its dynamic behaviour is also analysed. The influence of the distribution of people on the modal parameters of the joint Human-Grandstand system is analysed by means of numerical simulations.

Chapter 2

Literature review

This Chapter proposes a summary of the most relevant aspects regarding HSI. At first an analysis of the literature regarding vertical vibrations is proposed. Particularly, recorded experimental cases, HSI models and force models are reviewed. Due to its importance for a correct modelling of H-S systems, an overview of the dynamics of the whole human body when subject to vibrations is proposed. For the sake of completeness an overview of problems related to lateral vibrations is also proposed. Reference to possible vibration mitigation methods and to current design guidances is also provided in the last part of the Chapter.

2.1 Background of Human- Structure interaction

In the last few years, an increasing attention has been paid to human induced vibrations and HSI. In the recent years an increasing number of problems related to unexpected vibration amplitudes have been recorded. Reported problems regard various kinds of structures such as footbridges [6],[7], football stadia [8],[9] and long-cantilevered structures [10]. Indeed, the improvement of the mechanical characteristics of materials has enabled engineers to design structures increasingly lighter and more slender. As a consequence, pedestrian constructions have become more and more susceptible to vibrations when subject to dynamic loads [2]. Section 2.2 and Section 2.6 report an overview of experimental recorded cases of HSI phenomena.

People's influence is difficult to predict as it depends on many factors, such as the modal parameters of the empty structure, the posture and the number of people on the structure. Thus, at least two aspects should be considered in a design against human induced vibrations. The first aspect regards a correct characterization of the dynamic properties of joint H-S systems. Indeed, the modal properties of joint H-S systems should be considered in order to get reliable predictions of vibration levels at the design stage. In literature few attempts were made to include the effect of people on the dynamic properties of a structure. An overview of these methods is proposed in Section 2.3. The second aspect regards a correct characterization of the active forces induced by people on the structure. The majority of standards and codes suggest to model human-induced forces as deterministic harmonic forces. However, this assumption is too simplistic and does not reflect the real trend of human-induced forces. This problem was addressed in many works such as [21], and approaches to correctly identify such forces were proposed [22]-[25]. An overview of current available models of human induced forces is proposed in Section 2.4.

In order to predict changes of modal parameters due to the people's presence, biomechanical research and models of the whole human body are often used. A review the models considered more suitable to simulate the dynamics of H-S systems is proposed in Section 2.5.

When brand new structures fail the vibration serviceability check, an a-posteriori mitigation of vibration amplitudes is often required [26],[27]. To this purpose many kinds of solutions were proposed in the past years [28],[29]. An overview of these methods is proposed in Section 2.7. However, such solutions imply additional costs. A better knowledge of the effect of people on the dynamic behaviour of structures would allow a more accurate evaluation of the vibration

amplitudes at the design stage. As a consequence, the cost and effort to mitigate vibration amplitudes a-posteriori could be avoided or at least reduced.

2.2 Vertical vibrations

Many works available in literature report recorded cases of the influence of people on the dynamic properties of a structure. These cases can be divided in two main subcategories, i.e. structures mainly vibrating in the vertical direction ad structures mainly vibrating in the horizontal (lateral) direction. The effect of people has significant differences in the two cases. Indeed, the dynamics of people is considerably different for different vibration directions. This section proposes an overview of people's effect in the case of vertical vibrations, while a brief overview of the cases regarding lateral vibrations is reported in Section 2.6.

As for the vertical vibrations, the experimental evidence suggests that people interacting with a structure are a source of added damping [30]-[32]. Considering the dynamic properties of the structure when empty for estimating the structural response can lead to a high overestimation of the amplitudes of vibration [33],[34] when damping ratios change significantly due to people's presence.

The following subsections summarise the main available information regarding people's influence on structures vibrating in the vertical direction and occupied by passive (Subsection 2.2.1) and by active (Subsection 2.2.2) subjects respectively.

2.2.1 Passive people

The influence of passive people on the dynamic properties of a structure has been widely studied for the last decades for structural engineering purposes and it is now well known that people can significantly change the natural frequencies and damping ratios of the structure they occupy.

As for vertical vibrations, a significant increase of structural damping due to passive people has been widely evidenced in literature [30],[31],[32],[35] and the 1990s saw several attempts to quantify the effect of stationary occupants experimentally [30],[36]-[40]. Particularly, Brownjohn [30] investigated people's effects under laboratory conditions analysing the influence of a subject on the modal parameters of a concrete plank. He pointed out that even a single subject could increase the damping ratio of a concrete plank from 0.8% to 9.2% of critical. Frequency shifts (usually decreases) in the slab apparent resonant frequency were also recorded. People's influence was found to be determined by the subject's posture. Other studies, such as [41], investigated the influence of posture, crowd size and distribution, on the modal properties of an occupied test structure. Besides laboratory conditions, other works such as [32] and [35] investigated such

an influence on the dynamic properties of a football stadium and a sports hall respectively.

As for the natural frequencies of structures occupied by passive people, the majority of the recorded cases reports a decrease of natural frequencies due to people's presence. However, some cases showed an increase of natural frequencies [34] or an additional mode due to people's presence [38].

2.2.2 Active people

Initially it was thought that a person who runs and jumps on site could not change the dynamic properties of a structure (Ellis and Ji [36]), unlike what happened in the case of a passive subject. However, this is in contrast with what was found later by other researchers. For instance, Pimentel [42] pointed out that a moving subject could reduce the natural frequency of the structure, while Ohlsson [43], dealing with the study of wooden walkways (low frequencies structures), reported that a moving subject could increases the damping of the structure. More recent works such as [44],[45] reported similar results. Thus, the experimental evidence suggests that also moving occupants can affect both the natural frequencies and damping ratios of a structure.

2.3 Models of HSI

The first and simplest way to simulate people's presence on a structure is to model human occupants as added masses. As demonstrated by many works dealing with this topic [46]-[48], such an approach has been accepted for a long time, as it could explain the reduction of structure natural frequencies due to people's presence. Nevertheless, it could not explain the changes in structural damping due to passive people. The limitation of considering human occupants as mere added masses was first raised by Ohlson [43] and Rainer and Pernica [49] who suggested to use damped dynamic models of human occupants in order to obtain an accurate description of HSI. Foschi and Gupta [50] were among the firsts to adopt this approach.

Along with experimental researches, some models to quantify the effect of human occupants on the dynamic properties of a slender structure have been proposed in the past decade too.

Brownjohn [30] investigated people's effects under laboratory conditions and proposed a 2 Degrees Of Freedom (DOF) model for the plank-human system. Sachse [14]-[16] investigated the influence of human occupants on the dynamic properties of civil engineering structures, combining analytical studies and experiments.

Sachse proposed to model the Human-Structure (H-S) system as a 2 DOF system to explain the influence of human occupants on natural frequencies, damping ratios and Frequency Response Functions (FRFs). Her work proposed an extensive experimental investigation, deriving damped SDOF human models from experimental data and suggesting their use to predict the dynamic behaviour of the H-S system. However, according to the author, the properties of the human model to be adopted vary with the natural frequency of the empty structure, which is a non-physical assumption. As stated by the author herself, the structure modelling as a SDOF system is one of Sachse's work limitations. Therefore, the effect of closely spaced modes may not be considered. In addition, the effect of people's presence is evaluated in terms of mass ratio (mass of people over mass of structure). However, this does not explain the effect for people's distribution on the structure – e.g. a subject on a node of the structure would not modify the dynamic behaviour even though his mass is comparable to the mass of the structure.

A few years later, Sim [17] and Sim et al. [18],[19], proposed a dynamic model to represent a crowd as a system added to the main structure. In contrast to Sachse's work, Sim developed a crowd model employing the extensive research by Griffin et al. [51]-[54] carried out on seated and standing individuals. Using the results of the researches by Griffin et al., Sim derived an equivalent model to represent the dynamic behaviour of the crowd. In his work the author proposed to represent the crowd using a transfer function based on the apparent mass. As made by Sachse, Sim supposed the structure to be a SDOF system as well and the effect of people's distribution was not considered.

A work by Alexander [55] proposed a theoretical analysis of the dynamics of the crowd-structure system in which the author investigated the role of higher vibration modes.

Pavic and Reynolds [56] have recently proposed a 3 DOF model to describe the interaction between a grandstand and the crowd on it. The 3 DOF represents the dynamics of the structure and of passive and active people respectively. In their work the authors suggest to scale the physical mass of people using mode shape amplitudes of the most relevant mode of the empty structure. This was proved to be a reasonably correct assumption [57]. However, no mathematical justification to support such an assumption is proposed. In this case, too, the structure is modelled as a SDOF system.

According to the above-mentioned researches, the reviewed models may explain only qualitatively the influence of human occupants on natural frequencies, damping ratios and FRFs and they may not provide an accurate estimation of the behaviour of the joint H-S system.

In literature few attempts were made to include the effect of moving people. Particularly, a paper by Qin et al. [58] faced the problem of pedestrian-bridge interaction using a bipedal walking model. The proposed method consists in a feedback control force applied by the pedestrian. The results of the numerical study show that the effect of people increase with the amplitude of vibration. However, despite an increase of damping ratios due to the people's presence, results show an increase of the predicted amplitudes of vibration using the model of Human-Structure Interaction (HSI) and this result is against the experimental evidence.

A work by Pavic and Reynolds [56] proposed the use of a 3DOF model to represent the dynamics of a structure occupied by passive and active subjects. In the proposed model each DOF represents the structure, the passive crowd and the active crowd respectively. The model was used to predict the response of a stadium grandstand with good results. Another work by Shahabapoor et al. [59] proposed the use of a mass-spring-damper (MSD) model of the human body to predict the effect of walking pedestrians on the dynamic properties of a structure. In their work the authors report a theoretical analysis of the proposed approach. However, as evidenced by the authors, experimental data are required to validate the methodology. A common assumption and limitation of the last two above-mentioned approaches is the structure and the people modelling as a SDOF system.

2.4 Human induced forces

A correct characterization of human-induced forces is a key aspect for a successful prediction of vibration levels due to human activity. The majority of standards and codes suggests to model human-induced forces as deterministic harmonic forces. However, this assumption is too simplistic and does not reflect the real trend of human induced forces.

In the past years researches made a great effort in order provide an experimental and analytical characterization of such forces. A recent review by Racic et Al. [23], with its 270 references, demonstrates the high amount of work on the topic.

Human induced forces significantly vary not only between individuals but also for a single individual. In addition such forces are influenced by many parameters such as the frequency step, the kind of motion (e.g. walking, running) or the structure itself.

2.4.1 Walking

A walking pedestrian produces a dynamic force along three directions: vertical, horizontal-longitudinal and horizontal-lateral. The vertical component of the force is the most studied as it is the one that reaches the highest values. However, as in recent years many problems related to horizontal vibrations have been recorded, an increasing amount of researchers have focused on horizontal forces. The force transmitted to the ground has proved to be dependent on several factors such as the walking speed, the weight of the subject and the walking frequency. Typical frequency ranges are 1.6-2.4 Hz for walking and 2.0-3.5 Hz for running [60].

Pedestrian induced loading is commonly measured by means of force plates [24],[43]. However, such a choice could lead to measured forces not properly representing the reality. Indeed, the subject must control and target his/her footstep to land at a particular location, and the ability to walk naturally can be negatively affected. An alternative solution is the use of instrumented force measuring treadmills [61]-[63]. The use of treadmills enables continuous force measurements. However, the constrained speed of movement, imposed by the rotation of the treadmill belt, can alter the exerted forces with respect to normal walking. Some attempts to use instrumented shoes or pressure insoles [64],[65] are also recorded. However, such methods universally lack of accuracy when compared with the above-mentioned [66]. Innovative methods based on 'free field' measurement of human walking forces using motion capturing technology are also proposed [23]. To this purpose the motion of tracking markers attached to the subject is recorded. Then, the kinematics is calculated and the externally applied forces are calculated through inverse dynamic analysis.

2.4.2 Ascending and descending staircases

As most of the experimental cases analysed in this work regard staircases, a brief hint to human induced forces for such case is proposed. Few studies [24],[67],[68] propose analyses of the forces exerted when ascending or descending stairs. The main differences between such motion and normal walking are:

- The difference in height between two successive steps;
- The fixed length of the step due to the geometry of the stairs.

In [24] an extensive analysis of human induce forces is proposed. During the tests subjects were asked to climb up and down at an imposed frequency and to provide a feedback about which pace they felt more comfortable with. Experimental results show that preferred natural frequencies are 2 Hz (walking) and 3.3 Hz (running) for both ascending and descending. However, when

descending most of the subjects were comfortable at any footfall rate in the range 2-3.3 Hz. The main difference between ascending and descending lies in the second harmonic of the recorded forces. Indeed, when descending the second harmonics are much higher for a greater range of footfall rates.

2.4.3 Force models

The available force models proposed to date can be divided in time-domain and frequency-domain models. Time-domain models can be further divided in deterministic and probabilistic models. One of the main limitation of deterministic models is the use of a uniform force for each individual. The walking force is expressed in the time domain as a sum of Fourier harmonic components [69]. Thus, the intrinsic random variation among different subjects is not accounted for. Conversely, probabilistic force models are based on the assumption that, as human forces are considerably variable and uncertain, their characterization is better provided from a probabilistic and statistical perspective. To generate realistic synthetic vertical force signals, the use of a stochastic and narrow band model is proposed in literature [70],[71],[72] . An approach based on the use of "free-field" continuous walking/running forces, measured using motion capturing technology and, thus, without artificial constrains, is also proposed [22],[73],[74].

2.5 Human body dynamics

In order to obtain a correct prediction of the structural response due to human activity, a detailed knowledge of the dynamic behaviour of the human body when subject to vibrations is required.

The human body is a very complex dynamic system, whose properties strongly vary with the posture, the direction of vibration, the subject (inter-subject variability) and between individuals themselves (intra-subject variability). Thus, many studies regarding the characterization of human body dynamic were proposed in the past years. The properties of the human body are commonly expressed in terms of apparent mass. Such a quantity is obtained by placing a subject on a shaking table and measuring force and acceleration at the contact point. Many of the studies available in literature propose experimental results. Fewer studies also propose lumped modal parameters models obtained by curve-fitting the experimental data.

2.5.1 Standing subjects

As for standing subjects, the experimental evidence shows that the dynamics of the human body is dominated by a highly damped (30%-50%) mode with natural

frequency depending on the posture of the subject. Some studies were published in the past years. In [54],[75] the influence of posture and vibration magnitude was investigated. Experimental results showed that the first natural frequency of the human body tends to decrease with increasing vibration magnitude, e.g. from 6.75 Hz to 5.25 Hz for a subject in the normal posture when increasing vibration magnitude from 0.125 to 2.0 ms^{-2} root mean square (rms) in the frequency range 0.5 – 30 Hz. The natural frequency of the main resonance was proved to be highly dependent on the posture. Such natural frequency could vary from 2.75 Hz for a subject in the legs bent posture to 3.75 Hz in the one leg posture or 5.5 Hz in the normal posture.

In [53] linear lumped parameter models of the apparent mass are proposed. Such models were optimised using the mean apparent mass of 12 subjects and using the results of previous studies. Several 1 degree of freedom (DOF) and 2 DOFs models were used. Figure 2.1 shows a schematic expression of the models used in [53].

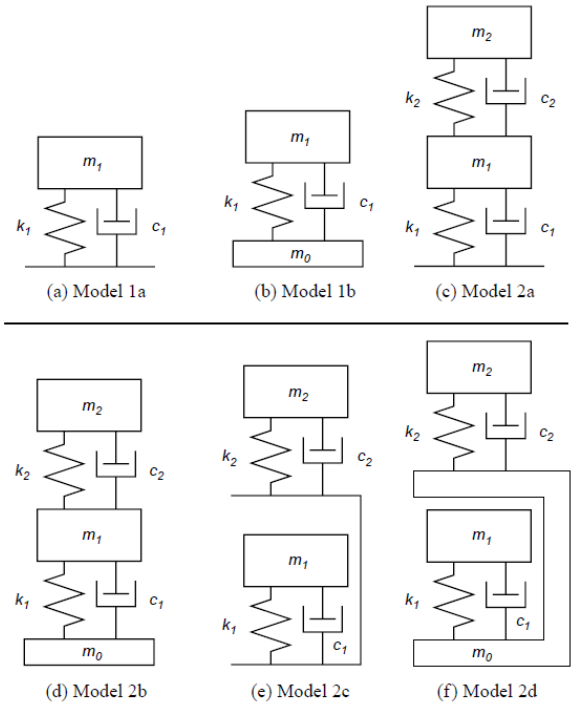

Figure 2.1: Lumped parameter model as in [53]

Results showed that the 2 DOFs models represent the apparent mass of standing subjects better than the 1 DOF models. Furthermore, the high agreement

between measured apparent masses and 2 DOFs models suggested that models with more than 2 DOFs are not required.

2.5.2 Seated subjects

As for seated subjects, the experimental evidence suggests that the frequency of the main resonance tends to be lower than that measured for the normal standing posture [76]. However, the differences are low (less than 1 Hz for most subjects) compared to the differences with respect to other postures.

Also for seated subjects the influence of inter-subject variability was investigated [77]. In addition, the influence of the seat (with or without backrest, with reclined rigid/foam backrest [77] or backrests inclined at various angles [78]) was investigated.

Like for standing subjects, mathematical models for the apparent mass are proposed [51]. Also in this case the 2 DOFs model provided results closer to the experimental data

2.6 Lateral vibrations

This work mainly deals with structures vibrating in the vertical direction. Only a few initial considerations about structures vibrating in the lateral direction are given in Chapter 6. However, for the sake of completeness, a brief summary of the state of the art regarding lateral vibrations is reported.

Two main problems concerning lateral vibrations can be defined as human-human (i.e. influence of surrounding people) and human-structure (i.e. change in the walking pattern due to structural movement) interaction.

Although cases of problems related to lateral vibrations of pedestrian structures had been previously recorded [79], the striking cases of the Solferino Bridge [80] and the Millennium bridge [81] have led to an increasing attention towards this topic. From that moment on many cases, such as [82][83]-[84], of footbridges subject to excessive vibrations have been recorded. Consequently, since that time several working groups were created to define design guidelines and thus the amount of research on the topic underwent a considerable growth. In many recorded cases it was seen that a large number of pedestrian could produce a considerable lateral response. Furthermore, a small increase of pedestrian could trigger a sudden increment of vibration amplitudes. Thus, in order to explain the mechanism of HSI a great amount of full scale testing and laboratory testing was performed. An instability type behaviour was assumed in several cases. Such a phenomenon is commonly referred to as Synchronous lateral Excitation), namely

the synchronisation between the movement of the pedestrian and that of the bridge. However, recent research showed that excessive vibrations could also occur without synchronization [84]. Indeed, pedestrian can act as negative dampers on low-frequency lateral vibration modes [84].

HSI appears to be governed by a number of coexisting phenomena. Such a fact makes the development of general mathematical models to predict HSI a difficult task. A great amount of models and criteria were proposed in recent years, ranging from stability criteria [81],[85],[86], which provide a critical number of pedestrian needed to trigger excessive vibrations, to models that represent the human body as an inverted pendulum [87] or as a load with nonlinear velocity dependency [88]. However, as stated in [88], these models are usually calibrated against a limited number of empirical observations and cannot accurately describe the full spectrum of involved phenomena. Consequently, despite the large amount of research, there is still only a limited connection between the mathematical models and the empirical observations [79].

2.7 Vibrations mitigation

When brand new structures fail the vibration serviceability check, an a-posteriori mitigation of vibrations is often required. Thus, in recent years researchers concentrated on the development and verification of various vibration mitigation methods [90].

The first and simplest way to mitigate excessive vibrations is the use of passive control systems. Common techniques, such as Tuned Mass Dampers (TMDs) are widely employed [91],[92],[93]. As an example, the above mentioned case of the Solferino bridge was solved by installing 14 TMDs. The excessive vibrations of the Millennium bridge were reduced by installing 37 viscous dampers and 29 pairs of vertically acting TMDs. Mitigation of human-induced lateral vibrations can also be obtained by shaping the walkway in order to modify the pedestrian density, speed and walking frequency [94].

Semi-active [95] and active vibration control is also gaining an increasing attention, as it is considered to be suitable for this kinds of applications. To this purpose various approaches based on different control schemes were proposed in the past year [96]. Examples include direct or compensated acceleration feedback control [97],[98], direct [97] or on-off nonlinear [99],[100] or response-dependent [101] velocity feedback control, integral resonant control [102].

Both passive and active control schemes present advantages and disadvantages [103]. Thus, the use of hybrid techniques (i.e. combination of active and passive control) is also proposed [104],[105].

2.8 Guidances

This section proposes a brief summary of some of the main guidelines for the design of pedestrian structures.

The majority of standards suggest to design structures without vibration modes in the range of the natural frequencies that can be easily forced by human occupants. However, such a restriction is a strong limit to possible design solutions.

As for footbridges, the limits set by the various guidelines vary greatly. The more restrictive criterion is the one proposed in ISO 10137 [12]. In [12] it is established that a verification of the comfort criteria should be performed if the first natural frequency of the structure is lower than:

- 5 Hz for vertical vibrations;

- 2.5 Hz for horizontal and torsional vibrations.

If the structure does not satisfy the limits in terms of natural frequencies, it becomes necessary to proceed with an analysis in terms of maxima of the accelerations.

With regard to Eurocode EN 1990 [11] and Sètra Guideline [13], both standards provide limits on the maximum peak acceleration. In particular, the Eurocode EN 1990 states a maximum peak of 0.7 ms^{-2} in the vertical direction and 0.2 ms^{-2} in the horizontal direction. Sètra proposes a range of accelerations depending on the desired level of comfort. To have maximum comfort, the upper limit is placed at 0.5 ms^{-2} in the vertical direction, while the horizontal accelerations are in any case limited to 0.1 ms^{-2} to avoid synchronization phenomena. However, it should be noted that since the limits are given in terms of maximum acceleration, a different filtering of the data can lead to completely different results. With regard to ISO 10137, paragraph Annex C shows the limit curve basis for the acceleration levels measured in octave bands. As prescribed by the regulations for pedestrian walkways, ISO 10137 paragraph C 1.2, the curve must be multiplied by 60 or 30 depending on whether or not there is the possibility that someone remains still on the structure, and is therefore subject to vibration for a longer period. Thus, while frequency weighting according to the ISO standard is clearly explained, no hints are given in the EUROCODE and in the Sètra guideline on the frequency weighting of the measured vibrations. This is probably due to the fact that these codes are intended to provide guidance at the design stage where forcing and response are given by numerical models and therefore their frequency content is

clearly stated. Therefore, when dealing with the measured time history, the kind of frequency weighting applied to real measured data strongly affects the results.

A special focus is also devoted to the design of stadia grandstands. Indeed, grandstands are often subject to rhythmic activities, especially during concerts where the crowd synchronizes its movement with the music. In some cases excessive vibrations, which can cause discomfort and in some cases panic, were recorded.

To overcome the problem, guidelines such as the National Building Code of Canada [106] and the BS 6399 [107] recommend to perform a dynamic analysis if the natural frequencies of the grandstand is below a certain threshold value. In BS 6399 this limit value is to 8.4 Hz. Indeed, it is seen that a crowd can introduce energy in a frequency range from 1.5 to 2.8 Hz. Thus, the limit value is obtained by considering the multiple harmonics of the upper limit of this frequency band.

Despite the experimental evidence, the majority of international standards and codes neglect the influence of human occupants in terms of changes of structural modal parameters. Therefore, at the design stage it is common practice to consider people interacting with a structure as a source of force only. This fact is explained with the lack of appropriate models to predict such a complex phenomenon. A recent guidance [20] (Joint Working Group, 2008) regarding dynamic performance requirements for permanent grandstands subject to crowd action is an exception to this. Indeed, the guidance underlines that if the effects due to human structure interaction are ignored in calculations, the response of the structure will be incorrectly represented in the analysis. Thus, in this guidance recommendation to considered human structure interaction is provided and an analytical method for treating human structure interaction is proposed. This approach was developed using the most recent research, such as [56], and available experimental data, with the aim of reproducing the patterns of behaviour observed in actual structures subject to dynamic crowd loading. However, as evidenced in the guidance, the method cannot deal with all the variations in human behaviour and physical characteristics that affect the structural dynamics

Chapter 3

H-S model for passive people

This chapter proposes a model to predict changes of modal parameters of a structure occupied by passive people. First, the mathematical formulation of the method is presented. The proposed approach requires to accurately know the modal model of the empty structure, expressed in terms of natural frequencies, damping ratios and mode shapes. No restriction on the number of degrees of freedom of the structural model is required. Each passive subject on the structure is modelled using the so called apparent mass and is introduced locally on the empty structure to obtain a model of the joint H-S system. As for the apparent mass of the subjects, both measurements and models already available in literature were used.

The proposed model was validated by means of experimental tests carried out on two lightly damped staircases and using some data available in literature.

3.1 Numerical model

This section presents a mathematical model to represent the dynamics of joint H-S systems in the case of passive people. Such a model can be used to assess the changes in the structure modal parameters induced by people's presence. Two elements are required to this purpose:

1. a dynamic model of the empty structure;
2. a description of the dynamic behaviour of each person on the structure.

As for point 1, a modal model of the structure is employed. Such a model may be obtained from experimental data or from existing structural models (e.g. a finite element model).

As for point 2, the quantity commonly used to represent the dynamic behaviour of the whole human body is the driving point FRF, i.e. the transfer function between the force f^{Human} exerted by the person on the structure (Figure 3.1) at the contact point (Ground Reaction Force - GRF) and the corresponding structure displacement (x), velocity ($\dot{x}$) or acceleration ($\ddot{x}$) in the frequency domain.

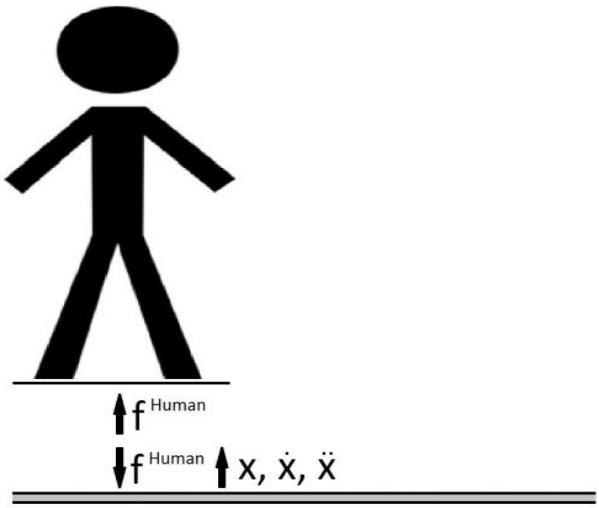

Figure 3.1: Dynamic modelling of a subject in contact with the structure

In case of acceleration, this transfer function is commonly referred to as the apparent mass in literature [108]. Defined here as $M^*(\omega) = \frac{f^{\mathrm{Human}}(\omega)}{\ddot{x}(\omega)}$, the apparent mass basically represents the relationship between the acceleration at the contact point and the GRF. $M^*(\omega)$ is a complex function in the frequency domain. Obviously, the GRF of each person on the structure depends on his/her

dynamic properties (e.g. mass, stiffness, damping). In Section 3.2 a discussion regarding possible apparent mass values is proposed.

The approach proposed by Krenk [109] has been considered and modified to find a method that is able to account for people's presence on the structure. Krenk's model was originally developed for the introduction of dampers on discretised structural systems. The effect of each damper is introduced through the force exerted by the damper on the structure. In the frequency domain, this force may be expressed as the product between the FRF of the damper and the displacement of the point where the damper is located. This model was modified to introduce passive people on the structure. One of the advantages of this model is the possibility to introduce each subject and evaluate the corresponding effect individually.

The basic steps to obtain the transfer function of the joint H-S system are reported here below.

The FRFs (between a generic force vector $\mathbf{f}(\omega)$ and structure displacement $\mathbf{x}(\omega)$) of the empty structure $\mathbf{G}(\omega)$ may be expressed as [108]:

$$\mathbf{G}(\omega) = \sum_{\mathrm{j}=1}^{\mathrm{n}} \frac{\boldsymbol{\phi}_\mathrm{j} \boldsymbol{\phi}_\mathrm{j}^\mathrm{T}}{\omega_\mathrm{j}^2 - \omega^2 + 2\mathrm{i}\zeta_j \omega \omega_j} \tag{3.1}$$

where $\boldsymbol{\phi}_\mathrm{j}$ is the jth mode shape vector (scaled to the unit modal mass) measured at discrete points, ω_j is the natural frequency of the jth mode, ζ_j is the jth non-dimensional damping ratio and n is the (arbitrary) number of modes taken into consideration.

The dynamic behaviour of the empty structure may be expressed as [108]:

$$\mathbf{x}(\omega) = \mathbf{G}(\omega)\mathbf{f}(\omega) \tag{3.2}$$

Since the eigenvectors are measured at discrete points, $\mathbf{G}(\omega)$ is the matrix containing the FRFs associated to these points. Accordingly, $\mathbf{x}(\omega)$ is the vector that contains the responses in the points taken into consideration, while $\mathbf{f}(\omega)$ is a generic force vector containing the forces applied in each point.

After defining the modal model of the empty structure $\mathbf{G}(\omega)$, people's contribution has to be added.

According to the definition of apparent mass, each person fixed to the k^{th} point of the structure introduces a force depending on the apparent mass and on the structure acceleration $\ddot{x}_k$ of the point itself (Figure 3.1). Therefore, the GRF of each passive subject connected to the k^{th} point of the structure can be expressed as

$$f_{\mathrm{k}}^{\mathrm{Human}}(\omega) = M_k^*(\omega)\ddot{x}_{\mathrm{k}}(\omega) = -\omega^2 M_k^*(\omega)x_{\mathrm{k}}(\omega) = H_k(\omega)x_{\mathrm{k}}(\omega) \tag{3.3}$$

where $M_k^*(\omega)$ is the apparent mass of the subject in point k.

In terms of the full displacement vector $\mathbf{x}(\omega)$, Eq. (3.3) may be expressed in the following matrix form:

$$\mathbf{f}^{\mathrm{Human}}(\omega) = H_k(\omega)\mathbf{w}_k\mathbf{w}_k^{\mathrm{T}}\mathbf{x}(\omega) \tag{3.4}$$

where $\mathbf{w}_{\mathrm{k}}$ identifies the connection of the subject to the structure, as exemplified in Figure 3.2.

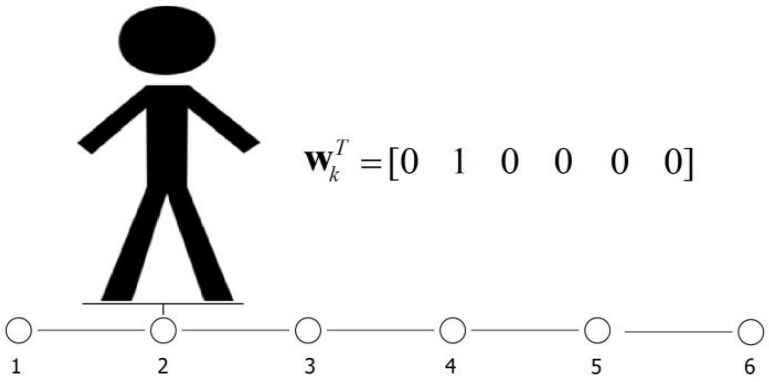

Figure 3.2: Connection of one subject to point #2 of the structure

The total force vector in the case of m people on the structure may be expressed as:

$$\mathbf{f}^{\mathrm{Human}}(\omega) = \mathbf{W}\mathbf{H}(\omega)\mathbf{W}^{\mathrm{T}}\mathbf{x}(\omega) \tag{3.5}$$

where $\mathbf{W} = [\mathbf{w}_1, \ldots, \mathbf{w}_m]$ represents the connection of m subjects and $\mathbf{H}(\omega)$ is the (diagonal) transfer function matrix, containing the H(ω) functions of all the subjects.

Including the force vector expressed by Eq. (3.5) in Eq. (3.2), Eq. (3.6) is obtained (refer to Figure 3.1):

$$\mathbf{G}^{-1}(\omega)\mathbf{x}(\omega) = \mathbf{f}(\omega) - \mathbf{f}^{\mathrm{Human}}(\omega) = \mathbf{f}(\omega) - \mathbf{W}\mathbf{H}(\omega)\mathbf{W}^{\mathrm{T}}\mathbf{x}(\omega) \tag{3.6}$$

Thus, the modified equation of motion becomes

$$[\mathbf{G}^{-1}(\omega) + \mathbf{W}\mathbf{H}(\omega)\mathbf{W}^{\mathrm{T}}]\mathbf{x}(\omega) = \mathbf{G}_{\mathrm{H}}^{-1}(\omega)\mathbf{x}(\omega) = \mathbf{f}(\omega) \tag{3.7}$$

In Eq. (3.7) $\mathbf{G}_{\mathrm{H}}(\omega)$ represents the new transfer function of the H-S system. The new frequency response function may be expressed explicitly in terms of the frequency response function $\mathbf{G}(\omega)$ by the Woodbury matrix identity [110]:

$$(\mathbf{A} + \mathbf{U}\mathbf{C}\mathbf{V})^{-1} = \mathbf{A}^{-1} - \mathbf{A}^{-1}\mathbf{U}(\mathbf{C}^{-1} + \mathbf{V}\mathbf{A}^{-1}\mathbf{U})^{-1}\mathbf{V}\mathbf{A}^{-1} \tag{3.8}$$

as

$$\begin{aligned}\mathbf{G}_{\mathrm{H}}(\omega) &= [\mathbf{G}(\omega)^{-1} + \mathbf{W}\mathbf{H}(\omega)\mathbf{W}^{\mathrm{T}}]^{-1} \\ &= \mathbf{G}(\omega) - \mathbf{G}(\omega)\mathbf{W}(\mathbf{H}(\omega)^{-1} + \mathbf{W}^{\mathrm{T}}\mathbf{G}(\omega)\mathbf{W})^{-1}\mathbf{W}^{\mathrm{T}}\mathbf{G}(\omega)\end{aligned} \tag{3.9}$$

This simple equation allows to calculate the transfer function of the joint H-S system. This approach allows to evaluate the effect due to the presence of each subject separately. This effect is a function of the subject's characteristics and posture (e.g. standing, one leg), as it depends on the subject's apparent mass. The driving point FRFs contained in the matrix $\mathbf{H}(\omega)$ depends upon these properties. In addition, the effect of each subject is a function of the point where the subject is located (i.e. a function of the mode shape components). The matrix $\mathbf{W}$ allows taking into account the position of each subject.

The proposed method has been validated by means of experimental tests that are summarised in Sections 3.3-3.5. The next section proposes different apparent mass curves that are used in the subsequent analysis.

3.2 Apparent mass curves

As described in Section 3, an apparent mass representative of the dynamic behaviour of the human body is required in order to apply the proposed approach.

Some of the problems occurring when modelling the dynamic characteristics of the human body deal with the variation of the following properties:

- the posture;
- the subjects (inter-subject variability, which means that two subjects do not have the same dynamic behaviour);
- the subject (intra-subject variability, which means that there is a spread in results when a subject undergoes the same dynamic test several times);
- the vibration amplitude (for the same subject);

To validate the proposed approach tests with subjects standing in a normal posture were performed. Thus, tests were performed to characterize the actual values of apparent mass of some subjects involved in the subsequent tests. The results are discussed in the next Subsection (3.2.1).

Then, average values of apparent masses available in literature were also considered in order to extend the validity of the proposed approach, as the actual apparent mass of the people occupying the structure is unknown in practical applications. Such values are discussed in Subsection 3.2.2.

In order to obtain a further verification of the proposed approach, some data available [14] in literature regarding the dynamic properties of a structure occupied by passive subjects were also used. As in some of these tests the subjects were sitting on the structure, Subsection 3.2.3 reports the apparent mass value used to simulate the dynamic of a subject in this posture.

3.2.1 Measurement of apparent mass values – standing subjects

This section describes the experimental set-up and procedure used to measure the apparent mass $M^*(\omega)$ of some of the subjects involved in the experimental tests on one staircase (Section 3.3).

The apparent mass was measured imposing a vertical vibration with a large electro-dynamic shaker (maximum displacement of ± 50 mm). The subjects were standing over a rigid surface (0.6 m x 0.6 m in size), whose natural frequency was higher than 60 Hz. According to the characteristics of the tested staircase, the stimulus was white noise in a frequency range between 4 and 25 Hz with a

vibration amplitude set to 0.5 ms^{-2} rms. The plate acceleration was measured with an accelerometer, while the force was measured by three piezoelectric load cells interposed between the shaker head and the plate.

Table 3.1 shows the measurement chain metrological characteristics

Sensor	Measurement Range	Frequency Range (±5%)	Sensitivity
Accelerometer	± 50 g	0.5 Hz – 3000 Hz	0.1 V/g
Load cell	≤ 44.48 kN	up to 60 KHz	4047 pC/kN

Table 3.1 Sensors metrological characteristics (apparent mass measurement setup)

Figure 3.3 shows the experimental set-up.

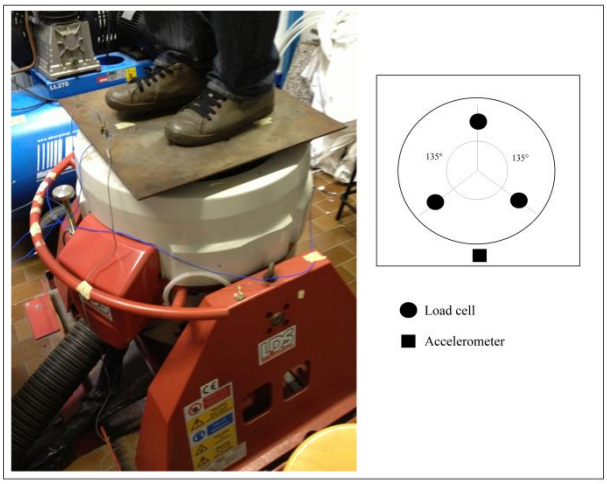

Figure 3.3: Setup to measure apparent mass values

An example of measured apparent masses, estimated as explained in [51], is shown in Figure 3.4.

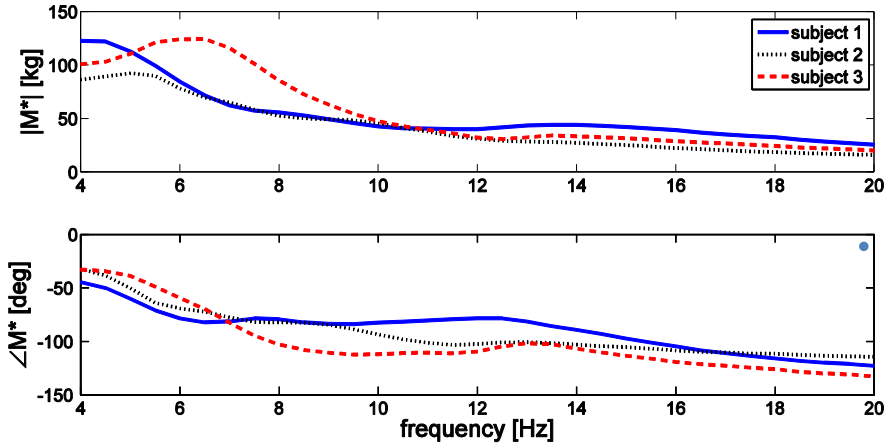

Figure 3.4: Examples of measured apparent masses

In the next section average models available in literature are discussed.

3.2.2 Lumped parameter models of the apparent mass – standing subjects

In addition to the experimental values reported in Section 3.2.1, the average values proposed by Matsumoto and Griffin [51] were also employed. In [51] mathematical models to represent the dynamic behaviour of standing subjects are proposed. Particularly, the authors propose different lumped parameter models (Figure 2.1, Chapter 1) to represent the dynamic behaviour of subjects – in different postures – exposed to vertical whole-body vibration. Furthermore, the models proposed by Matsumoto and Griffin [51] may be suitably employed to the purpose of this work because they represent people's dynamic behaviour through apparent mass curves, as made in the approach proposed in Section 3.1.

As previously mentioned, the apparent mass values vary with the posture, the subject (inter and intra-subject variability) and the vibration amplitude. In their work Matsumoto and Griffin investigated all these aspects. Particularly, they analysed the cases of subjects in normal standing posture, in legs bent posture and in one-leg posture. In all the cases taken into consideration in [51], Matsumoto and Griffin proposed optimized parameters based on the average of the apparent mass curves of 12 male subjects. The parameters are computed for all the models reported in Figure 2.1.

The models considered in this work are those named 2a, 2c and 2d in Figure 2.1. The apparent masses corresponding to these models (standing posture) are reported in Figure 3.5 and Table 3.2 reports the associated coefficients.

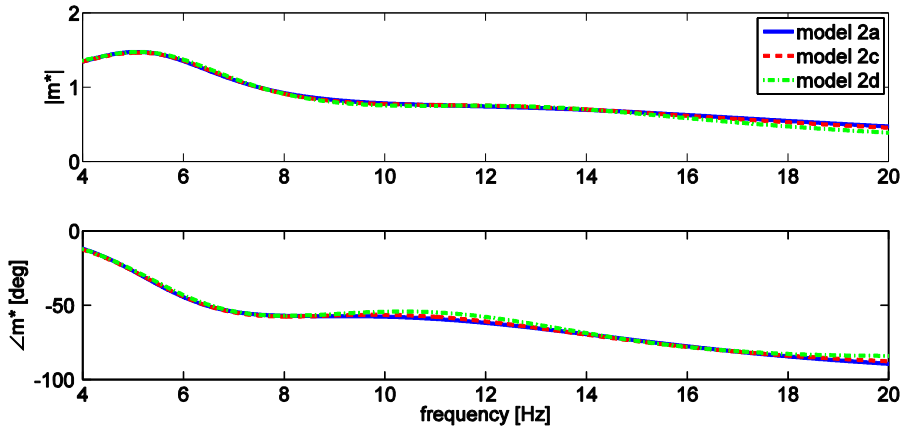

Figure 3.5: Apparent masses – standing posture – various models

		Stiffness [$Nm^{-1}kg^{-1}$]		Damping [$Nsm^{-1}kg^{-1}$]		Mass (no unit)	
	k_1	k_2	c_1	c_2	m_0	m_1	m_2
Mod 2a	$4.39 \cdot 10^3$	$5.53 \cdot 10^2$	$3.71 \cdot 10^1$	$1.18 \cdot 10^1$	-	$5.74 \cdot 10^{-1}$	$3.94 \cdot 10^{-1}$
Mod 2c	$2.37 \cdot 10^3$	$8.49 \cdot 10^2$	$2.48 \cdot 10^1$	$1.65 \cdot 10^1$	-	$3.45 \cdot 10^{-1}$	$6.33 \cdot 10^{-1}$
Mod 2d	$1.82 \cdot 10^3$	$8.93 \cdot 10^2$	$1.42 \cdot 10^1$	$1.76 \cdot 10^1$	$9.09 \cdot 10^{-2}$	$2.54 \cdot 10^{-1}$	$6.55 \cdot 10^{-1}$

Table 3.2: Optimized model parameters for models 2a, 2c and 2d (from [51]) – vibration amplitude: 1.0 ms^{-2}

Equations (3.10)-(3.12) show the analytical expressions of the apparent mass curves reported in Figure 2.1, Table 3.2, and used in this work.

$$\text{Model 2a:} \quad M_{2a}(\mathrm{i}\omega) = \frac{(\mathrm{i}c_1\omega + k_1)\{m_1(-m_2\omega^2 + \mathrm{i}c_2\omega + k_2) + m_2(\mathrm{i}c_2\omega + k_2)\}}{\{-m_1\omega^2 + \mathrm{i}(c_1 + c_2)\omega + k_1 + k_2\}(-m_2\omega^2 + \mathrm{i}c_2\omega + k_2) - (\mathrm{i}c_2\omega + k_2)^2} \tag{3.10}$$

$$\text{Model 2c:} \quad M_{2c}(\mathrm{i}\omega) = \frac{m_1(\mathrm{i}c_1\omega + k_1)}{(-m_1\omega^2 + \mathrm{i}c_1\omega + k_1)} + \frac{m_2(\mathrm{i}c_2\omega + k_2)}{(-m_2\omega^2 + \mathrm{i}c_2\omega + k_2)} \tag{3.11}$$

$$\text{Model 2d:} \quad M_{2d}(\mathrm{i}\omega) = M_{2c}(\mathrm{i}\omega) + m_0 \tag{3.12}$$

Figure 3.5 shows that the choice of the model has little impact on the apparent mass values. It should be noted that the apparent mass values differ from those reported in Figure 3.4 as they are normalized by the static weight of the subjects.

As for the case of normal standing posture, Matsumoto and Griffin also investigated the effect of the vibration amplitude on the results.

Figure 3.6 shows the apparent masses obtained with model 2a and for various vibration amplitudes (rms in the frequency range 0.5-30 Hz) and Table 3.3 reports the associated coefficients (Figure 2.1).

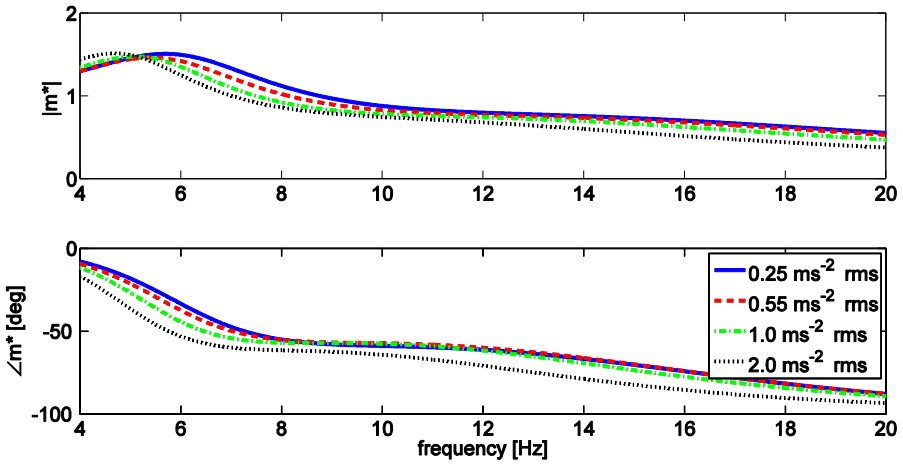

Figure 3.6: Apparent masses – standing posture – various amplitudes of vibration

Vibration magnitude (ms^{-2} rms)	Stiffness [$Nm^{-1}kg^{-1}$]		Damping [$Nsm^{-1}kg^{-1}$]		Mass (no unit)	
	k_1	k_2	c_1	c_2	m_1	m_2
0.25	$5.56 \cdot 10^{3}$	$7.29 \cdot 10^{2}$	$3.86 \cdot 10^{1}$	$1.47 \cdot 10^{1}$	$5.74 \cdot 10^{-1}$	$4.17 \cdot 10^{-1}$
0.5	$5.25 \cdot 10^{3}$	$6.48 \cdot 10^{2}$	$3.79 \cdot 10^{1}$	$1.37 \cdot 10^{1}$	$5.63 \cdot 10^{-1}$	$4.11 \cdot 10^{-1}$
1.0	$4.39 \cdot 10^{3}$	$5.53 \cdot 10^{2}$	$3.71 \cdot 10^{1}$	$1.18 \cdot 10^{1}$	$5.74 \cdot 10^{-1}$	$3.94 \cdot 10^{-1}$
2.0	$3.32 \cdot 10^{3}$	$4.86 \cdot 10^{2}$	$3.26 \cdot 10^{1}$	$1.16 \cdot 10^{1}$	$5.70 \cdot 10^{-1}$	$4.04 \cdot 10^{-1}$

Table 3.3: Optimized model parameters at four vibration magnitudes – model 2a (from [51])

Figure 3.6 shows that the amplitude of vibration impacts on the apparent mass values (the main resonance decreases when the amplitude of vibration increases).

3.2.3 Apparent mass – sitting subjects

In order to simulate the dynamic behaviour of the joint H-S system described in [14], an apparent mass of the sitting human body was needed. To this purpose the work by Toward and Griffin [78] was employed. Particularly, among the apparent mass values reported in [78], the median vertical apparent mass of 12 subject sitting without backrest was used, as this was the posture of the subjects during the tests reported in [14]. Figure 3.7 reports the apparent mass curve extracted from the figures reported in [78].

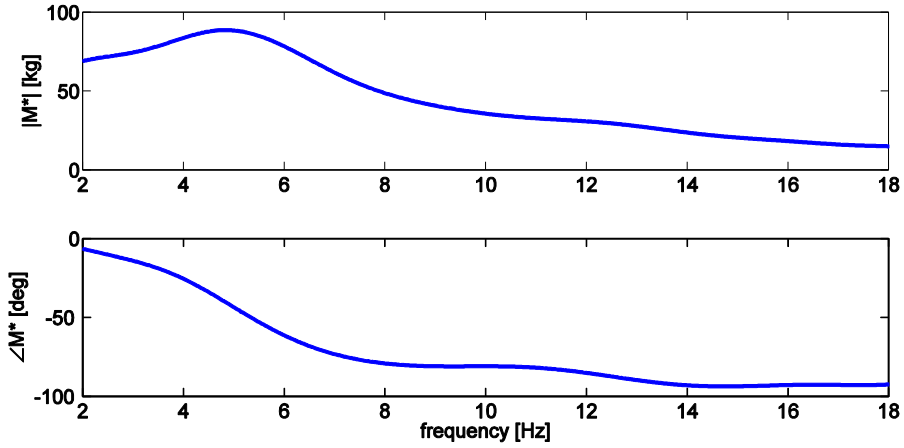

Figure 3.7: Apparent mass – sitting posture

The above-described values of apparent masses were used to simulate the dynamics of the joint H-S systems. The results are proposed in the next Sections.

3.3 Test case 1: Campus Bovisa Sud Staircase

3.3.1 Test case structure and experimental tests

The first considered case study is a slender staircase (Figure 3.8) connecting the ground and the first floors in the main building of the Politecnico di Milano Bovisa Sud Campus. The structure under test is very flexible: even a few people on it are able to change the damping considerably.

Several tests were carried out to verify the effectiveness of the proposed approach. The structure was first tested without people to attain its FRFs. Then, it was tested with people standing still in defined points. This allowed to determine the FRFs of the joint H-S system. All the FRFs were processed to obtain the corresponding modal parameters by means of experimental modal analysis techniques [108],[111].

Figure 3.8: Staircase – Campus Bovisa

This section describes the experiments carried out on the staircase and the corresponding results in terms of FRFs and modal parameters..

The first step was a modal characterisation of the structure with and without people. Therefore, the structure was instrumented with 18 accelerometers measuring in the vertical direction and forced by accelerating a known mass with an electro-dynamic shaker. Figure 3.9 shows the accelerometers positions.

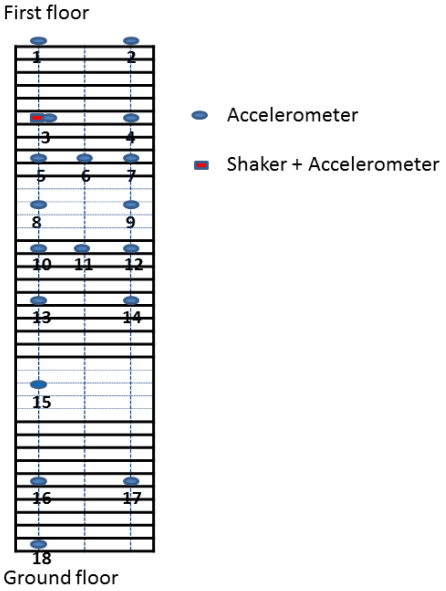

Figure 3.9: Staircase – Campus Bovisa – Experimental setup

The force exerted on the structure by the moving mass could be estimated by multiplying the value of the mass and its acceleration. The acceleration was measured with an accelerometer placed on the mass itself.

The preliminary tests showed that the first natural frequency of the structure is approximately 8 Hz. Therefore, the structure was forced with band-limited random noise between 5 and 20 Hz. In this frequency band the force rms value was 16.8 N. At first, some experimental tests on the empty structure were performed in order to extract its modal properties. Then, additional tests with respectively 3, 6 and 9 people standing still in different points of the structure were carried out. In all the cases, the structure was forced to determine the corresponding FRFs with the shaker.

Figure 3.10 shows an example of experimental FRFs for:

- the empty structure;
- the structure with 2 groups of 3 different people placed in correspondence of the accelerometers 5, 7, 10;
- the structure with 6 people placed in correspondence of the accelerometers 4,5,7,10,12,14;
- the structure with 9 people placed in correspondence of the accelerometers 4, 5, 7, 8, 9, 10, 11, 12, 14.

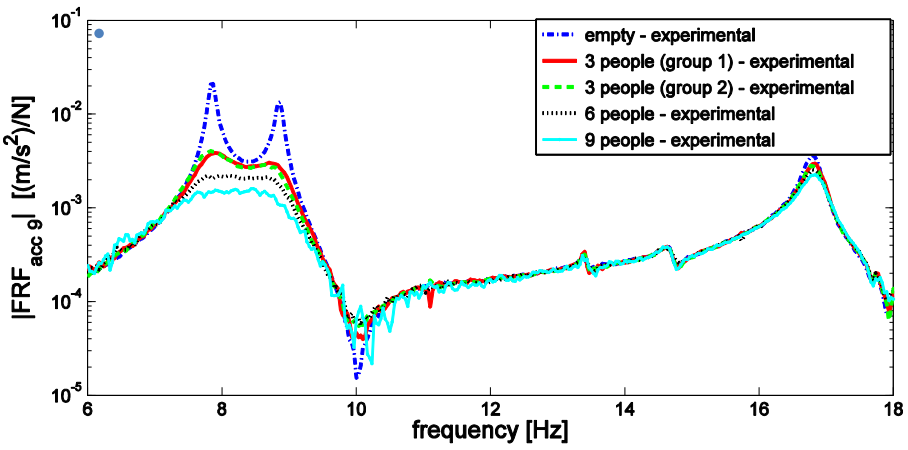

Figure 3.10: Experimental FRFs

Table 3.4 shows the modal properties (i.e. eigenfrequencies f_n and non-dimensional damping ratios ζ) associated to these configurations, identified through the Polyreference Least Square Frequency Domain method [111][111].

empty		3 people, group 1		3 people, group 2		6 people		9 people	
f_n [Hz]	ζ [%]	f_n [Hz]	ζ [%]	f_n [Hz]	ζ [%]	f_n [Hz]	ζ [%]	f_n [Hz]	ζ [%]
7.85	0.48	7.85	3.14	7.79	2.92	7.76	5.31	7.67	7.83
8.86	0.50	8.85	2.60	8.80	2.84	8.81	3.60	8.78	5.22
16.80	0.61	16.84	0.78	16.87	0.90	16.85	0.91	16.89	0.99

Table 3.4: Experimental modal parameters

Figure 3.11 and Figure 3.12 show the mode shapes of the first two modes. The figures were obtained by interpolating the mode shapes. At this point the interpolation was performed only for graphical purposes. Indeed, in the analysis the experimental values were used. The experimental mode shapes of the empty structure are reported in Annex A, Table A.1.

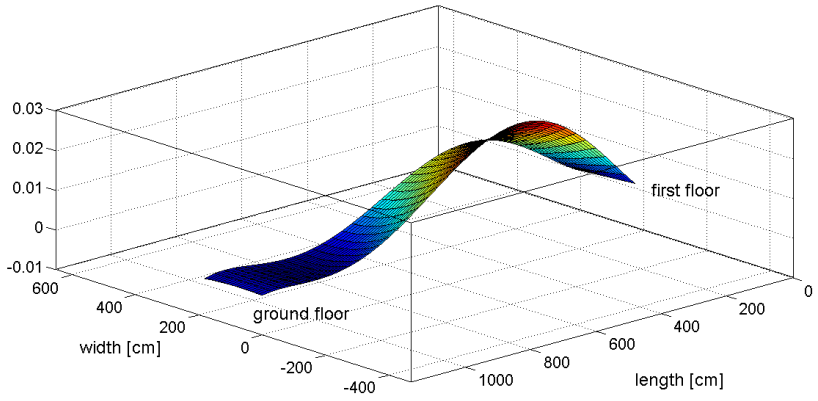

Figure 3.11: Campus Bovisa Staircase – mode shape – mode 1 (7.85 Hz)

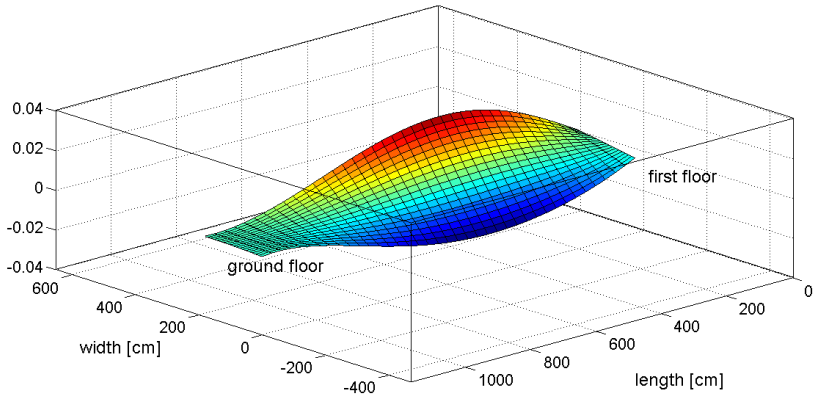

Figure 3.12: Campus Bovisa Staircase – mode shape – mode 2 (8.86 Hz)

As it is formulated, the model proposed in this paper requires the FRFs of the empty structure (Section 3.1). No constrains are placed on the number of vibration modes used to reconstruct these FRFs, as in Eq. (3.1). All the modes in the frequency range of interest may and should be considered. The vibration modes reported in Table 3.4 are those having an appreciable amplitude in the range of frequencies of interest for the structure taken into consideration (i.e. the frequency range where the effect of people is considerable). These modes were used to reconstruct the FRFs of the empty structure and perform the subsequent analysis.

The values reported in Table 3.4 show that people might cause a high increase of damping in correspondence of the first two eigenmodes. A slight increase may be noticed in correspondence of the third mode as well (Figure 3.10 and Table 3.4). In addition, the results of the tests performed with different groups of people showed that different subjects do not behave in the same way and the effect on the modal parameters of the structure is not merely proportional to the mass of the subjects standing on the structure. In the two tests with three people (group 1 and group 2) the mass of each subject in group 1 is lower than that of the corresponding subject in group 2 and the total mass is about 15% higher in this second case. Despite this, as for group 1, the damping associated to the first mode is higher. This highlights how the characteristics of the subject may play a crucial role for the final effect on the dynamic behaviour of the joint H-S system.

The above-mentioned experimental data were used to validate the approach proposed in Section 3.1. Such an issue requires to add people's effect. At first the measured $M^*(\omega)$ curves (Subsection 3.2.1) are used in the model, as explained by Eqs. (3.3) to (3.9).

3.3.2 Prediction of people's effect using measured apparent masses

The model presented in Section 3.1 was used to predict the behaviour of the structure occupied by people. The results were compared with those obtained experimentally. To do this, each subject was added to the model using its measured apparent mass (Section 3.2.1), and using the model described in Section 3.1 (Eqs. (3.3) to (3.9)).

Figure 3.13 shows the comparison between a measured FRF and a predicted FRF for the test with 3 people (group 1), while Table 3.5 shows the corresponding identified modal parameters.

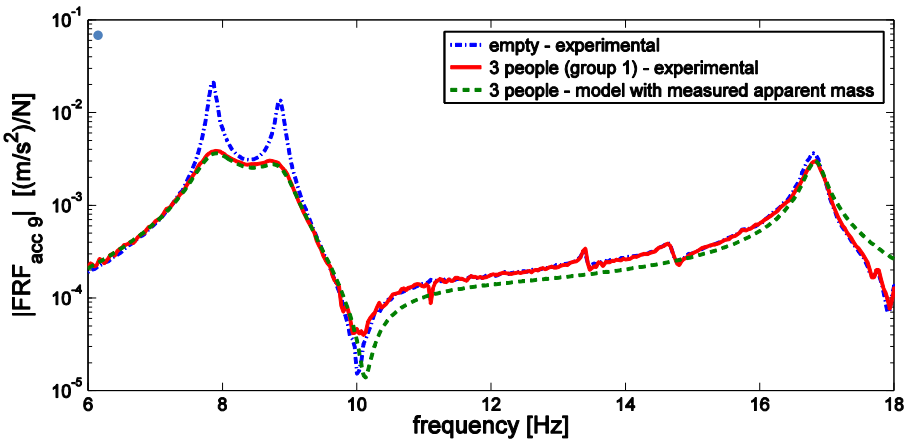

Figure 3.13: Experimental and predicted FRFs (3 people, group 1) using measured apparent mass values

empty		3 people, group 1, experimental		3 people, group 1, model with actual app. mass.	
f_n [Hz]	ζ [%]	f_n [Hz]	ζ [%]	f_n [Hz]	ζ [%]
7.85	0.48	7.85	3.14	7.85	3.26
8.86	0.50	8.85	2. 60	8.85	2.73
16.80	0.61	16.84	0.78	16.83	0.76

Table 3.5: Experimental and predicted (using measured apparent masses) modal parameters – tests with 3 people

The model results well fit the experimental ones, both in terms of natural frequencies and damping ratios, proving the reliability of the proposed model.

In this case, people were added in the model through the measured apparent masses. In practice, this is not feasible because in the design phase it is not possible to know the exact characteristics of all the people that will be using the structure. Thus, the next section discusses and verifies the possibility of using the average values of apparent masses (Section 3.2.2) instead of the measured ones.

3.3.3 Prediction of people's effect using average apparent masses

The previous Section showed the reliability of the results obtained with the model using the actual apparent masses of the subjects on the structure. However, the actual apparent mass of the people occupying the structure is unknown in usual applications.

Thus, in such cases, only an average estimate may be obtained. The average models available in literature were also employed to verify the applicability of the

proposed model, instead of using the actual apparent mass of each subject. This allowed to verify the robustness of the model.

Thus, the results of the simulations proposed in this section differ from those proposed in Section 3.3.2 for the use of the average values of the apparent masses in place of the measured ones.

Figure 3.14 gives an example of the results concerning the case of three people (group 1).

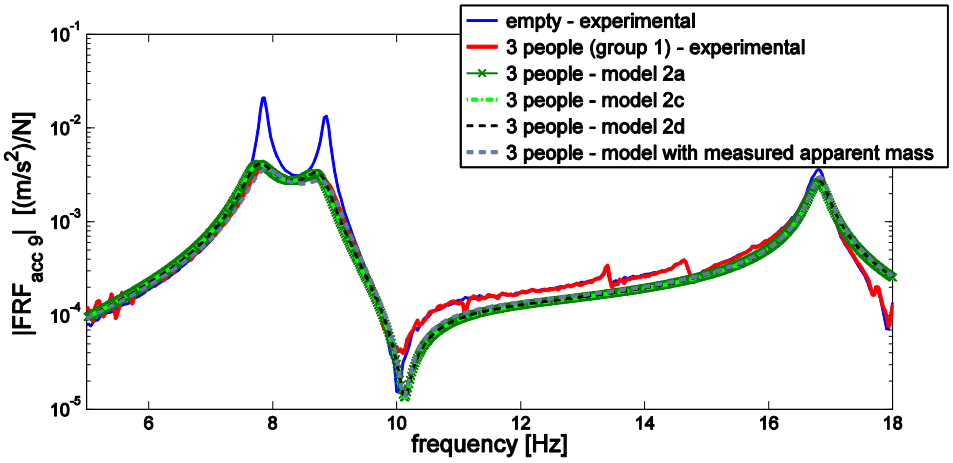

Figure 3.14: Experimental and predicted FRFs (3 people, group 1) using average apparent mass values and different models

The figure shows a comparison among the predicted FRFs using the measured apparent masses (the same as Figure 3.13) and those achieved by means of the optimised numerical apparent mass curves coming from three different models proposed by Matsumoto and Griffin (described in Section 3.2.2).

Figure 3.14 shows that the choice of the apparent mass model has little influence on the results. In addition, all the FRFs are in good agreement with the experimental ones and with that obtained by using measured apparent masses. Since the choice of the model has little influence on the result, 2a was used in the following as it is the model that best fits the measured apparent mass data, according to Matsumoto and Griffin.

In addition, the optimised coefficients for vibration amplitudes of 0.25 ms^{-2}, 0.5 ms^{-2}, 1.0 ms^{-2} and 2.0 ms^{-2} (Section 3.2.2) were also used . Indeed, the apparent mass depends on the amplitude of vibration which the subject is exposed to. As for actual applications, it is not possible to know a priori these amplitudes of vibration. Therefore, the effect of employing apparent masses yielded with different vibration amplitudes was investigated as well. Figure 3.15 shows the obtained results.

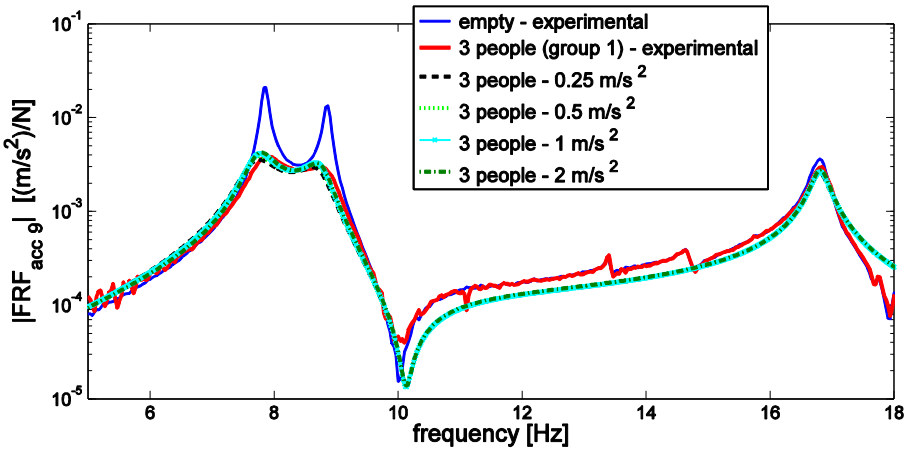

Figure 3.15: Experimental and predicted FRFs (3 people, group 1) using average apparent mass values obtained with different vibration amplitudes

The same results are also reported using a linear scale (Figure 3.16), which allows to better appreciate the difference between the different curves. The results are reported using both a logarithmic and linear scale as each of the two allows to appreciate different characteristics of the results.

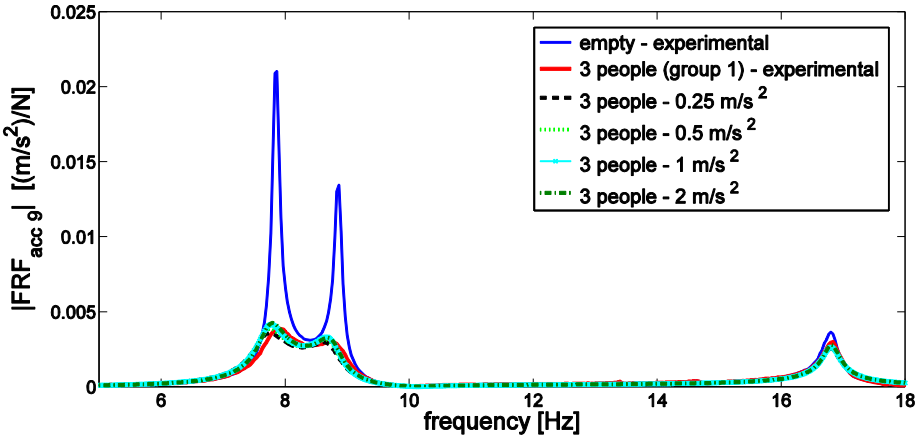

Figure 3.16: Experimental and predicted FRFs (3 people, group 1) using average apparent mass values obtained with different vibration amplitudes – linear scale

The difference among the FRFs in Figure 3.15 or Figure 3.16 is hardly noticeable and all the results are in good agreement with the experimental evidence. Such a result suggests that no strong assumptions are required on the amount of the vibration amplitudes of the structure in order to yield reliable information regarding the dynamic behaviour of the joint H-S system.

Table 3.6 reports the modal parameters identified using the FRFs computed using the apparent mass obtained with vibration amplitudes of 1.0 ms^{-2} (a high value if related to common civil applications) compared to the experimental results.

f_n [Hz], empty experimental	f_n [Hz], 3 people experimental	f_n [Hz], 3 people (Matsumoto and Griffin's apparent mass)	ζ [%], empty experimental	ζ [%], 3 people experimental	ζ [%], 3 people (Matsumoto and Griffin's apparent mass)
7.85	7.85	7.74	0.48	3.14	2.89
8.86	8.85	8.74	0.50	2.60	2.37
16.80	16.84	16.81	0.61	0.78	0.85

Table 3.6: Experimental and predicted modal parameters – tests with 3 people – measured vs average apparent masses

As might be expected, the obtained prediction of the modal parameters are less close to the experimental values than those obtained by using the experimental values of the apparent masses (Section 3.3.2). However, also in this case reliable predictions were obtained. Again, this result proves the effectiveness and robustness of the proposed approach.

The effect of a higher number of people on the structure was also investigated. Figure 3.17 and Figure 3.18 show the comparison between the experimental and predicted FRFs for two other tests, in the presence of 6 and 9 people on the structure respectively.

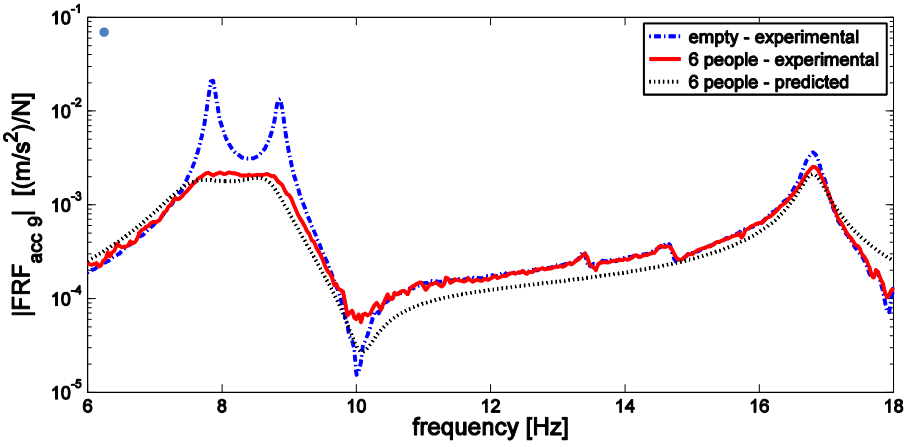

Figure 3.17: Experimental and predicted FRFs – 6 people

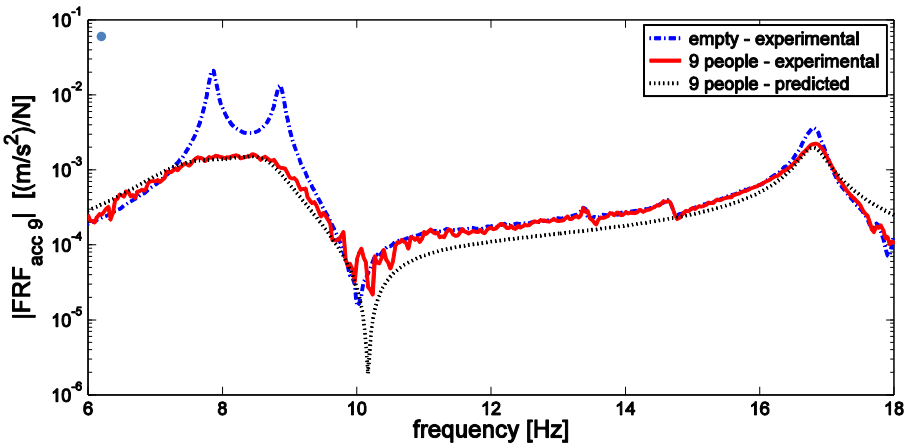

Figure 3.18: Experimental and predicted FRFs – 9 people

Table 3.7 and Table 3.8 show the comparison between experimental and predicted modal parameters (obtained using the average apparent mass values, model 2a, 1 ms^{-2} rms). The experimental results show a high increase of the damping ratios of the first two modes and a small decrease of the natural frequencies. The third mode is little influenced by people's presence.

f_n [Hz], empty experimental	f_n [Hz], 6 people experimental	f_n [Hz], 6 people (Matsumoto and Griffin's apparent mass)	ζ [%], empty experimental	ζ [%], 6 people experimental	ζ [%], 6 people (Matsumoto and Griffin's apparent mass)
7.85	7.76	7.57	0.48	5.31	6.21
8.86	8.81	8.68	0.50	3.60	3.50
16.80	16.85	16.80	0.61	0.91	1.05

Table 3.7: Experimental and predicted modal parameters – tests with 6 people

f_n [Hz], empty experimental	f_n [Hz], 9 people experimental	f_n [Hz], 9 people (Matsumoto and Griffin's apparent mass)	ζ [%], empty experimental	ζ [%], 9 people experimental	ζ [%], 9 people (Matsumoto and Griffin's apparent mass)
7.85	7.67	7.46	0.48	7.83	8.93
8.86	8.78	8.64	0.50	5.22	4.42
16.80	16.89	16.80	0.61	0.99	1.11

Table 3.8: Experimental and predicted modal parameters – tests with 9 people

Also in this case the modal parameters predicted with the H-S model are in good agreement with the experimental values. Particularly, the predicted damping ratios of all the three modes are well predicted and the differences between the foreseen and experimental values are very small compared to those of the empty structure in all cases. Therefore, the model proposed to describe the dynamics of H-S systems is able to predict changes of modal parameters due to people's presence, even employing the average analytical apparent masses determined by Matsumoto and Griffin.

3.4 Test case 2: Campus Bicocca Staircase

The second considered case study is another slender staircase (Figure 3.19) connecting the ground and the basement floors in the building U2 of the Università degli studi Milano-Bicocca. This second structure was used in order to provide a further confirmation of the effectiveness of the proposed approach.

Figure 3.19: Staircase – Campus Bicocca

This section describes the experiments carried out on the staircase and the corresponding results in terms of FRFs and modal parameters.

The first step was a modal characterisation of the structure with and without people. Therefore, the structure was instrumented with 24 accelerometers measuring in the vertical direction and forced by accelerating a known mass with an electro-dynamic shaker. Figure 3.20 shows the position of the accelerometers and of the shaker.

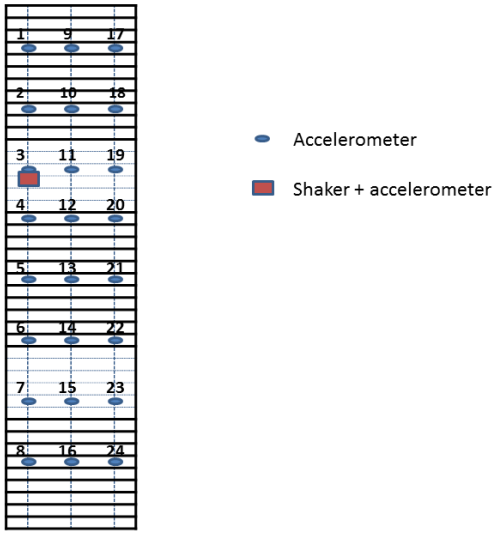

Figure 3.20: Staircase – Campus Bicocca – Experimental setup

The preliminary tests showed that the first natural frequency of the structure is approximately at 6.7 Hz. Therefore, the structure was forced with band-limited random noise between 4 and 20 Hz.

First, some experimental tests on the empty structure were performed in order to extract its modal properties. Then, additional tests with respectively 3, 5 and 10 people standing in different points of the structure were carried out. In all the cases, the structure was forced to determine the corresponding FRFs with the shaker.

Figure 3.10 shows an example of experimental FRFs for:

- the empty structure;
- the structure with 3 people placed in correspondence of the accelerometers 5,20,22;
- the structure with 5 people placed in correspondence of the accelerometers 5,9,11,20,22;
- the structure with 10 people placed in correspondence of the accelerometers 5,6,7,9,10,13,14,16,20,23.

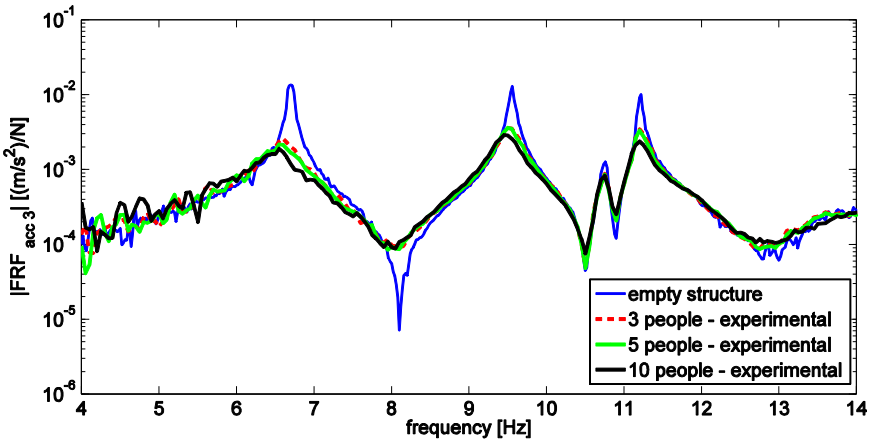

Figure 3.21: Experimental FRFs – Campus Bicocca

Table 3.9 shows the modal properties (i.e. eigenfrequencies f_n and non-dimensional damping ratios ζ) associated to these configurations, identified through the Polyreference Least Square Frequency Domain method [111].

empty		3 people		5 people		10 people	
f_n [Hz]	ζ [%]	f_n [Hz]	ζ [%]	f_n [Hz]	ζ [%]	f_n [Hz]	ζ [%]
6.70	0.33	6.61	2.40	6.57	2.97	6.53	3.68
9.55	0.28	9.55	1.11	9.52	1.14	9.48	1.41
10.75	0.29	10.75	0.44	10.75	0.44	10.74	0.56
11.21	0.17	11.21	0.62	11.20	0.66	11.20	0.83

Table 3.9: Experimental modal parameters – Campus Bicocca staircase

Figure 3.22, Figure 3.23, Figure 3.24 and Figure 3.25 show the mode shapes associated to the modes reported in Table 3.9. The figures were obtained by interpolating the mode shapes, though also in this case in the analysis the experimental values were used. The experimental mode shapes of the empty structure and of the structure plus passive people are reported in Annex A, Table A.2-A.5.

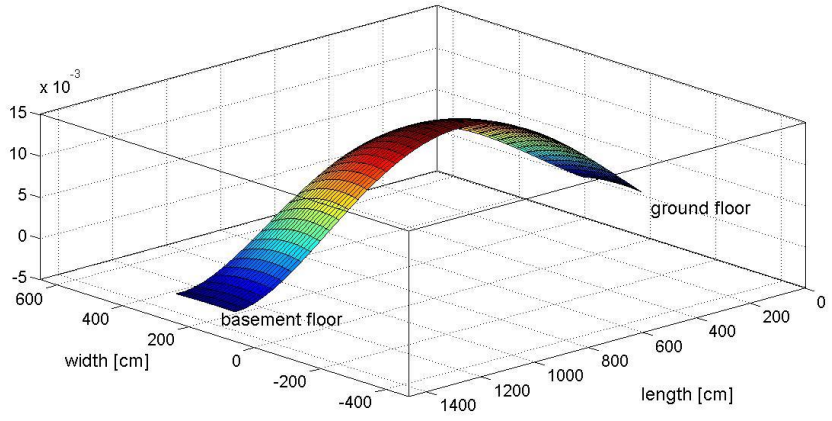

Figure 3.22: Campus Bicocca Staircase – mode shape – mode 1 (6.70 Hz)

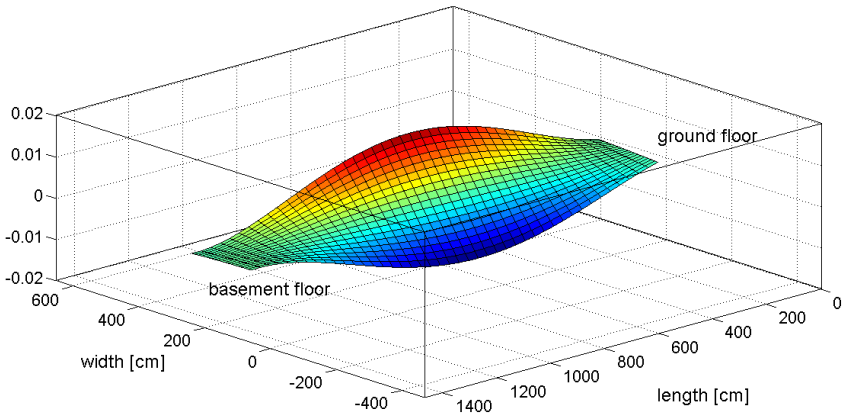

Figure 3.23: Campus Bicocca Staircase – mode shape – mode 2 (9.55 Hz)

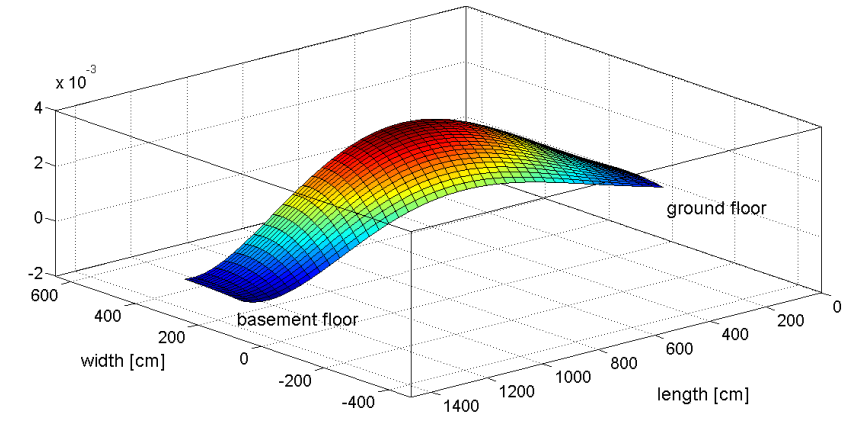

Figure 3.24: Campus Bicocca Staircase – mode shape – mode 3 (10.75 Hz)

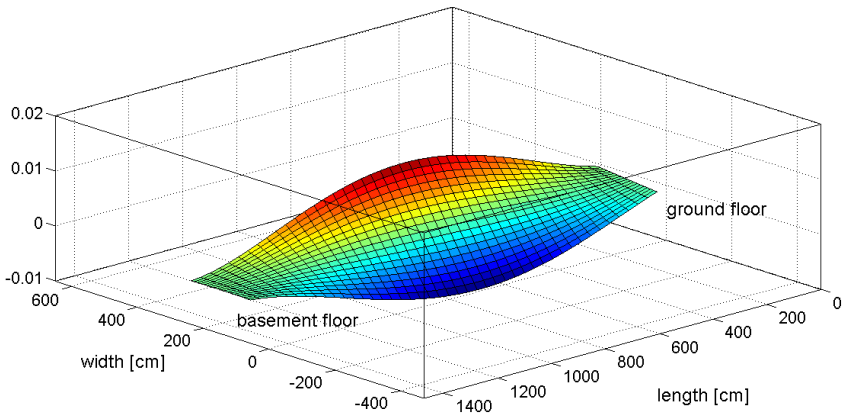

Figure 3.25: Campus Bicocca Staircase – mode shape – mode 4 (11.21 Hz)

The vibration modes reported in Table 3.9 are those having an appreciable amplitude in the range of frequencies of interest for the structure taken into consideration (i.e. the frequency range where the effect of passive people is considerable). These modes were used to reconstruct the FRFs of the empty structure and perform the subsequent analysis. It is possible to notice that also in this case people cause an increase of damping ratios and a decrease of natural frequencies. The modal parameters variation is higher for the first mode and lower for the mode having the smallest amplitude (third mode).

The model presented in Section 3.1 was used to predict the behaviour of the structure occupied by people. The results were compared to those obtained

experimentally. The next subsections present the results of the tests with 3, 5 and 10 people respectively. In this case only average apparent mass values were used.

3.4.1 Test with 3 people

Figure 3.26 shows a comparison between experimental and predicted FRFs for the test with 3 people. Predictions were performed using the 2DOF lumped parameters model of the apparent mass named 2a ([51], Figure 2.1 in Chapter 1) and for 2 rms vibration amplitudes (0.25 ms^{-2} and 1.0 ms^{-2}). The same results are also reported using a linear scale in Figure 3.27.

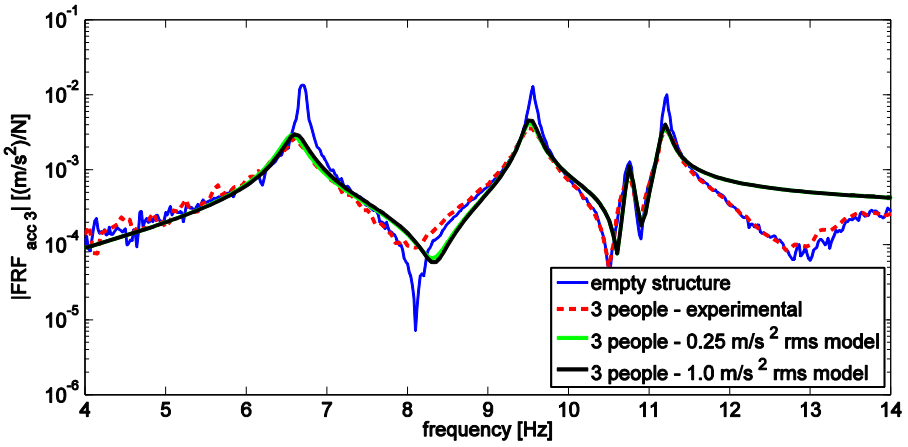

Figure 3.26: Experimental and predicted FRFs (3 people) – Campus Bicocca staircase

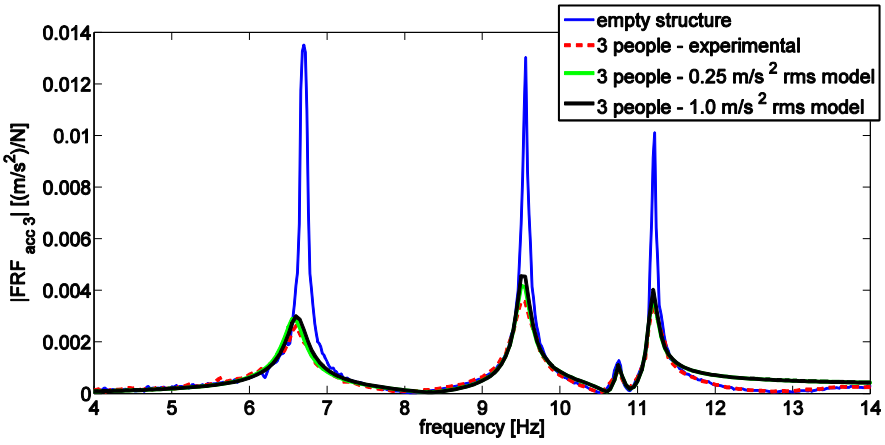

Figure 3.27: Experimental and predicted FRFs (3 people) – Campus Bicocca staircase – linear scale

The associated modal parameters are reported in Table 3.10.

empty		3 people - experimental		3 people – average mass (0.25 ms^{-2})		3 people – average mass (1.0 ms^{-2})	
f_n [Hz]	ζ [%]	f_n [Hz]	ζ [%]	f_n [Hz]	ζ [%]	f_n [Hz]	ζ [%]
6.70	0.33	6.61	2.40	5.57	2.02	6.61	1.99
9.55	0.28	9.55	1.11	9.52	0.94	9.52	0.84
10.75	0.29	10.75	0.44	10.75	0.33	10.75	0.33
11.21	0.17	11.21	0.62	11.19	0.52	11.19	0.49

Table 3.10: Experimental and predicted modal parameters – test with 3 people – Campus Bicocca Staircase

The predicted modal parameters little underestimate the experimental results. However, in this case too, results show that there is a general good agreement between experiments and predictions. Indeed, the predicted damping ratios of the 3rd and 4th mode (second last and last line) confirm the small variation of such a parameter. Conversely, the predicted damping ratios of the 1st and 2nd mode are very close to the experimental values. Furthermore, the choice of the model has a small influence on the results.

3.4.2 Test with 5 people

Figure 3.28 shows a comparison between predicted and measured FRFs for the test with 5 people. Table 3.11 shows the associated modal parameters.

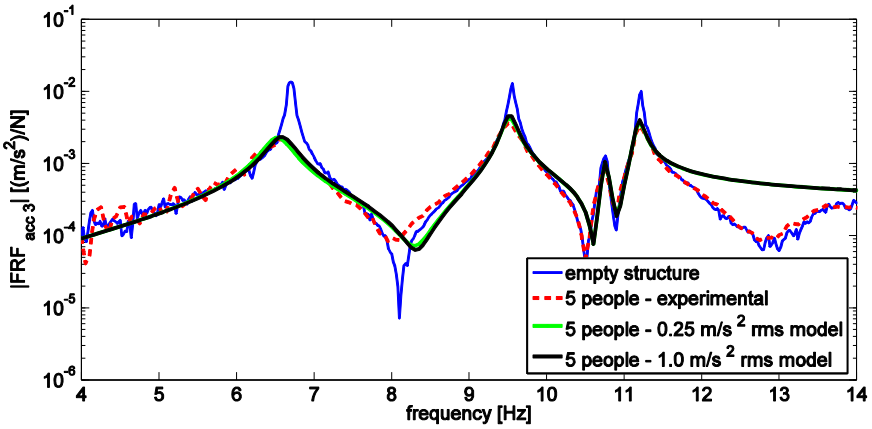

Figure 3.28: Experimental and predicted FRFs (5 people) – Campus Bicocca staircase

empty		5 people - experimental		5 people – average mass (0.25 ms^{-2})		5 people – average mass (1.0 ms^{-2})	
f_n [Hz]	ζ [%]	f_n [Hz]	ζ [%]	f_n [Hz]	ζ [%]	f_n [Hz]	ζ [%]
6.70	0.33	6.57	2.97	6.53	2.59	6.58	2.58
9.55	0.28	9.52	1.14	9.52	0.94	9.52	0.85
10.75	0.29	10.75	0.44	10.75	0.35	10.75	0.34
11.21	0.17	11.20	0.66	11.19	0.52	11.19	0.50

Table 3.11: Experimental and predicted modal parameters – test with 5 people – Campus Bicocca Staircase

The introduction of two additional subjects has a small influence on the modal parameters of the first mode and a negligible influence on the modal parameters of the other modes. The following section reports the results of tests with double the individuals on the staircase.

3.4.3 Test with 10 people

Figure 3.29 show a comparison between predicted and measured FRFs for the test with 10 people and Table 3.12 shows the associated modal parameters.

Also in this case, despite the use of average models of the apparent mass, predictions are in good agreement with the experimental values. Indeed, the FRF is well predicted by using the proposed approach. Results confirm that the rms of the acceleration used to estimate the apparent mass (0.25 ms^{-2} or 1.0 ms^{-1}) has a small impact on the results.

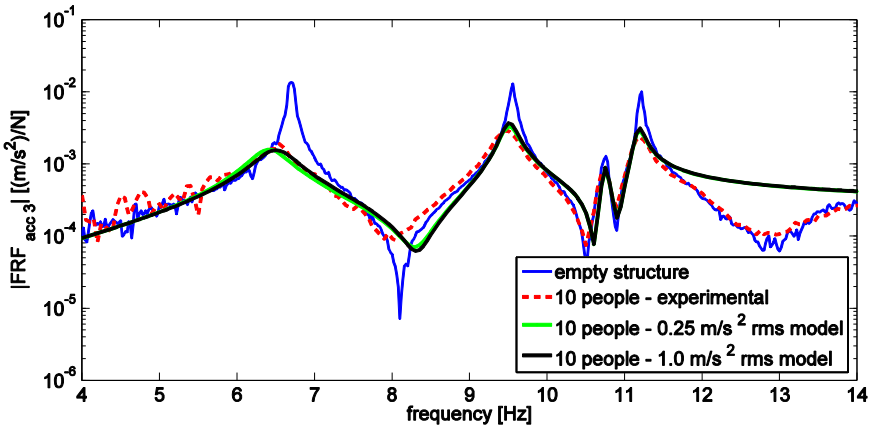

Figure 3.29: Experimental and predicted FRFs (10 people) – Campus Bicocca staircase

empty		10 people - experimental		10 people – average mass (0.25 ms^{-2})		10 people – average mass (1.0 ms^{-2})	
f_n [Hz]	ζ [%]	f_n [Hz]	ζ [%]	f_n [Hz]	ζ [%]	f_n [Hz]	ζ [%]
6.70	0.33	6.53	3.68	6.41	3.88	6.50	4.01
9.55	0.28	9.48	1.41	9.51	1.18	9.51	1.05
10.75	0.29	10.74	0.56	10.74	0.41	10.74	0.40
11.21	0.17	11.20	0.83	11.18	0.64	11.18	0.60

Table 3.12: Experimental and predicted modal parameters – test with 10 people – Campus Bicocca Staircase

The results of the tests performed on the campus Bicocca staircase confirmed the results obtained in the previous case. For the two considered structures, passive people's presence causes small changes in the natural frequencies and a high increase of the damping ratios. In all the considered cases a reliable prediction of modal parameters was obtained by using the H-S model proposed in Section 3.1.

3.5 Test case 3: verification of Sachse's results

In order to obtain a further verification of the model proposed in Section 3.1, the extensive research by Sachse [14] was also employed.

The structure tested by Sachse is a prestressed concrete slab of about 15000 kg, 2 m wide and spanned 10.8 m between a pair of 'knife-edges' near its ends. The structure was instrumented with 9 accelerometers and forced with an electro-mechanical shaker in order to measure its FRFs. In her work the author identified the dynamic properties of the empty structure by performing several tests. Table 3.13 reports the indicative values of such parameters, while Figure 3.30 reports the associated mode shapes.

empty		
f_n [Hz]	ζ [%]	Modal mass [kg]
4.54	0.32	7040
16.93	0.35	7370

Table 3.13: Modal parameters of the concrete slab

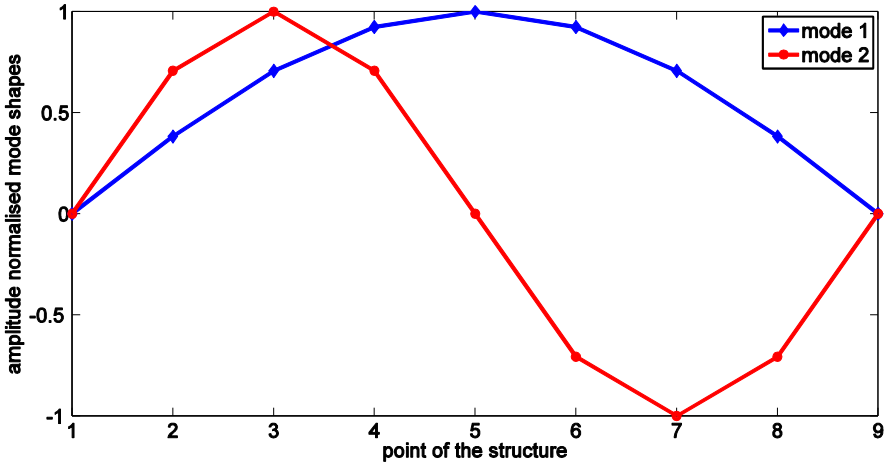

Figure 3.30: Mode shapes of the concrete slab

Using this structure Sachse performed many tests introducing one or more subjects on the structure and measuring the experimental FRFs of the joint H-S system. The results of some of these tests are compared with those obtained with the H-S model proposed in Section 3.1 and the apparent masses described in Section 3.2.2 (model 2a, 1.0 ms^{-2} rms) and 3.2.3.

Table 3.14 summarises the tests proposed by Sachse that are used in this work.

Case #	Configurations	Sachse's test #
1	1 Test Subject (TS) sitting at Test Point (TP) 5	21-25,36-45
2	1 TS sitting at TP 7	26-30
3	1 TS sitting at TP 9	31-35
4	1 TS standing at TP 5	48-52,63-72
5	1 TS standing at TP 7	53-57
6	1 TS standing at TP 9	58-62
7	2 TSs sitting at TP 5	116-120
8	3 TSs sitting at TP 5	96-100
9	4 TSs sitting at TP 5	101-105
10	5 TSs sitting at TP 5	123-127
11	2 TSs sitting at TP 3 and 3 TSs sitting at TP 7	128-132

Table 3.14: Sachse's tests

Table 3.15 and Table 3.16 compare the experimental results (average values) obtained by Sachse (natural frequencies and damping ratios) with those obtained with the approach proposed in Section 3.

Case #	f_n [Hz] experimental	f_n [Hz] predicted	ζ [%] experimental	ζ [%] predicted
1	4.49	4.52	0.51	0.67
2	4.52	4.53	0.43	0.50
3	4.52	4.54	0.35	0.32
4	4.50	4.51	0.50	0.51
5	4.51	4.53	0.42	0.42
6	4.52	4.54	0.34	0.32
7	4.43	4.46	0.74	1.00
8	4.41	4.44	0.88	1.32
9	4.38	4.41	1.32	1.63
10	4.34	4.39	1.69	1.92
11	4.42	4.45	1.20	1.17

Table 3.15: Experimental and predicted modal parameters – mode 1

Case #	f_n [Hz] experimental	f_n [Hz] predicted	ζ [%] experimental	ζ [%] predicted
1	16.95	16.93	0.35	0.35
2	16.94	16.93	0.47	0.46
3	16.96	16.93	0.35	0.35
4	16.95	16.93	0.34	0.35
5	16.96	16.93	0.56	0.59
6	16.95	16.93	0.34	0.35
7	16.95	16.93	0.36	0.35
8	16.95	16.93	0.36	0.35
9	16.95	16.93	0.38	0.35
10	16.94	16.93	0.41	0.35
11	16.98	16.94	1.40	0.90

Table 3.16: Experimental and predicted modal parameters – mode 2

Results show a general agreement between the experimental results and the obtained predictions. In addition, possible differences could be due to the following approximations:

- not exact correspondence between the nominal and the actual contact point, especially for the tests with more than 1 subject (Table 3.13Table 3.14, tests 7-11). Indeed, the assumption of having more than 1 subject located at the same point necessary introduces approximations in the results;
- intra-subject variability (average models were used to simulate people's presence).

Nevertheless it is possible to observe that also in this case the model proposed in Section 3.1 is able to predict well the general trend of changes of modal parameters.

3.6 Summary

This chapter proposed a model to estimate the effects of passive people on the modal parameters of a generic structure. The method only requires the knowledge of the modal parameters of the empty structure as an input. Each subject is then added locally on the structure by means of his/her apparent mass. With respect to other methods currently available in literature, the proposed approach places no constraints on the number of structural degrees of freedom taken into consideration. In addition, the proposed method considers the effect produced on the structure by each subject locally. Therefore, such a procedure allows a reliable quantification of people's effect.

Two slender staircases and data available in literature were used to validate this approach. Initially, in order to simulate the dynamics of the joint H-S system people were included in the modal model of the empty structure using their measured apparent mass to verify the method. In this case, the results obtained were very close to the experimental data. This proved the effectiveness of the proposed approach. Then, people's presence was simulated by employing average values of the apparent mass found in literature in order to extend the results to real-life applications. Satisfactory results were obtained also in this case in terms of identification of changes of modal parameters due to people's presence.

Chapter 4

H-S model - moving people

Model validation

Chapter 3 proposed an approach to evaluate the influence of passive people on the dynamic behaviour of a structure. This Chapter investigates the possibility to extend this approach to the case of moving people. The idea behind such an extension is the identification of an equivalent model to represent the dynamic behaviour of the joint structure-moving people system. An appropriate active force is then applied to this equivalent model in order to get a prediction of vibration levels.

The method was first tested under controlled conditions using two slender structures as test cases.

4.1 An approach to evaluate structural responses due to people's presence

Chapter 3 proposed a model to evaluate the effect of passive people on the dynamic behaviour of a slender structure. This Chapter proposes an extension of such a method to the case of moving people.

To this purpose the effect of moving subjects is decoupled in two contributions, i.e. (passive) Ground Reaction Forces (GRFs) and active forces (Figure 4.1).

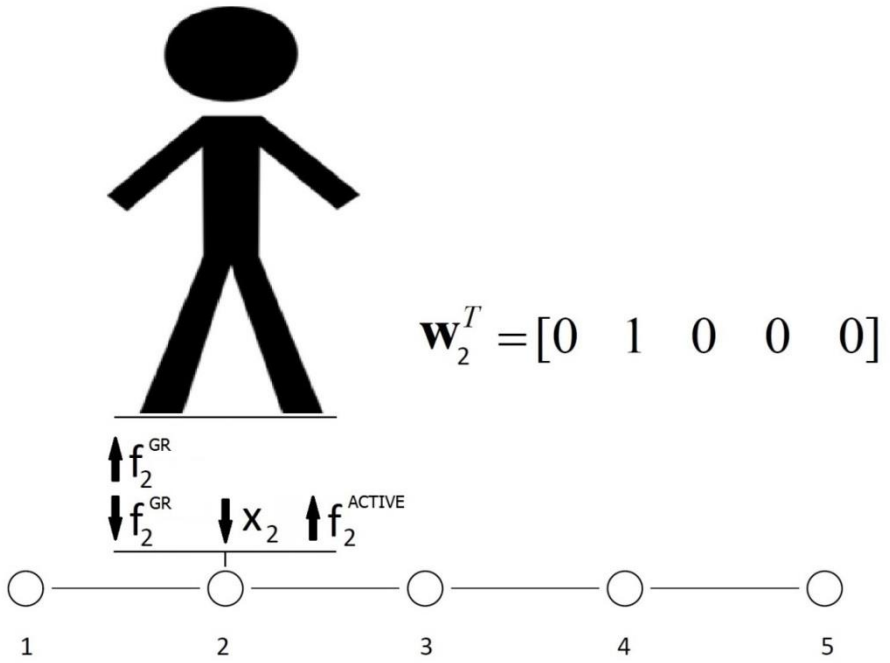

Figure 4.1: Connection of a moving subject to the structure

Under this hypothesis, Eq. (3.2) can be rewritten in the form:

$$\mathbf{x}(\omega) = \mathbf{G}(\omega)(\mathbf{f}^{\mathrm{ACTIVE}}(\omega) - \mathbf{f}^{\mathrm{GR}}(\omega)) \tag{4.1}$$

Combining Eq. (3.5) and Eq. (4.1), Eq. (4.2) is obtained

$$[\mathbf{G}^{-1}(\omega) + \mathbf{W}\mathbf{H}(\omega)\mathbf{W}^{\mathrm{T}}]\mathbf{x}(\omega) = \mathbf{G}_{\mathrm{H}}^{-1}(\omega)\mathbf{x}(\omega) = \mathbf{f}^{\mathrm{ACTIVE}}(\omega) \tag{4.2}$$

In Eq. (4.2) the modified matrix of FRFs $\mathbf{G_H}(\omega)$ includes the GRFs while the vector $\mathbf{f}^{\mathrm{ACTIVE}}(\omega)$ includes all the active forces exerted by people on the structure.

Therefore, the problem is decoupled in two main tasks, i.e. the identification of passive GRFs of moving people and active forces respectively.

In summary, the steps to obtain an estimation of the structural response of a structure due to people presence are:

I. Find an equivalent transfer function $\mathbf{G}_{\mathrm{H}}(\omega)$ to represent the dynamic behaviour of the joint structure-moving people system

II. Identify the active forces induced by people on the structure

III. Apply the active load (Eq. (4.2)) to estimate the structural response

Opposite to passive people, GRFs of moving people significantly change in time. The proposed approach assumes average GRFs can be used to identify a single matrix of FRFs $\mathbf{G}_{\mathrm{H}}(\omega)$. This seems to be a reasonable assumption as the number of people increases. Even though this is an approximate approach, it will be proved to provide results much more reliable than those achieved using the model of the empty structure to foresee structural vibrations. Nevertheless, a great effort is necessary to identify a correct equivalent model to represent the human behaviour during motion.

This Chapter proposes a validation of the approach outlined above. The focus is the verification of the appropriateness of the proposed approach, i.e. the separation of GRFs and active forces. To this purpose, tests with a subject walking on a dynamometric plate were performed. Such an approach allowed measuring the actual force exerted by the subject on the structure. The only unknown quantity was the equivalent model $\mathbf{G}_{\mathrm{H}}(\omega)$. In Chapter 5 the same approach will be used to evaluate the structural response of a slender staircase under operating conditions. In this case both the GRFs and the active forces are unknown.

The next section proposes a possible procedure to identify the equivalent GRF of a moving subject.

4.2 Equivalent model of a moving subject

As described in Section 4.1, there is need to identify an equivalent matrix of FRFs $\mathbf{G}_{\mathrm{H}}(\omega)$ in order to apply the proposed approach. $\mathbf{G}_{\mathrm{H}}(\omega)$ represents the dynamic behaviour of the joint structure-moving people system and accounts for the passive GRFs at the contact points. The active force $\mathbf{f}^{\mathrm{ACTIVE}}(\omega)$ is then applied on this equivalent set of FRFs in order to obtain the structural response.

In this section a general approach to estimate equivalent GRFs and an equivalent matrices of FRFs $\mathbf{G}_{\mathrm{H}}(\omega)$ is proposed. This approach is then applied to

the particular case of a subject walking on the spot in order to simulate the dynamics of a subject walking on the force plate.

As outlined in Chapter 3, the GRF can be expressed in terms of an apparent mass $M^*(\omega)$ (Eq. (3.3)). The apparent mass depends on many factors, such as: a) the particular subject (inter-subject variability); b) his posture; c) the amplitude of vibration. Papers related to the topic, such as [51] and [54], analysed such an influence. Particularly:

a) The posture is found to have a high influence on the apparent mass.

b) As for the inter-subject variability, the apparent mass depends on the characteristics of the particular subject. However, for practical applications it is reasonable to assume that the average behaviour of a high number of people is properly modelled using average values of apparent mass.

c) The vibration magnitude is found to have a smaller relevance, as proved also in Chapter 3 for the case of passive people.

Ultimately, for the purpose of this work, the parameter mostly affecting the apparent mass is the posture. As regards passive people, it is likely to assume the posture does not change in time. This assumption is definitely not true for the case of moving people. To deal with this case, a possible approach is proposed in this work. Its steps are outlined as follows:

I. Identify one cycle T (i.e. time elapsing between two touches on the ground of the same foot) of the particular motion.

II. Divide the cycle in an appropriate number (P) of positions. These positions must be representative of the overall behaviour during the motion.

III. Identify an apparent mass ${M_a}^*(\omega)$ for each position.

IV. Define an equivalent apparent mass as the weighted average of the apparent masses:

$$ {M_{eq}}^*(\omega) = \sum_{a=1}^{P} \alpha_a {M_a}^*(\omega) \tag{4.3} $$

The so determined equivalent apparent mass is used to define the equivalent GRF, as in Eq. (5.1), and then the equivalent matrix of FRFs $\mathbf{G}_H(\omega)$ (Eq. (4.2)).

Considering the case of a subject walking on the spot, experimental tests were performed to obtain information on the posture of some subjects performing this action. The motion was divided in three postures (P=3), i.e. standing, one leg (left) and one leg (right).

The equivalent apparent mass is obtained as in Eq. (4.4).

$$M_{\mathrm{eq}}{}^{*}(\omega) = \alpha_1 M^{*}{}_{(\mathrm{standing})} + \alpha_2 M^{*}{}_{(\mathrm{one\ leg-left})} + \alpha_3 M^{*}{}_{(\mathrm{one\ leg-right})} \quad (4.4)$$

with

$$\sum_{a=1}^{P} \alpha_a = 1 \quad (4.5)$$

During 1 cycle each subject was seen to stand on two legs for a time from 0.05·T to 0.15·T and on one leg (left or right) for the remaining time. The coefficients $\alpha_{\mathbf{a}}$ were varied accordingly in order to investigate their influence on the results.

For the apparent masses in standing and on one leg postures, both experimental measurements on some subjects involved in the tests and values available from the literature were used. In particular the work of Mastumoto and Griffin [51], proposing mathematical models to represent the dynamic behaviour of subjects exposed to vertical vibrations, was employed. The results obtained using both experimental measurements of the apparent mass and values available in literature are discussed in the next sections.

4.3 Test case 1: Campus Bovisa Staircase

The first considered test case structure is the staircase described in Chapter 3, Section 3.3. The next Section describes the experimental setup and the performed tests.

4.3.1 Experimental setup and tests

The experimental setup used to perform the tests reported in this section consisted of 23 accelerometers, an electro-mechanical shaker used to force the structure and a dynamometric plate used to measure the force exerted by a single walking subject. Figure 4.2 shows the experimental setup.

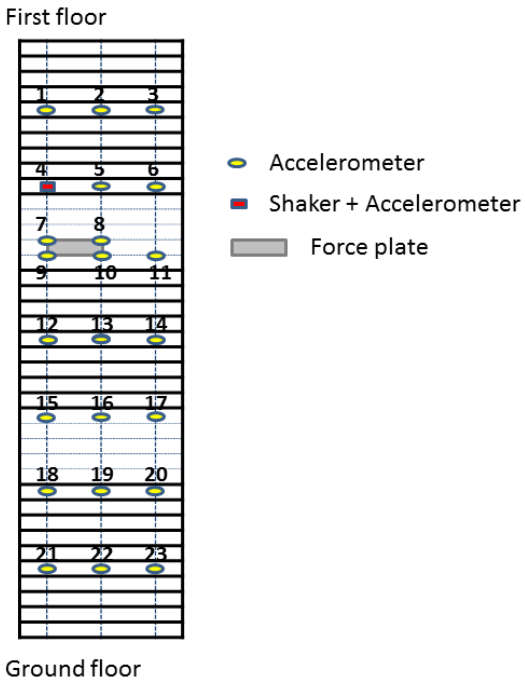

Figure 4.2: Experimental setup – Campus Bovisa Staircase – one moving subject

The considered structure has two dominant modes around 8 and 9 Hz (Chapter 3). Since the third dominant mode is around 17 Hz and such frequency is not likely to be forced by human walk, only the first two modes were considered in this Chapter.

Since the tests discussed in this Section were performed at a different time of the year with respect to the tests reported in Chapter 3, a new modal characterization of the empty structure was performed. Table 4.1 shows the identified modal parameters. Results show that the modal parameters slightly change with respect to those reported in Chapter 3 (Table 3.4).

f_n [Hz]	ζ [%]
7.84	0.33
8.89	0.43

Table 4.1: Modal parameters of the empty structure – Campus Bovisa Staircase

All the tests reported in this Section involved two subjects per test. In all cases one subject was asked to walk on the dynamometric plate (positioned as sho wn in Figure 4.2). The second subject was asked to stand (passive) on different points of

the structure while the active subject was walking. Each subject was asked to walk on a spot: 1) freely; 2) at a frequency as close as possible to a submultiple of the first natural frequency of the structure; 3) at a frequency as close as possible to a submultiple of the second natural frequency of the structure. The layout of the tests is reported in Table 4.2. Tests 1 to 6 differ from tests 7 to 12 because different subjects were involved in the experiments (named Test Subject (TS) 1 and 2).

Test #	Walk frequency	Passive subject's location (Figure 4.2)
1	Free – TS1	13 – TS2
2	1.96 Hz – TS1	13 – TS2
3	2.20 Hz – TS1	13 – TS2
4	Free – TS1	11 – TS2
5	1.96 Hz – TS1	11 – TS2
6	2.20 Hz – TS1	11 – TS2
7	Free – TS2	13 – TS1
8	1.96 Hz – TS2	13 – TS1
9	2.20 Hz – TS2	13 – TS1
10	Free – TS2	11 – TS1
11	1.96 Hz – TS2	11 – TS1
12	2.20 Hz – TS2	11 – TS1

Table 4.2: Tests layout – Bovisa staircase – one moving subject

The results of the tests were used to validate the proposed approach. The next section reports the comparison between experimental measurements and results predicted using the proposed approach.

4.3.2 Experimental results and model validation

This section reports the results of the experimental tests summarized in Table 4.2 compared to those obtained by means of simulations.

The proposed approach was used to determine the equivalent transfer function $\mathbf{G}_{\mathrm{H}}(\omega)$ of the joint H-S system. The measured force was used to simulate the structural response and the results were compared to the measured accelerations. To simulate the structural response both the FRFs of the empty structure and the predicted FRFs of the joint H-S system were used.

Subsection 4.3.2.1 reports the modal parameters of the FRFs of the joint H-S system. Subsections 4.3.2.2 and 4.3.2.3 propose a comparison between experimental and predicted results.

4.3.2.1 Equivalent matrix $G_H(\omega)$

The determination of the equivalent matrix of FRFs $\mathbf{G_H}(\omega)$ requires the definition of:

I. The apparent mass of the passive subject (standing posture)
II. The apparent masses of the moving subject (standing posture and one leg left-right posture)
III. The coefficients α_1, α_2, α_3 (Eq. (4.4))

The apparent mass in standing and one leg postures was defined using:

a) Average values proposed in [51]. Particularly, also in this case the model named 2a was used. The normalized apparent masses proposed in [51] were multiplied by the real mass of the considered subjects.
b) Measurements performed to determine the actual apparent mass of the subjects involved in the tests. The experimental setup described in Section 3.2.1 was used and the experimental apparent mass was determined as in [51].

Figure 4.3 shows, as an example, the average normalized apparent masses proposed in [51] (model 2a and 1.0 ms^{-2} rms) for subjects in standing and one leg posture.

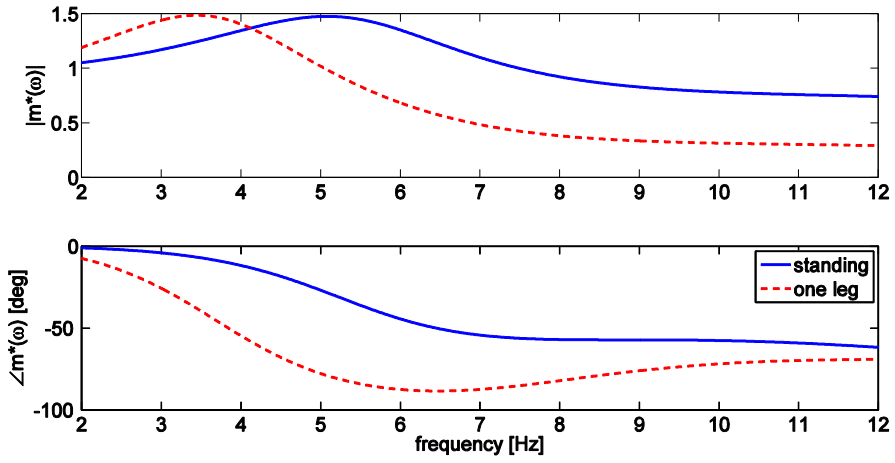

Figure 4.3: Normalized apparent masses (from [51])– standing and one leg posture – model 2a – 1,0 ms^{-2} rms

The coefficients α_1, α_2, α_3 were varied to investigate their influence on the results. Accordingly to the experimental evidence, three cases were considered, i.e. 1) $\alpha_1 = 0$, $\alpha_2 = \alpha_3 = 0.5$; 2) $\alpha_1 = 0.1$, $\alpha_2 = \alpha_3 = 0.45$; 3) $\alpha_1 = 0.2$, $\alpha_2 = \alpha_3 = 0.4$.

Figure 4.4 reports an example of equivalent apparent masses of an 80 kg subject obtained using the average values proposed in [51].

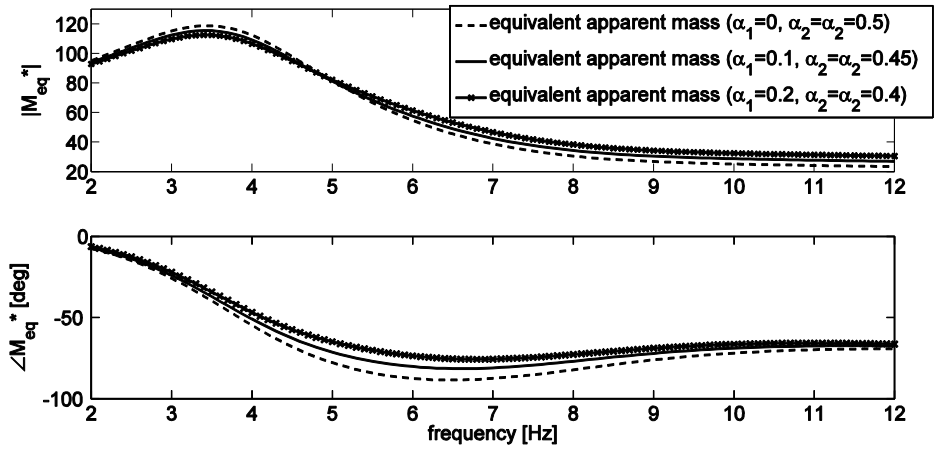

Figure 4.4: Equivalent apparent masses – one moving subject

The above-described apparent mass curves were used to simulate the dynamics of the joint H-S system. Table 4.4, Table 4.5 and Table 4.6 report a summary of the modal parameters associated to the FRFs $\mathbf{G_H}(\omega)$. These FRFs were obtained combining all the possible cases outlined above.

	f_1 [Hz]					
	$\alpha_1 = 0$, $\alpha_2 = \alpha_3 = 0.5$		$\alpha_1 = 0.1$, $\alpha_2 = \alpha_3 = 0.45$		$\alpha_1 = 0.2$ $\alpha_2 = \alpha_3 = 0.4$	
Test #	M_{eq} with measured apparent masses	M_{eq} with model 2a apparent masses	M_{eq} with measured apparent masses	M_{eq} with model 2a apparent masses	M_{eq} with measured apparent masses	M_{eq} with model 2a apparent masses
1,2,3	7.86	7.82	7.86	7.82	7.86	7.81
4,5,6	7.89	7.77	7.89	7.77	7.89	7.76
7,8,9	7.86	7.82	7.86	7.82	7.86	7.81
10,11,12	7.87	7.76	7.87	7.75	7.87	7.75

Table 4.3: Equivalent $G_H(\omega)$ – one moving subject: f_1

	ζ_1 [%]					
	$\alpha_1 = 0, \alpha_2 = \alpha_3 = 0.5$		$\alpha_1 = 0.1, \alpha_2 = \alpha_3 = 0.45$		$\alpha_1 = 0.2\ \alpha_2 = \alpha_3 = 0.4$	
Test #	M_{eq} with measured apparent masses	M_{eq} with model 2a apparent masses	M_{eq} with measured apparent masses	M_{eq} with model 2a apparent masses	M_{eq} with measured apparent masses	M_{eq} with model 2a apparent masses
1,2,3	1.50	1.30	1.58	1.36	1.65	1.41
4,5,6	3.02	2.29	3.10	2.34	3.17	2.38
7,8,9	1.25	1.31	1.35	1.35	1.46	1.40
10,11,12	2.62	2.55	2.72	2.59	2.83	2.63

Table 4.4: Equivalent $G_H(\omega)$ – one moving subject: ζ_1

	f_2 [Hz]					
	$\alpha_1 = 0, \alpha_2 = \alpha_3 = 0.5$		$\alpha_1 = 0.1, \alpha_2 = \alpha_3 = 0.45$		$\alpha_1 = 0.2\ \alpha_2 = \alpha_3 = 0.4$	
Test #	M_{eq} with measured apparent masses	M_{eq} with model 2a apparent masses	M_{eq} with measured apparent masses	M_{eq} with model 2a apparent masses	M_{eq} with measured apparent masses	M_{eq} with model 2a apparent masses
1,2,3	8.88	8.87	8.88	8.86	8.88	8.86
4,5,6	8.89	8.85	8.89	8.84	8.89	8.84
7,8,9	8.88	8.87	8-88	8.87	8.88	8.86
10,11,12	8.87	8.84	8.88	8.84	8.88	8.84

Table 4.5: Equivalent $G_H(\omega)$ – one moving subject: f_2

	ζ_2 [%]					
	$\alpha_1 = 0, \alpha_2 = \alpha_3 = 0.5$		$\alpha_1 = 0.1, \alpha_2 = \alpha_3 = 0.45$		$\alpha_1 = 0.2\ \alpha_2 = \alpha_3 = 0.4$	
Test #	M_{eq} with measured apparent masses	M_{eq} with model 2a apparent masses	M_{eq} with measured apparent masses	M_{eq} with model 2a apparent masses	M_{eq} with measured apparent masses	M_{eq} with model 2a apparent masses
1,2,3	0.61	0.65	0.66	0.69	0.70	0.72
4,5,6	1.09	1.03	1.13	1.07	1.17	1.11
7,8,9	0.51	0.60	0.56	0.63	0.61	0.65
10,11,12	1.01	1.04	1.05	1.08	1.11	1.11

Table 4.6: Equivalent $G_H(\omega)$ – one moving subject: ζ_2

Results show that the two subjects can change the damping ratios of the structure significantly. Particularly, Table 4.4 and Table 4.6 show that the influence of people is higher for the first vibration mode. Conversely, the natural frequencies are slightly influenced by the presence of people. In addition, results

show how the influence of the same subject can differ according to the point where the subject is located. Indeed, the damping increases when the passive subject moves from point 13 (tests 1,2,3,7,8,9) to point 11 (tests 4,5,6,10,11,12) of the structure (Figure 4.2).

Furthermore, Table 4.3, Table 4.4, Table 4.5 and Table 4.6 show that the αi parameters have a negligible influence on the results. As an example, the damping ratio of the first mode (Table 4.4) for the tests with two subjects (second and fourth line of the table) changes of maximum 8%. Therefore, the values reported in the subsequent analysis refer to the case of $\alpha_1 = \mathbf{0.1}$, $\alpha_2 = \alpha_3 = \mathbf{0.45}$ which are the average values determined experimentally.

The modal parameters reported in Table 4.3, Table 4.4, Table 4.5 and Table 4.6 and the force measured with the force plate were used to simulate the structural response and the results were compared to the measured accelerations. The results were also compared with those obtained using the modal parameters of the empty structure to simulate the structural response. Results were compared in terms of Power Spectra and rms of the accelerations in the frequency band 0-15 Hz. The reported values refer to accelerometer 11 (Figure 4.2), i.e. the point of maximum response.

4.3.2.2 Experimental and predicted results – Power Spectra

The modal parameters of the empty structure and the modal parameters predicted using the model of the joint H-S systems were used to predict the structural response. The measured force was used to simulate the response and the results were compared with the experimental measurements. Figure 4.5 and Figure 4.6 show, for the case of test 4, accelerometer 11, a comparison between the power-spectrum of the measured acceleration and the power-spectrum of the acceleration predicted using the model of both the empty structure $\mathbf{G(\omega)}$ and of the subjects+structure $\mathbf{G_H(\omega)}$ respectively. Results reported in Figure 4.5 refer to the equivalent transfer function $\mathbf{G_H(\omega)}$ obtained with the measured apparent masses of the subjects involved in the tests, while results reported in Figure 4.6 refer to the transfer function obtained with the average values proposed in [51].

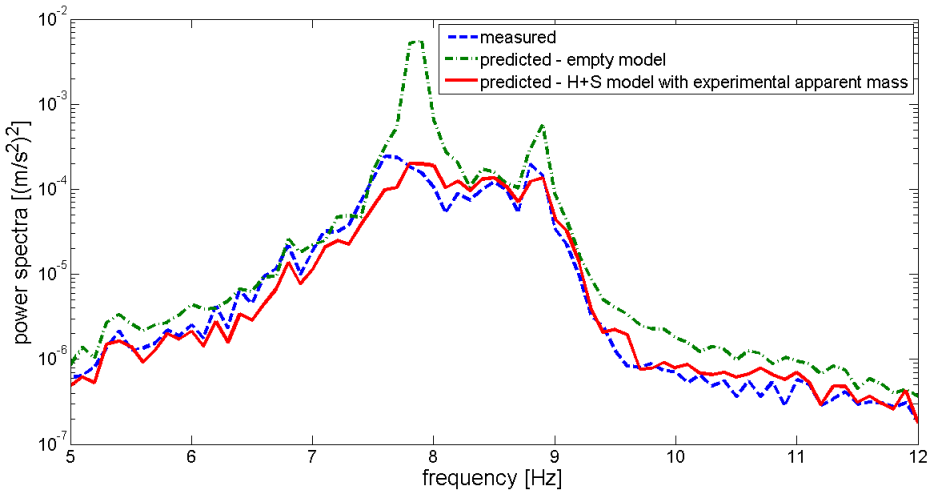

Figure 4.5: Test 4 – one moving subject – power spectra, accelerometer 11 – experimental apparent mass

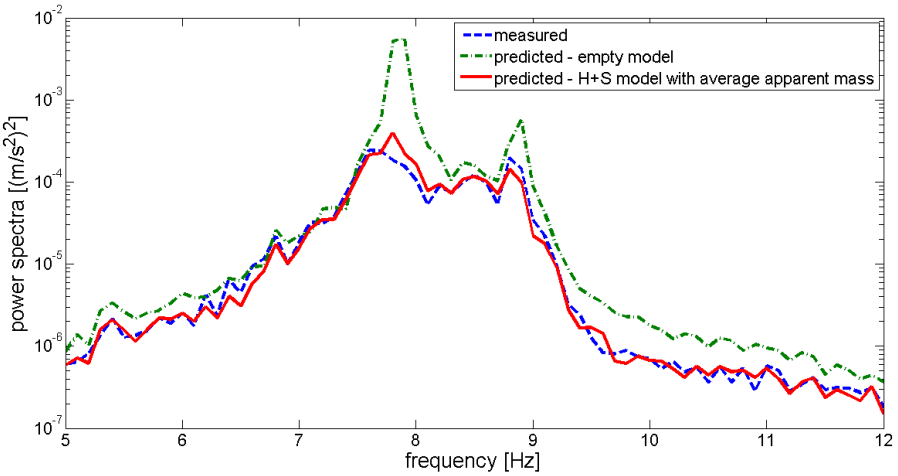

Figure 4.6: Test 4 – one moving subject – power spectra, accelerometer 11 – average apparent mass

Both figures clearly show how the use of the model of the empty structure to simulate the structural vibrations would lead to an overestimation of the amplitudes of vibration. Conversely, using the proposed approach the results are much closer to the experimental data in both cases.

4.3.2.3 Experimental and predicted results – rms

Table 4.7 reports a comparison of the results in terms of rms of the acceleration in the frequency band 0-15 Hz. The rms were predicted using both the FRFs of the

empty structure $\mathbf{G}(\boldsymbol{\omega})$ and of the H+S system $\mathbf{G_H}(\boldsymbol{\omega})$ with measured and average apparent masses. The corresponding relative errors estimated as in Eq. (4.6) and Eq. (4.7) are also reported. In Eq. (4.6) and Eq. (4.7) (rms empty) is the rms of the acceleration estimated using the FRFs of the empty structure, (rms H-S) is the rms of the acceleration estimated using the FRFs of Human+Structure system and (rms exp.) is the rms of the measured acceleration.

$$Error\ \%\ empty = \frac{(rms\ \ empty) - (rms\ exp.)}{(rms\ exp.)} \tag{4.6}$$

$$Error\ \%\ H-S = \frac{(rms\ H-S) - (rms\ exp.)}{(rms\ exp.)} \tag{4.7}$$

Test #	rms exp. [ms^{-2}]	rms $\mathbf{G}(\omega)$ [ms^{-2}]	rms $\mathbf{G_H}(\omega)$ [ms^{-2}] (meas. M^*)	rms $\mathbf{G_H}(\omega)$ [ms^{-2}] (av. M^*)	Error % empty	Error % H-S (meas. M^*)	Error % H-S (av. M^*)
1	0.067	0.101	0.066	0.067	51.5	-0.7	0.1
2	0.060	0.129	0.061	0.064	116.4	1.7	6.8
3	0.099	0.169	0.093	0.097	69.6	-6.3	-2.5
4	0.048	0.123	0.051	0.051	153.7	4.2	5.6
5	0.046	0.135	0.053	0.054	193.8	14.5	18.2
6	0.081	0.190	0.086	0.092	133.8	5.8	13.2
7	0.062	0.109	0.059	0.058	76.2	-4.2	-7.0
8	0.095	0.251	0.092	0.087	163.5	-3.6	-8.4
9	0.101	0.117	0.079	0.079	15.5	-21.6	-22.2
10	0.091	0.204	0.090	0.092	122.8	-1.0	0.6
11	0.049	0.182	0.053	0.050	272.5	9.0	1.8
12	0.056	0.103	0.054	0.053	84.6	-3.9	-4.5

Table 4.7: Rms and relative errors - α_1=0.1, α_2=α_3=0.45 – campus Bovisa staircase – one moving subject

Table 4.7 again highlights how the use the matrix of FRFs $\mathbf{G}(\omega)$ of the empty structure can lead to an overestimation of the results. The overestimation can be as high as 270% (Test #11). The error obtained using the model of the empty structure $\mathbf{G}(\omega)$ is higher for the tests with the passive subject located in point 11. Indeed, a subject located in point 11 introduces a higher damping than the same

subject located in point 13 (see Table 4.3, Table 4.4, Table 4.5 and Table 4.6). Furthermore the overestimation of the response is higher when the force has a dominant harmonic around 1.96 Hz, as people introduce more damping on the first mode of the structure. The use of the matrix of FRFs $\mathbf{G}_{\mathrm{H}}(\omega)$ leads to results that are much closer to the experimental values, with an exception for test #9. As for test #9, in this case the model fails in the prediction of the structural response. However, in this particular test the applied force was at a frequency of 2.20 Hz (second vibration mode) and the passive subject was located in point 13. In this case (Table 4.6) a small increase of damping of the second vibration mode is experienced and the approximations can play a significant role. Indeed, small errors on the prediction of the natural frequencies can result in a high error in the prediction of vibration levels in the case of a single subject and nearly harmonic force. As for tests 5 and 6, the prediction obtained with the H-S model slightly overestimates the experimental results. However, the overestimation is much lower than those obtained with the model of the empty structure. Still, a good prediction of the experimental results was mostly obtained using the proposed approach.

4.4 Test case 2: Campus Bicocca Staircase

The second considered test case structure is the staircase described in Chapter 3, Section 3.4. The next Section reports the experimental setup and the performed tests.

4.4.1 Experimental setup and tests

The experimental setup described in Section 3.4 was changed in order to introduce the dynamometric plate on the staircase. Furthermore, the position of the accelerometers numbered 11,12 and 20 was changed in order to measure the accelerations at the contact points between the dynamometric plate and the staircase. Figure 4.7 shows the experimental setup.

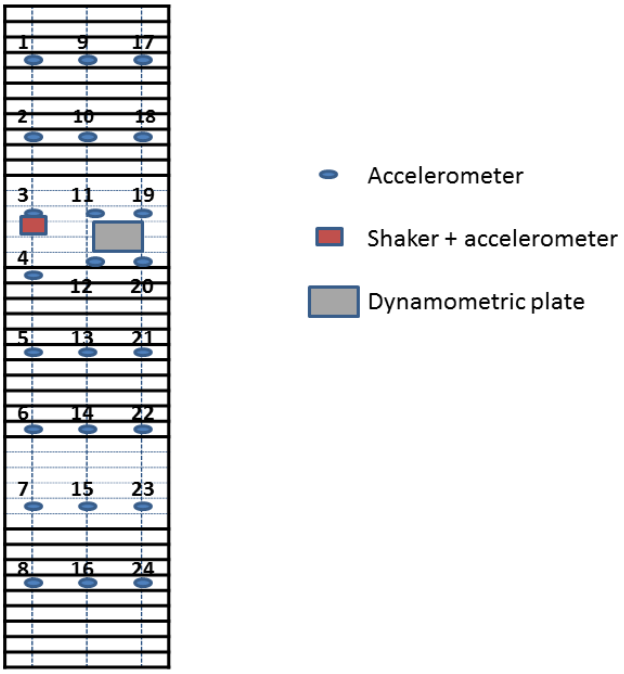

Figure 4.7: Experimental setup – Campus Bicocca Staircase – one moving subject

Test #	First Passive subject's location (Figure 4.7)	Second Passive subject's location (Figure 4.7)
1 – TS1	-	-
2 – TS2	-	-
3 – TS3	-	-
4 – TS1	21 – TS2	-
5 – TS1	10 – TS2	-
6 – TS2	21 – TS1	-
7 – TS2	10 – TS1	-
8 – TS3	21 – TS2	-
9 – TS3	10 – TS2	-
10 – TS1	21 – TS2	10 – TS3
11 – TS2	21 – TS1	10 – TS3
12 – TS3	21 – TS1	10 – TS2

Table 4.8: Tests layout – Bicocca staircase – one moving subject

Like for the campus Bovisa staircase, also in this case experimental tests with one subject walking on the dynamometric plate and one or two passive subjects standing on the structure were performed. In this case three Test Subjects (TS) were involved in the tests. Table 4.8 summarises the performed tests.

The experimental data were compared with predictions obtained by means of numerical simulations. The same procedure outlined in Sections 4.2 and 4.3.2.1 was employed. The next subsections summarise the obtained results. In this case only the average models of the apparent mass were used, with $\alpha_1 = 0.1$, $\alpha_2 = \alpha_3 = 0.45$.

4.4.2 Experimental and predicted results - modal parameters

As for the Campus Bicocca staircase, a slightly different experimental setup was employed. Particularly, the force measured with the dynamometric plate was measured synchronously with the accelerations. Thus, the experimental FRFs could be estimated. The modal parameters determined from the analysis of these FRFs were compared with those obtained with the H-S model. It should be noticed that the modal parameters extracted from the experimental FRFs (multi input FRFs) are subject to a high uncertainty due to the nature of the available data. In order to obtain a proper comparison between experiments and predicted results, the modal parameters of the joint H-S were also identified through the analysis of simulated multi input FRFs.

Test #	f_1 [Hz] exp.	f_1 [Hz] model	ζ_1 [%] exp	ζ_1 [%] model
1	6.64	6.69	0.73	1.04
2	6.66	6.69	0.55	0.86
3	6.67	6.69	0.68	0.91
4	6.61	6.66	1.29	1.53
5	6.65	6.68	0.89	1.04
6	6.66	6.68	0.77	1.09
7	6.67	6.68	0.58	0.86
8	6.60	6.66	1.24	1.35
9	6.65	6.69	0.73	0.86
10	6.60	6.64	2.24	2.04
11	6.63	6.65	1.60	1.67
12	6.60	6.63	1.41	1.49

Table 4.9: Experimental and predicted modal parameters – mode 1 – Campus Bicocca Staircase – one moving subject

The obtained results are summarised in Table 4.9, Table 4.10, Table 4.11 and Table 4.12.

Test #	f_2 [Hz] exp.	f_2 [Hz] model	ζ_2 [%] exp	ζ_2 [%] model
1	9.53	9.58	0.51	0.49
2	9.53	9.56	0.41	0.44
3	9.53	9.56	0.44	0.40
4	9.54	9.56	0.76	0.63
5	9.53	9.58	0.48	0.42
6	9.55	9.55	0.42	0.59
7	9.54	9.57	0.47	0.48
8	9.52	9.57	0.43	0.44
9	9.52	9.56	0.51	0.53
10	9.55	9.55	0.69	0.56
11	9.51	9.56	0.66	0.56
12	9.51	9.55	0.43	0.49

Table 4.10: Experimental and predicted modal parameters – mode 2 – Campus Bicocca Staircase – one moving subject

Test #	f_3 [Hz] exp.	f_3 [Hz] model	ζ_3 [%] exp	ζ_3 [%] model
1	10.72	10.75	0.44	0.40
2	10.74	10.74	0.37	0.37
3	10.74	10.76	0.38	0.40
4	10.75	10.75	0.37	0.38
5	10.76	10.76	0.45	0.45
6	10.78	10.77	0.42	0.40
7	10.76	10.75	0.40	0.45
8	10.80	10.74	0.23	0.21
9	10.76	10.76	0.40	0.47
10	10.75	10.75	0.32	0.40
11	10.73	10.73	0.42	0.40
12	10.76	10.74	0.44	0.43

Table 4.11: Experimental and predicted modal parameters – mode 3 – Campus Bicocca Staircase – one moving subject

Test #	f_4 [Hz] exp.	f_4 [Hz] model	ζ_4 [%] exp	ζ_4 [%] model
1	11.20	11.21	0.23	0.29
2	11.21	11.19	0.26	0.29
3	11.20	11.20	0.28	0.31
4	11.20	11.19	0.38	0.39
5	11.20	11.20	0.27	0.28
6	11.20	11.19	0.29	0.33
7	11.21	11.19	0.22	0.27
8	11.20	11.18	0.32	0.33
9	11.19	11.20	0.26	0.27
10	11.19	11.19	0.36	0.37
11	11.19	11.19	0.39	0.41
12	11.19	11.20	0.35	0.40

Table 4.12: Experimental and predicted modal parameters – mode 4 – Campus Bicocca Staircase – one moving subject

A small overestimation of the natural frequencies is obtained in most cases and a small overestimation of the damping ratio is found in the case of mode 1 (Table 4.9, last two columns). Such an effect will be deepened in the next Section. However, results show that modal parameters are generally well predicted by using the H-S model. Indeed, it should be noticed that, despite the use of average models, the trend of the predicted modal parameters well agrees with the experimental values.

4.4.3 Experimental and predicted results - rms

The results were also compared in terms of rms of the measured and predicted accelerations in the frequency band 0-15 Hz. The rms were predicted using both the FRFs of the empty structure $\mathbf{G}(\omega)$ and of the H+S system $\mathbf{G_H}(\omega)$

Table 4.13 reports the experimental/predicted rms and the relative errors estimated as in Eq. (4.6) and Eq. (4.7). Results refer to the point of maximum response (i.e. point 21).

Test #	rms exp. [ms^{-2}]	rms $\mathbf{G}(\omega)$ [ms^{-2}]	rms $\mathbf{G_H}(\omega)$ [ms^{-2}] (av. M*)	Error % empty	Error % H-S (av. M*)
1	0.065	0.070	0.055	7.4	-15.4
2	0.040	0.051	0.036	27.7	-9.8
3	0.057	0.071	0.054	23.5	-6.8
4	0.042	0.070	0.042	67.5	-0.3
5	0.058	0.081	0.056	39.3	-4.6
6	0.037	0.068	0.031	81.3	-15.8
7	0.035	0.054	0.033	53.1	-8.1
8	0.070	0.125	0.057	79.4	-17.9
9	0.094	0.130	0.083	38.2	-12.0
10	0.040	0.070	0.040	73.5	-0.6
11	0.063	0.120	0.062	89.7	-2.4
12	0.075	0.108	0.061	43.7	-18.8

Table 4.13: Rms and relative errors - α_1=0.1, α_2=α_3=0.45 – campus Bicocca staircase – one moving subject

Also in this case results show that the use the matrix of FRFs $\mathbf{G}(\omega)$ of the empty structure simulate the response can lead to an overestimation of the results. The error obtained using the model of the empty structure $\mathbf{G}(\omega)$ is higher for the tests with the passive subject located in point 21. Indeed, a subject located in point 21 introduces a higher damping than the same subject located in point 10 (Table 4.9).

The use of the proposed approach leads to a small underestimation of the amplitudes of vibration. This is in agreement with the overestimation of the damping ratio of the dominant mode underlined in Section 4.4.2. Once again, it is important to notice that the results were obtained by using average models of the apparent mass and that in this case the intra subject variability can play a significant role. Nevertheless, the results obtained using the H-S model are generally closer to the experimental values.

4.4.4 Experimental and predicted results - power spectra

Figure 4.8, Figure 4.9 and Figure 4.10 show a comparison among the power-spectrum of the measured acceleration and the power-spectrum of the acceleration predicted using the model of both the empty structure $\mathbf{G}(\omega)$ and of the subjects+structure $\mathbf{G_H}(\omega)$ respectively. Results are about test 4 (Figure 4.8),

test 8 (Figure 4.9) and test 11 (Figure 4.10) and refer to the point of maximum acceleration (point 21).

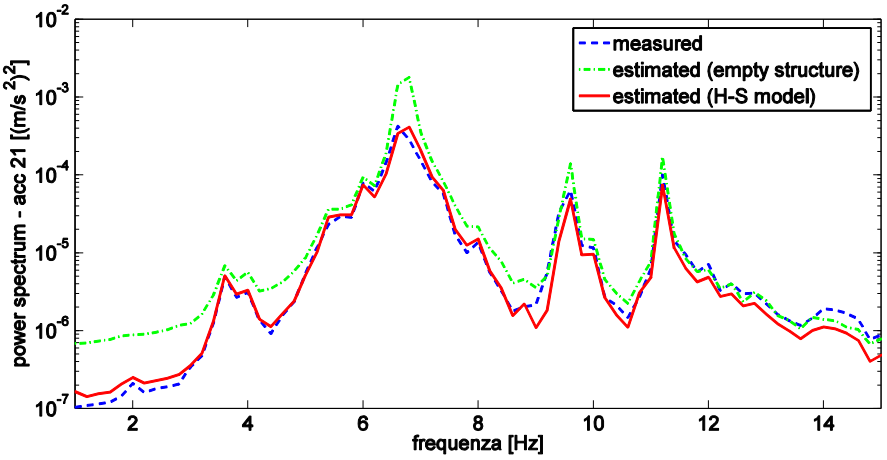

Figure 4.8: Test 4 – Campus Bicocca Staircase – experimental and predicted Power Spectra – acc 21 – one moving subject

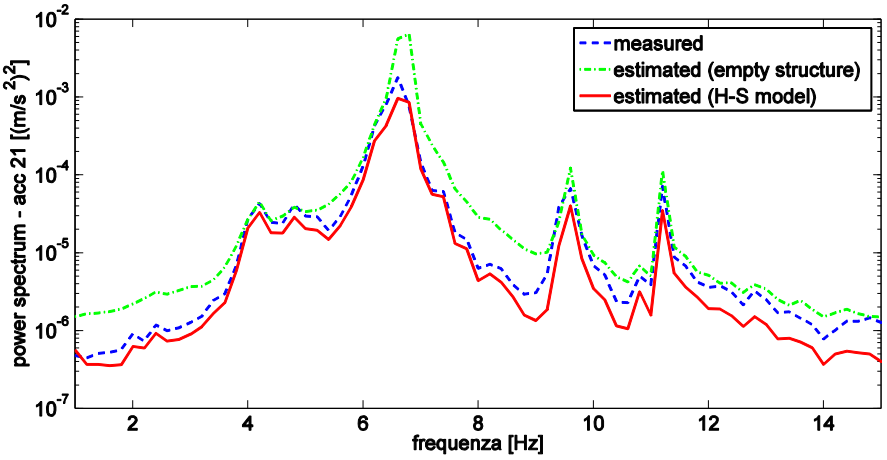

Figure 4.9: Test 8 – Campus Bicocca Staircase – experimental and predicted Power Spectra – acc 21

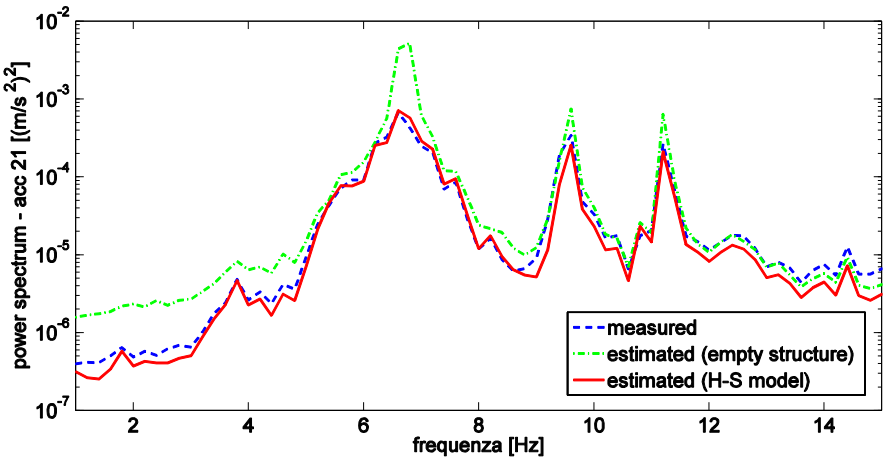

Figure 4.10: Test 11 – Campus Bicocca Staircase – experimental and predicted Power Spectra – acc 21 – one moving subject

Also in this case the results clearly show that the use of the model of the empty structure to simulate the structural vibrations would lead to an overestimation of the amplitudes of vibration. Conversely, using the proposed approach the results are much closer to the experimental data in all cases.

4.5 Summary

This Chapter aimed at proposing and validating an approach to predict the structural response of a slender structure due to people's presence. The methodology is based on the superposition of two contributions produced by people acting on a structure. Particularly, people's effect is decoupled in passive GRFs and active forces. The GRFs are used to find an appropriate equivalent model to represent the dynamics of a structure occupied by moving people. The active force is then introduced on this modified model to obtain a prediction of the structural vibrations.

Tests under controlled conditions were performed to validate the proposed approach. One subject was asked to march on a force plate, while a one or two subjects were standing still on the structure. The actual force induced by a single subject and the structural response were measured at the same time.

Results show that the use of the model of the empty structure to simulate the structural response causes an overestimation of the vibration amplitudes. Conversely, the use of the proposed methodology leads to results compatible with the experimental measurements. To represent the dynamic behaviour of moving subjects both experimental data and average models were used. Good results were

obtained in both cases. The obtained results support the use of the superposition of the effects (i.e. decoupling the effect of people in passive GRFs and active forces) to predict the structural vibrations.

Chapter 5

H-S model - moving people

Operating conditions

Chapter 4 proposed an approach to improve the prediction of the structural response due to people presence. In Chapter 4 the method was outlined and its effectiveness was verified through experimental tests performed under controlled conditions. In this Chapter the method is used to predict the vibration amplitudes during normal operating conditions. Tests performed on the same staircases described in Chapter 3 and Chapter 4 were used to verify the appropriateness of the proposed approach. To validate the approach under operating conditions people were asked to walk freely on the structures. In this case both the ground reaction forces and the active forces exerted by people on the structure were unknown. A statistical approach was used to simulate the structural response. Also in this case the performed tests allowed verifying that the use of the model of the empty structure to foresee the in service vibration levels led to an overestimation of the staircase response. Conversely, the proposed approach allowed obtaining results compatible with the experimental data.

In Chapter 4 an approach to predict vibration levels due to people's presence was proposed. In Chapter 4 the validity of superposition of the effects, i.e. considering separately GRFs and active forces was verified under controlled conditions.

In this Chapter the approach is extended to the case of normal operating conditions considering two slender staircases as test structures. In order to apply the proposed approach, the identification of two elements is required:

- GRFs: In the case of moving people, as the contact point of each subject with the structure changes with time, the GRFs can be hardly defined rigorously. In this work the use of average GRFs to represent the overall effect of moving people is proposed. The derivation of such GRFs for the case of people ascending and descending staircases is described in Section 5.
- Active forces: As for the active forces, some works available in literature [68],[24],[25], deals with the analysis of human induced dynamic forces on slender staircases. However, the information that can be extracted from these papers was not sufficient for the purpose of this work. Therefore, an experimental setup was developed to measure an appropriate set of active forces. The experimental setup and the results are discussed in Section 5.2.

Section 5.3 describes the experimental setup and tests, while Section 5.4 summarises the simulation procedure used to attain a prediction of vibration amplitudes. Section 5.5 presents and discusses the obtained results.

5.1 Experimental identification of GRFs

In order to apply the proposed approach, there is the need to identify the GRFs exerted by people during motion. Opposite to passive people, GRFs of moving people significantly change in time. Therefore, as for moving people, average GRFs are determined. Even though this is an approximate method, as the number of people increases, it seems reasonable to assume that average GRFs can be used.

As for the case considered in this Chapter, i.e. people walking on a staircase, in order to apply the proposed method it is necessary to determine an equivalent apparent mass representative of the average GRFs due to people's ascending and descending stairs. Like in Chapter 4, also in this case it will be proved that the proposed approach is able to provide results much more reliable than those achieved using the model of the empty structure to foresee structural vibrations. Indeed, if a correct equivalent model to represent the human behaviour during

motion is identified, the proposed method can provide reliable predictions of vibration levels.

5.1.1 Procedure to identify the equivalent apparent mass

As outlined in Chapter 4, the steps to identify the GRFs can be summarized as follows:

I. Perform a visual analysis in order to identify a given number of postures during one cycle of the particular motion. Particularly, for the tests reported in this Chapter, the motion during ascending and descending stairs was analysed. Figure 5.1 shows an example of frames extracted from one test performed to investigate such motion.

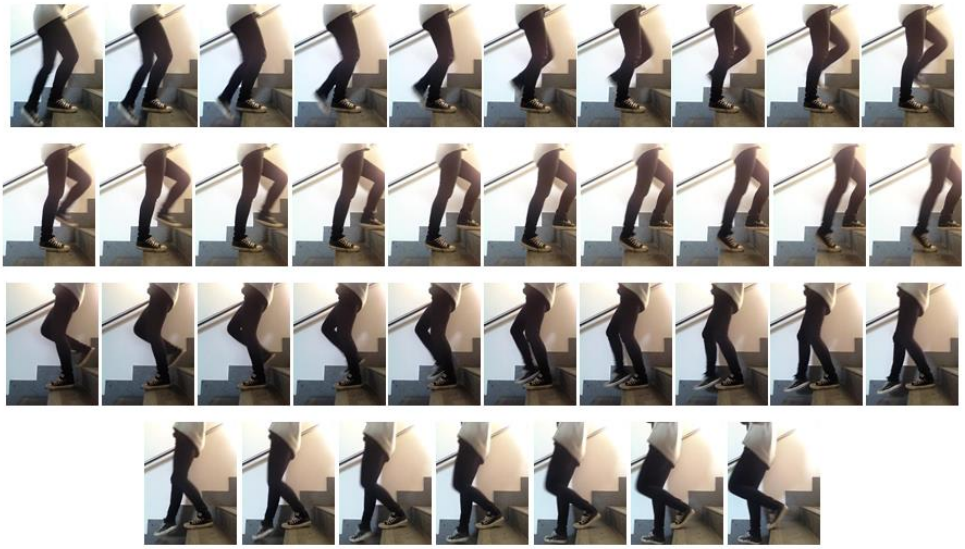

Figure 5.1: Visual analysis of ascending and descending stairs

As shown in Figure 5.1, the motion can be divided in an arbitrary number of postures that can be used to determine an equivalent apparent mass.

II. Choose an appropriate number (P) of positions. The positions must be representative of the overall behaviour during the motion. In this case 8 positions (4 postures, left and right foot) were chosen to represent the motion of people when ascending and descending stairs. The first 6 positions are shown in Figure 5.2 and are named with numbers from 1 to 3, left and right leg. The last chosen posture is the one defined as “one leg” in [51], i.e. stand on the leg being straight with comfortable and upright

upper-body. For each posture, the apparent mass was measured while the subject was standing on the left and right leg. The setup described in Section 3.2.1 was used to perform the measurements.

Figure 5.2: Selected positions (1 to 6)

III. Identify an average apparent mass $M_a^*(\omega)$, a=1:8, for each position. In this case no data available in literature could be used. Therefore, experimental tests were performed to measure such apparent masses. The experimental set-up described in Part I of this work was employed. For the 8 considered positions, the apparent masses of the 3 subjects involved in the tests were averaged.

IV. Define an equivalent apparent mass as the weighted average of the apparent masses, as in Eq. (4.3):

In this case the 8 apparent masses were averaged and all the weighting coefficients were set to $\alpha_a = 1/8$.

The so obtained equivalent apparent mass $M_{eq}^*(\omega)$ was used to determine the GRFs and thus the equivalent set of frequency response functions $\mathbf{G}_H(\omega)$ to represent the dynamic behaviour of the joint structure-moving people system.

5.1.2 Analysis of apparent masses

In order to determine an equivalent apparent mass describing the average GRFs of moving people, experimental tests were performed. Three subjects were involved in the tests. A total of 24 apparent mass curves was measured (3 subjects, 4 postures, left and right feet). The collected data were also used to analyze the influence of inter-subject variability (i.e. different subjects do not behave dynamically likewise) and posture on the apparent mass values. To this purpose, the apparent masses of different subjects in the same posture were first compared.

Figure 5.3 shows, as an example, the measured apparent masses (right foot) related to the postures reported in Figure 5.2.

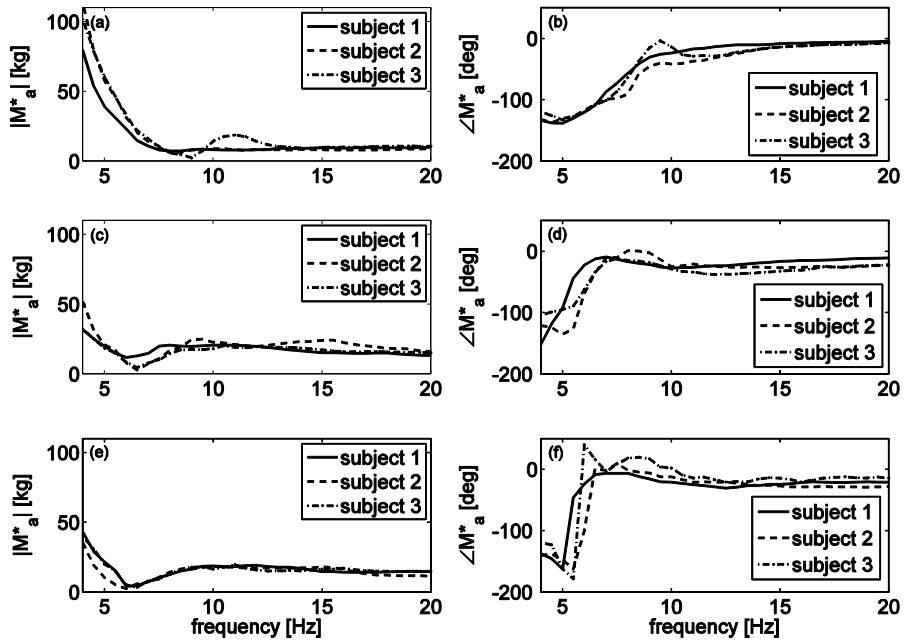

Figure 5.3: Apparent masses – 3 subjects – right foot, Position 1 – amplitude (a), Position 1 – phase (b), Position 2 – amplitude (c), Position 2 – phase (d), Position 3 – amplitude (e), Position 3 – phase (f)

Figure 5.4 shows, for a single subject, a comparison among the apparent masses measured in the 4 postures (right foot) considered in this analysis.

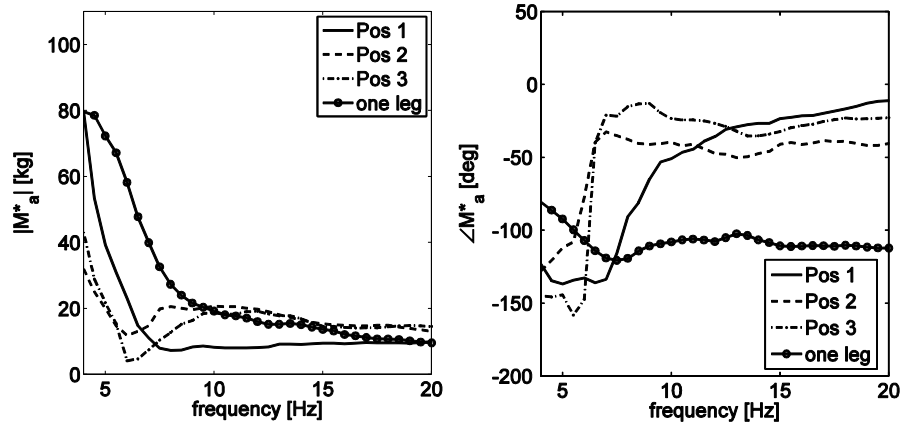

Figure 5.4: Apparent masses – subject 1 – right foot – amplitude (a), phase (b)

From a visual analysis of the apparent masses reported in Figure 5.4 it can be reasonably assumed that the apparent mass values are highly influenced by the

subject's posture. Conversely, the inter-subject variability seems to have a lower influence on the results (Figure 5.3). The obtained results confirm the experimental evidence reported in literature [54], i.e. the high influence of posture on the apparent mass values, and supports the use of average apparent mass values to identify the model of the joint H-S system. The next section summarizes the experimental tests performed to identify the active forces used to simulate the structural response.

5.2 Experimental identification of active forces

In order to characterize the active forces exerted by people on the structure, an appropriate set-up was built and several tests were performed.

To perform the experimental tests a force plate and two accelerometers were used. The force plate was located on a wooden auxiliary step at the end of a staircase (Figure 5.5). A second wooden auxiliary step was placed after the force plate. The two accelerometers were put on the two auxiliary steps respectively.

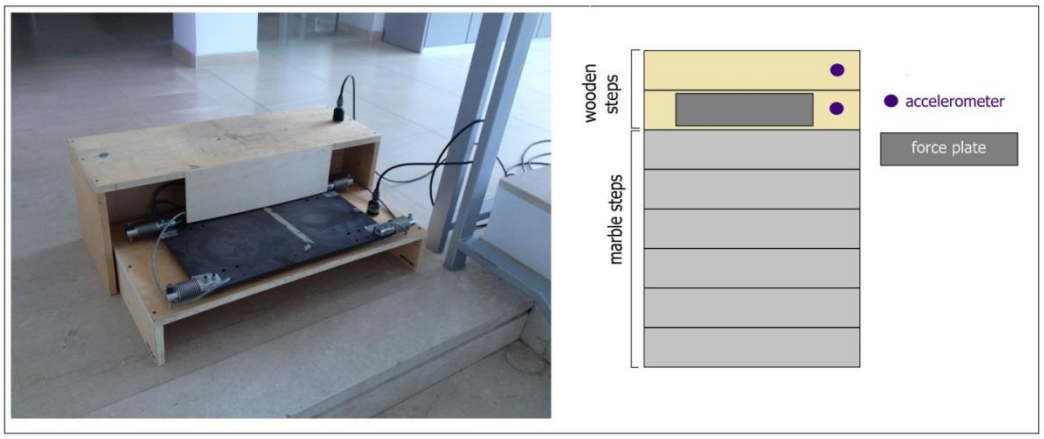

Figure 5.5: Experimental setup to measure the active forces

The acquired data were used to obtain a characterization of the active forces exerted by people when ascending and descending stairs. A total of 26 subjects were involved in the tests. Each subject was asked to ascend and descend the step three times with the right foot and three times with the left foot. An overall amount of 312 force time histories was measured. Figure 5.6 reports, as an example, the 12 forces exerted by one subject when ascending and descending the step with left and right foot

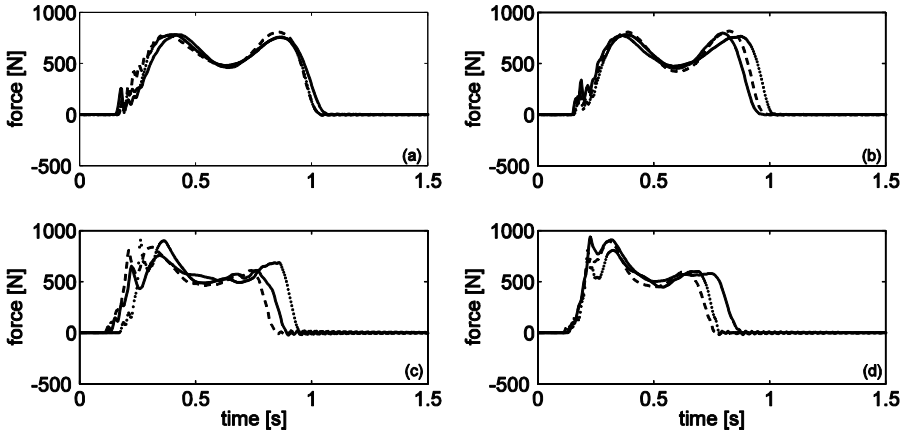

Figure 5.6: Example of recorded forces: ascending – right leg (a), ascending – left leg (b), descending – right leg (c), descending – left leg (d)

In addition, the collected data were also used to determine the step frequencies. To this purpose the cross correlation [112] of the accelerations measured in the two subsequent steps were used. Figure 5.7 reports the estimated step frequencies.

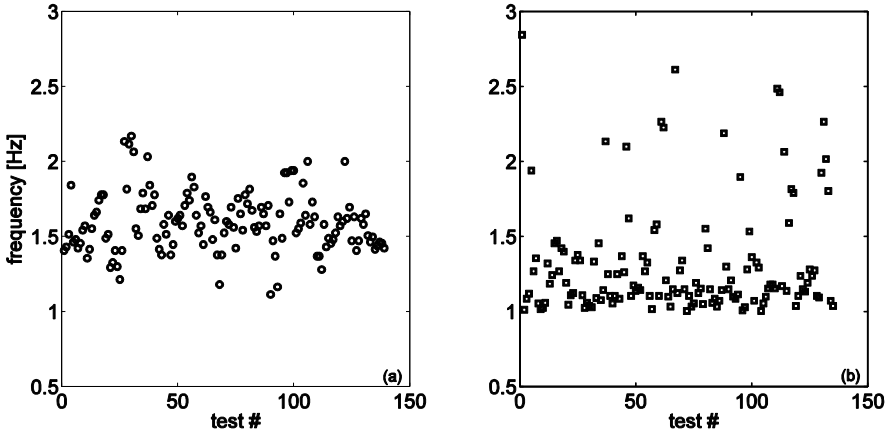

Figure 5.7: Frequency step – ascending (a) and descending (b)

The recorded time histories and the estimated step frequencies were used to simulate the structural response. The simulation procedure and the results are discussed in the next section.

5.3 Experimental setup and tests

5.3.1 Campus Bovisa staircase

In order to allow people walking freely on the structure, the experimental setup described in Chapter 4, Section 4.3.1, was changed. Particularly, only the accelerometers placed at the two sides of the staircase were left. Figure 5.8 shows the experimental setup.

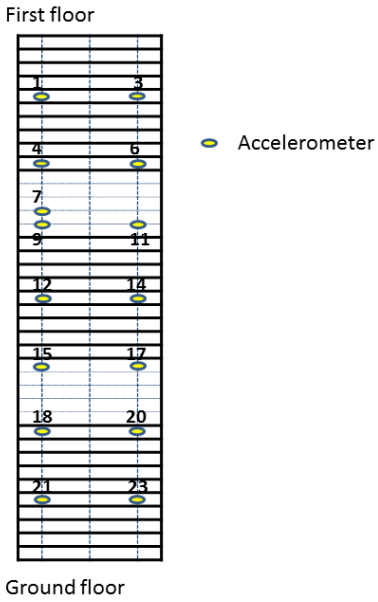

Figure 5.8: Experimental setup – tests in operating conditions – Campus Bovisa staircase

With the setup shown in Figure 5.8, two kinds of test were performed:

- 3 subjects walking on the structure
- 9 subjects walking on the structure

Figure 5.9 reports, as an example, one frame of the test with 9 subjects walking on the staircase.

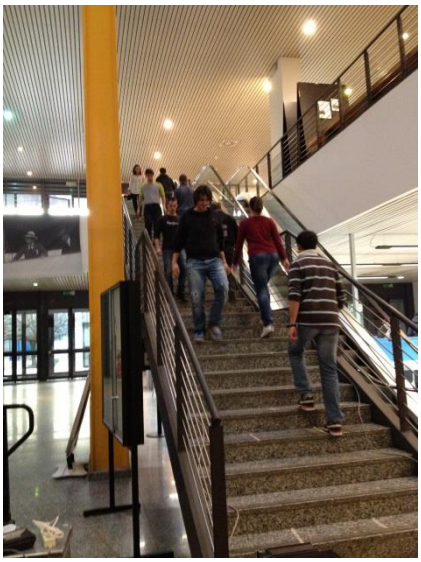

Figure 5.9: 9 subjects walking on the staircase – Campus Bovisa staircase

The accelerations collected during the tests described above were compared to those obtained by means of numerical simulations.

5.3.2 Campus Bicocca staircase

To perform tests in operating conditions on the Campus Bicocca staircase, the same experimental setup described in Chapter 3, Section 3.4, was employed.

Also in this case two kinds of test were performed, i.e.:

- 5 subjects walking on the structure
- 10 subjects walking on the structure

The next Section report the procedures used to determine the GRFs that were used to obtain the model of the joint H-S system.

5.4 Simulation procedure

As described in Chapter 4 of this work, in order to obtain a prediction of structural vibrations a two steps procedure was adopted. Particularly, average ground reaction forces were computed using the apparent masses estimated from the tests described in Section 5.1. These GRFs were used to determine an equivalent set of FRFs $\mathbf{G}_{\mathrm{H}}(\omega)$ representing the dynamic behaviour of the joint structure – moving people system. Then, the forces recorded during the tests described in Section 5.2 were used to simulate the structural response.

The adopted simulation procedure can be summarized in the following steps:

1) Discretization of the structure in K_p points. The discretization is exemplified in Figure 5.10 and results in K_p=78 for the Campus Bovisa staircase and K_p=86 for the Campus Bicocca staircase.

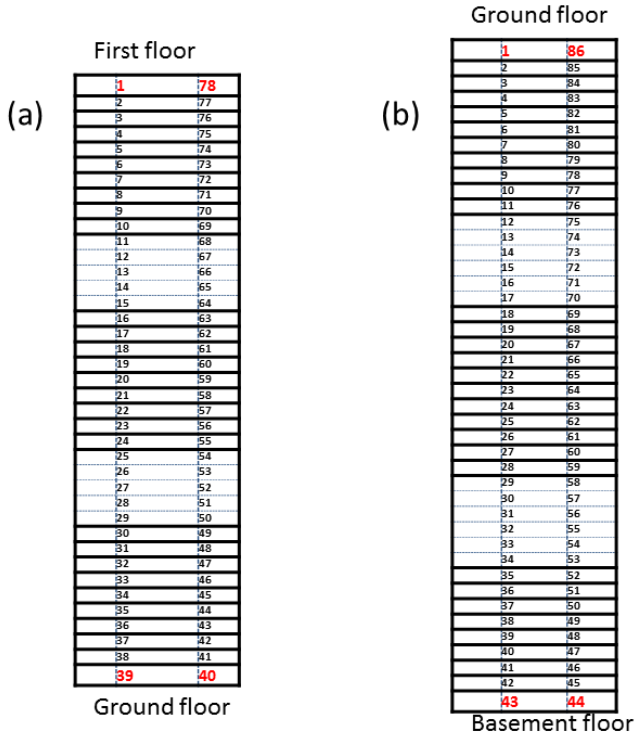

Figure 5.10: Structure discretization: campus Bovisa staircase (a) and campus Bicocca staircase (b).

2) Extraction of mode shape amplitudes for each of the K_p points represented in Figure 5.10 using interpolated mode shapes. The data collected during the tests reported in the previous Chapters were used to derive the modal model of the empty structure. Indeed, in the case treated in Chapters 3 and 4, the experimentally determined eigenvectors were enough to perform the analysis. Conversely, in this case there was the need to interpolate the mode shapes experimentally measured in order to extend the information to other points of the structure. Several interpolation methods were used and robustness checks, as explained later, were performed to verify the appropriateness of the obtained mode shapes. The low-influence of the interpolation method was verified via simulations.

3) Determination of the equivalent set of FRFs $\mathbf{G}_{\mathrm{H}}(\omega)$using the equivalent apparent mass $M_{\mathrm{eq}}{}^{*}(\omega)$. $M_{\mathrm{eq}}{}^{*}(\omega)$ is computed as in Eq. (4.3) and it is the average of the 3x8 considered apparent masses. To this purpose the total mass was distributed along the structure. Particularly, a fraction of mass equal to

$$M^{*}{}_{\mathrm{fr}}(\omega) = \frac{\mathrm{n_p}}{\mathrm{K_p}} M_{\mathrm{eq}}{}^{*}(\omega) \tag{5.1}$$

was introduced in each of the K_p points. In Eq. (5.1) $M_{\mathrm{eq}}{}^{*}(\omega)$ is the equivalent apparent mass computed as in Eq. (4.3) and $\mathrm{n_p}$ is the number of people walking on the structure.
Thus, the GRF in each point can be expressed as

$$f_{\mathrm{k}}^{\mathrm{GR}}(\omega) = M^{*}{}_{\mathrm{fr}}(\omega)\ddot{x}_{\mathrm{i}}(\omega) = -M^{*}{}_{\mathrm{fr}}(\omega)\omega^2 x_{\mathrm{k}}(\omega) \tag{5.2}$$

In terms of the full displacement vector $\mathbf{x}(\omega)$ Eq. (5.2) becomes

$$\mathbf{f}^{\mathrm{GR}}(\omega) = \mathbf{W}\mathbf{H}(\omega)\mathbf{W}^{\mathrm{T}}\mathbf{x}(\omega) = -\omega^2 M^{*}{}_{\mathrm{fr}}(\omega)\mathbf{W}\mathbf{x}(\omega) \tag{5.3}$$

with

- $\mathbf{W}$: K_p x K_p identity matrix
- $\mathbf{H}(\omega)$: K_p x K_p diagonal matrix containing the fractions of the equivalent apparent mass

Substituting Eq. (5.3) in Eq. 4.1, Eq. (5.4) is obtained

$$[\mathbf{G}^{-1}(\omega) + \omega^2 M^{*}{}_{\mathrm{fr}}(\omega)\mathbf{W}]\mathbf{x}(\omega) = \mathbf{G}_{\mathrm{H}}^{-1}(\omega)\mathbf{x}(\omega) = \mathbf{f}^{\mathrm{ACTIVE}}(\omega) \tag{5.4}$$

where $\mathbf{G}(\omega)$ is the K_p x K_p matrix containing the frequency response functions of the empty structure and $\mathbf{G}_{\mathrm{H}}(\omega)$ is the K_p x K_p matrix representing the equivalent set of frequency response functions representing the dynamic behaviour of the joint structure-moving people system.

4) Determination of K_p force time histories (1 for each discretization point, Figure 5.10)

The previous section described the experimental tests performed to determine a possible set of active forces exerted by 26 subjects ascending and descending a staircase. These values were used to generate the time histories of the active forces.

The following procedure was followed for each of the n_p subjects walking on the structure: for each subject the initial parameter were chosen trough a random selection of

I. one subject from the available database (26 subjects, Section 5.2). For each subject, 12 measured footsteps are available (3 ascending – right foot, 3 ascending – left foot, 3 descending – right foot, 3 descending – left foot).
II. the starting point (1 to K_p, Figure 5.10)
III. the initial foot (left or right)

At each subsequent iteration (step) the contact point was increased and the foot was changed (left $\rightarrow$ right or vice versa).
The direction of movement (ascending or descending) was determined on the base of the number of the contact point (descending if the $1 \leq$ contact point $\leq (K_p/2)$, ascending if $(K_p/2+1) \leq$ contact point $\leq (K_p)$, see Figure 5.10.

After defining the direction of movement (ascending or descending) and the foot (left or right), the force exerted by the subject at each contact point was randomly selected among the 3 available forces.

The procedure to generate the active force for one subject is exemplified in Figure 5.11. In the example the starting contact point is 45.

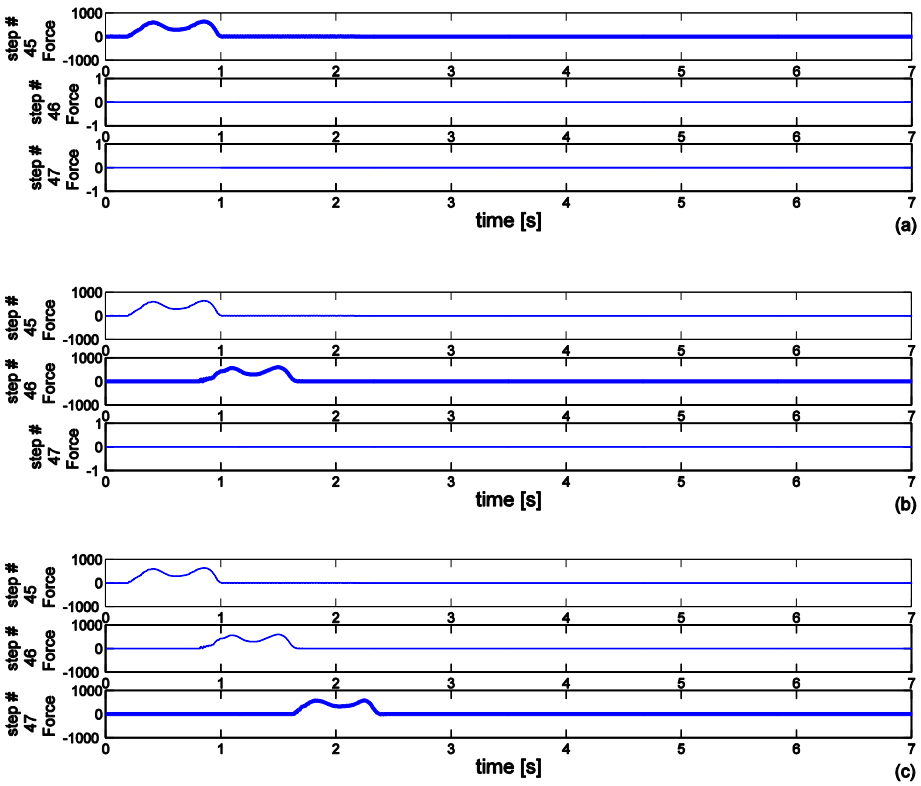

Figure 5.11: Active forces generation – iteration 1 (a), iteration 2 (b), iteration 3 (c)

At each step, the time delay between one step and the subsequent (Figure 5.11 (b)) was chosen on the base of a random selection of the step frequencies reported in Figure 5.7.

The above described procedure was repeated until the desired length of time history of the response had been reached and for all the n_p subjects walking on the staircase.

5) Simulation of the structural response via convolution using the Impulse Response Functions (IRFs) of the joint H-S systems and the simulated forces. The IRFs were obtained from the FRFs by using inverse Fourier transform.

To simulate the structural response statistically, points 4 and 5 were repeated 100 times for each test configuration (3 and 9 people). Each simulation required about 2 minutes to simulate a 480 s time history on a normal laptop.

The simulated accelerations were used to compare the experimental results with the numerical predictions. The results are discussed in the next subsection.

5.5 Experimental results and comparison with experimental simulations

This Section reports a comparison between the experimental results and those obtained by means of numerical simulations. The simulations were performed according to the procedure outlined in the previous Section. In addition to the modal model of the joint H-S system, other models were also used. Particularly, three different modal models were used to simulate the structural response and to compare the so obtained predictions with the experimental results.

The considered models are:

1. Modal model of the empty structure $\mathbf{G}(\omega)$
2. H-S modal model $\mathbf{G}_{\mathrm{H}}(\omega)$
3. Experimental modal model of the joint H-S system. To this purpose the experimental modal parameters were extracted from the experimental structural responses via Operational Modal Analysis techniques [118],[119].

5.5.1 Campus Bovisa staircase

5.5.1.1 Effect of mode shapes interpolation on the results

In order to investigate the influence of the interpolation of the mode shapes on the results, several simulations were carried out. Particularly, the robustness of the interpolation was verified:

- by using several interpolation methods (spline, harmonic, polynomial)
- performing the interpolating procedure using a reduced number of points.

The average, upper and lower limits (average $\pm 3\sigma$) of the mode shapes were used to simulate the structural response. The simulated results were analysed in terms of rms of the measured/simulated accelerations. The rms in the frequency range 0-15 Hz were compared.

Figure 5.12 shows the obtained results for the case of the test with 9 people. Results refer to the point of maximum acceleration (accelerometer 6 in Figure 5.8).

The points reported in Figure 5.12 refer to:

- The average of the 100 simulated rms (circle with bar)
- The average rms $\pm 2\sigma$ (square with bar), with σ standard deviation of the 100 simulated rms

Case 1, Case 2 and Case 3 in Figure 5.12 report the results of the tests performed using: 1) the average of all the interpolated mode shapes; 2) the average of all the interpolated mode shapes plus 3 times the standard deviation of all the interpolations; 3) the average of all the interpolated mode shapes minus 3 times the standard deviation of all the interpolations.

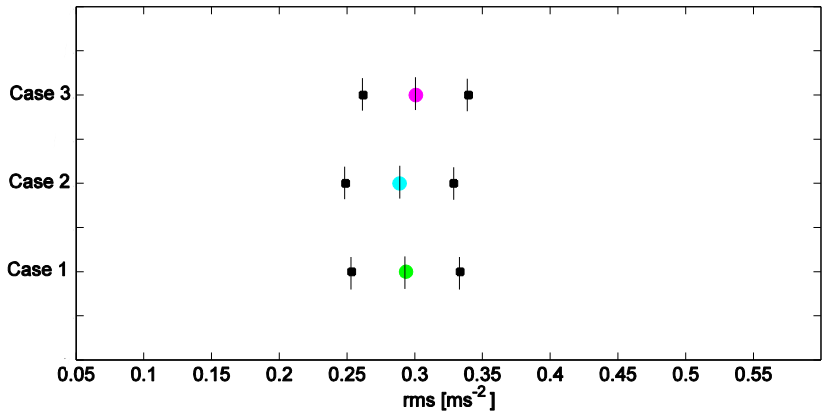

Figure 5.12: Test with 9 subjects walking on the campus Bovisa staircase - Case1: empty structure, Case 2: H-S model with average mode shapes, Case 3: H-S model with average - 3σ mode shapes, Case 3: H-S model with average + 3σ mode shapes

Results show that the uncertainty associated to the interpolation of the mode shapes have a small impact on the results. The obtained results are compared to those obtained experimentally in the next section.

5.5.1.2 Discussion of the results

Table 5.1 and Table 5.2 report the identified modal parameters for the tests with 3 and 9 people.

	empty	H-S model	H-S experimental
f_{n1} [Hz]	7.84	7.82	7.84
f_{n2} [Hz]	8.89	8.88	8.86
ζ_1 [%]	0.33	0.54	0.79
ζ_2 [%]	0.43	0.47	0.44

Table 5.1: modal parameters – test with 3 people – campus Bovisa Staircase

	empty	H-S model	H-S experimental
f_{n1} [Hz]	7.84	7.79	7.82
f_{n2} [Hz]	8.89	8.87	8.85
ζ_1 [%]	0.33	0.94	1.18
ζ_2 [%]	0.43	0.56	0.83

Table 5.2: modal parameters – test with 9 people – campus Bovisa Staircase

As for the test with 3 people, the experimental modal parameters show a small increase of damping ratios and a slight decrease of natural frequencies. The predicted modal parameters slightly underestimate the experimental values. However, since the forces exerted by people are not white noise, it is important to notice that the identification via Operational Modal Analysis techniques might be subject to biases, especially for the test with 3 people.

As for the test with 9 people, also in this case the experimental modal parameters show an increase of damping ratios and a slight decrease of natural frequencies. The model of the joint H-S system provides modal parameters that slightly underestimate the experimental values. However, the results obtained with the H-S model are much closer to the experimental values than the modal parameters of the empty structure.

Figure 5.13 and Figure 5.14 show a comparison among the experimental and predicted rms of the point of maximum acceleration (accelerometer 6 in Figure 5.8).

The points reported in Figure 5.13 and Figure 5.14 refer to:

- The experimental rms (triangle)
- The average of the 100 simulated rms (circle with bar)
- The average rms $\pm 2\sigma$ (square with bar), with σ standard deviation of the 100 simulated rms

Case 1, Case 2 and Case 3 in Figure 5.13 and Figure 5.14 report the results related to the modal model of the empty structure, the model of the joint H-S system and the experimental model respectively.

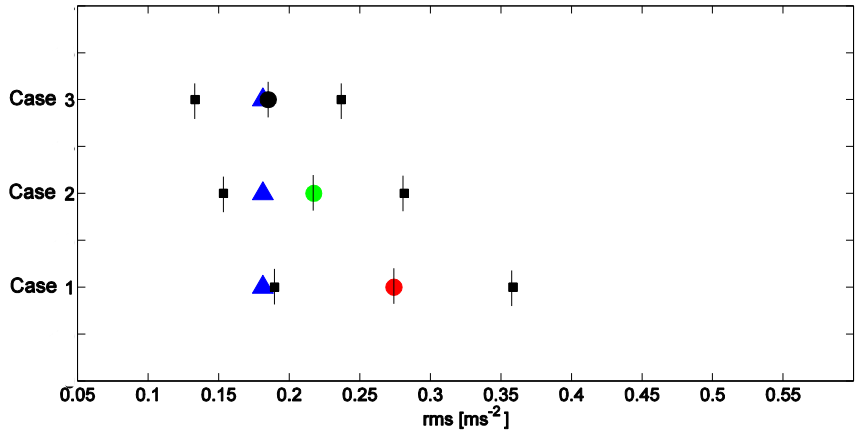

Figure 5.13: Test with 3 subjects walking on the campus Bovisa staircase – Case1: empty structure, Case 2: H-S model, Case 3: experimental modal parameters

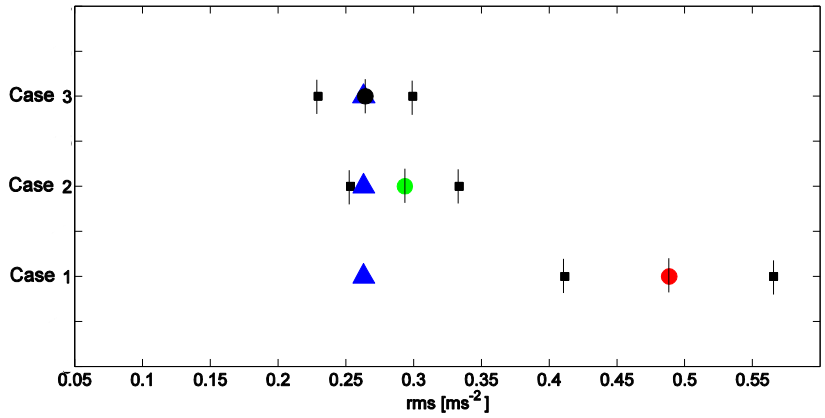

Figure 5.14: Test with 9 subjects walking on the campus Bovisa staircase - Case1: empty structure, Case 2: H-S model, Case 3: experimental modal parameters

The obtained results confirm that the use of the model of the empty structure causes an overestimation of predicted structural vibrations. Conversely, using the experimental modal parameters the and the model of the H-S systems accelerations are much better predicted.

5.5.2 Campus Bicocca staircase

Table 5.3 and Table 5.4 reports the identified and predicted modal parameters for the tests performed on the campus Bicocca staircase with 5 and 10 people.

	empty	H-S model	H-S experimental
f_{n1} [Hz]	6.70	6.68	6.60
f_{n2} [Hz]	9.56	9.55	9.47
f_{n3} [Hz]	10.75	10.75	10.75
f_{n4} [Hz]	11.21	11.21	11.18
ζ_1 [%]	0.33	0.64	0.75
ζ_2 [%]	0.28	0.33	0.42
ζ_3 [%]	0.29	0.30	0.22
ζ_4 [%]	0.17	0.20	0.20

Table 5.3: modal parameters – test with 5 people – campus Bicocca Staircase

	empty	H-S model	H-S experimental
f_{n1} [Hz]	6.70	6.67	6.59
f_{n2} [Hz]	9.56	9.54	9.44
f_{n3} [Hz]	10.75	10.75	10.74
f_{n4} [Hz]	11.21	11.20	11.18
ζ_1 [%]	0.33	0.95	1.25
ζ_2 [%]	0.28	0.37	0.60
ζ_3 [%]	0.29	0.30	0.32
ζ_4 [%]	0.17	0.23	0.24

Table 5.4: modal parameters – test with 10 people – campus Bicocca Staircase

As for the test with 5 people, the experimental modal parameters show a small increase of damping ratios and a slight decrease of natural frequencies. The predicted modal parameters generally slightly underestimate the damping ratios and overestimate the natural frequencies. Similar considerations apply to the case of the test with 10 people. However, it should be noticed that the results obtained with the H-S model are closer to the experimental values than the modal parameters of the empty structure.

Also in this case the simulated results were compared with the experimental measurements in terms of rms of the measured/simulated accelerations in the frequency range 0-15 Hz.

Figure 5.15 and Figure 5.16 show a comparison among the experimental and predicted RMSs of the point of maximum acceleration (accelerometer 21 in Figure 3.20).

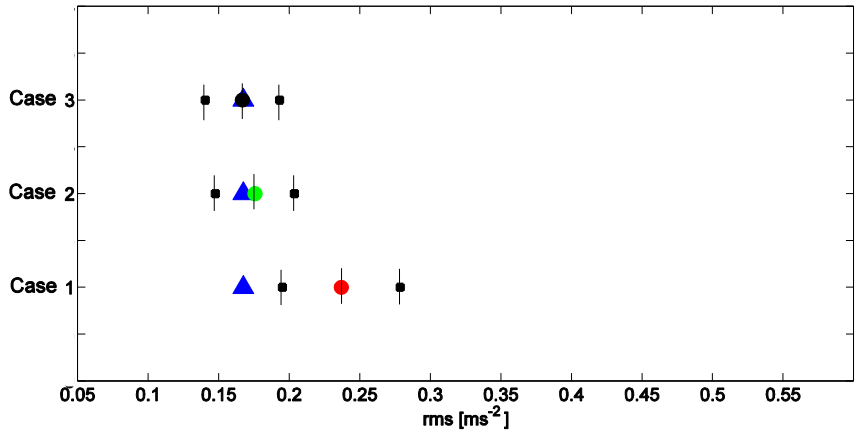

Figure 5.15: Test with 5 subjects walking on the campus Bicocca staircase – Case1: empty structure, Case 2: H-S model, Case 3: experimental modal parameters

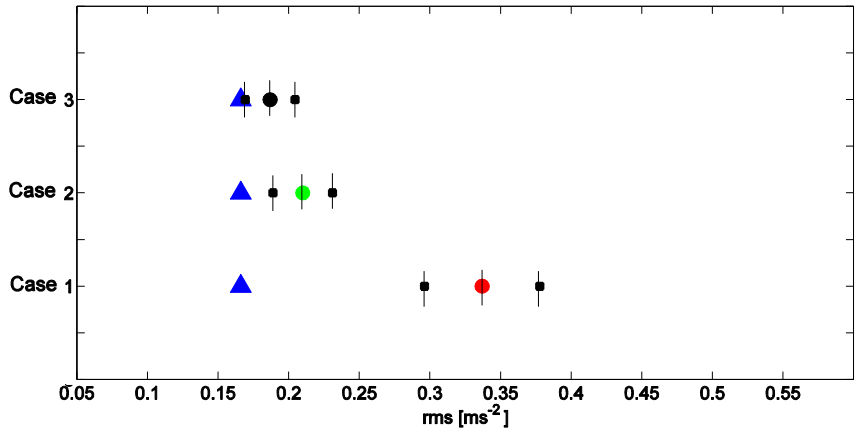

Figure 5.16: Test with 10 subjects walking on the campus Bicocca staircase – Case1: empty structure, Case 2: H-S model, Case 3: experimental modal parameters

Also in this case the obtained results confirm that the use of the model of the empty structure causes an overestimation of predicted structural vibrations. Conversely, using the modal parameters of the joint H-S system the accelerations are better predicted. This result supports the validity of the simulation method and shows that, if the modal parameters of the joint H-S system are correctly predicted, the structural vibrations can be obtained via superposition of effects. The use of the model of the joint H-S system to predict the structural response significantly improves the results with respect to the use of the model of the empty structure. Indeed, in this case the results of the simulations are much closer to the experimental values. Therefore, a key point for the success of the proposed approach is the identification of a correct set of equivalent FRFs accounting for the

GRFs of moving people. If the modal parameters are correctly predicted, the proposed approach can provide reliable predictions of vibration amplitudes.

5.6 Summary

This Chapter proposed an approach to predict in-service vibration amplitudes of a pedestrian structure. The method requires the knowledge of the modal model of the empty structure. The influence of people is decoupled in two main effects, i.e. GRFs and active forces. GRFs are included in the model using the apparent masses of the subjects in contact with the structure. The effect of such apparent masses is a modification of the FRFs (i.e. changes of structural modal parameters). An active force is applied using the new set of FRFs representing the dynamic behaviour of the joint H-S in order to obtain a prediction of the structural response.

In order to extend the method proposed in Chapter 4 two main problems are investigated in this Chapter.

The first issue regards the identification of GRFs representative of the average influence of moving people in terms of changes of modal parameters. To this purpose a set of apparent masses, representative of various postures taken by people during motion, was measured. Thus, an average apparent mass was obtained and used to assess people's influence.

The second issue regards the identification of appropriate active forces. As in normal operating conditions the actual force exerted by people could not be measured, an appropriate set of possible forces was measured. Thus, a statistical approach was used to simulate the structural response.

An appropriate simulation procedure was used to obtain predictions of the structural vibrations. The results show that by using the modal model of the empty structure the obtained amplitudes overestimate the actual structural response. Conversely, by using the approach proposed in this work, results are much closer to the experimental measurements.

Chapter 6

Theoretical Analysis of Human-Structure Interaction

This Chapter proposes a theoretical analysis of the behaviour of joint H-S systems. The study is based on an investigation of the mathematical properties of the model proposed in the previous chapters of this dissertation.

The first part of the Chapter aims at investigating the properties of the matrix of joint H-S systems. The differences between using a MDOFs structural model or the modal superposition of the effects are analysed. In case of applicability of the superposition of effects, it is proved that the determination of the matrix of the joint H-S system can be directly determined by solving an equation.

In the second part of the Chapter, a criterion to evaluate the influence of people based on the direct analysis of apparent mass curves is proposed. The criterion assumes that people's effect can be modelled via superposition of effects.

In the last part of the Chapter an analysis of the effects of subjects in different postures is proposed. The analysis was performed using various apparent mass curves representative of different postures and related to various directions of vibration.

6.1 Matrix approach

In order to investigate the mathematical properties of the matrix of the joint H-S system $\mathbf{G}_{\mathrm{H}}(\omega)$ the case of a structure with 3 passive subject is considered first.

The considered structure is shown schematically in Figure 6.1.

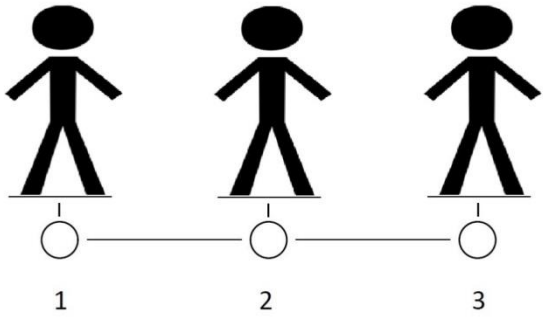

Figure 6.1: People's distribution on the structure

The modal matrix of the empty structure can be expressed as in Eq. (6.1).

$$\boldsymbol{G}(\omega) = \begin{bmatrix} G_{11}(\omega) & G_{12}(\omega) & G_{13}(\omega) \\ G_{21}(\omega) & G_{22}(\omega) & G_{23}(\omega) \\ G_{31}(\omega) & G_{32}(\omega) & G_{33}(\omega) \end{bmatrix} \tag{6.1}$$

Each term of the matrix $\boldsymbol{G}(\omega)$ is given by Eq. (6.2)

$$G_{ik}(\omega) = \sum_{j=1}^{n} \frac{\varphi_{i,j}\varphi_{k,j}}{\omega_{nj}^2 - \omega^2 + 2\mathrm{i}\zeta_j\omega\omega_{nj}} \tag{6.2}$$

where:

- n is the number of the considered vibration modes;
- ω_{nj} is the natural frequency of the j-th mode;
- ζ_j is the damping ratio of the j-th mode;
- $\varphi_{i,j}$, $\varphi_{k,j}$ are the modal constants of the j-th vibration mode in the i-th and k-th points respectively.

The matrix $\mathbf{G}(\omega)$ complies with the property expressed in Eq. (6.3). This property can be directly derived from Eq. (6.2).

$$G_{ik}(\omega) = G_{ki}(\omega) \tag{6.3}$$

The matrix defining the dynamic behaviour of the joint H-S system was derived in Chapter 2 and is recalled in Eq. (6.4).

$$\mathbf{G}_{\mathrm{H}}(\omega) = [\mathbf{G}(\omega)^{-\mathbf{1}} + \mathbf{W}\mathbf{H}(\omega)\mathbf{W}^{\mathbf{T}}]^{-\mathbf{1}} \tag{6.4}$$

As for the configuration reported in Figure 6.1, the terms $\mathbf{W}$ and $\mathbf{H}(\omega)$ in Eq. (6.4) can be expressed as in Eq. (6.5) and Eq. (6.6).

$$\mathbf{W} = \begin{bmatrix} 1 & 0 & 0 \\ 0 & 1 & 0 \\ 0 & 0 & 1 \end{bmatrix} \tag{6.5}$$

$$\mathbf{H}(\omega) = \begin{bmatrix} H_1(\omega) & 0 & 0 \\ 0 & H_2(\omega) & 0 \\ 0 & 0 & H_3(\omega) \end{bmatrix} \tag{6.6}$$

In Eq. (6.6) the terms $H_1(\omega)$, $H_2(\omega)$ and $H_3(\omega)$ represent the generic driving point FRFs of the three subjects located in point 1, 2 and 3 of the structure (Figure 6.1).

In order to compute the matrix $\mathbf{G_H}(\omega)$ (Eq. (6.4)), the inverse of the matrix of the empty structure is first computed. Its expression is reported in Eq. (6.7)

$$\mathbf{G}(\omega)^{-\mathbf{1}} = -\frac{1}{\det(\mathbf{G}(\omega))} \cdot \begin{bmatrix} G_{23}(\omega)^2 - G_{22}(\omega)G_{33}(\omega) & G_{12}(\omega)G_{33}(\omega) - G_{13}(\omega)G_{23}(\omega) & G_{13}(\omega)G_{22}(\omega) - G_{12}(\omega)G_{23}(\omega) \\ G_{12}(\omega)G_{33}(\omega) - G_{13}(\omega)G_{23}(\omega) & G_{13}(\omega)^2 - G_{11}(\omega)G_{33}(\omega) & G_{23}(\omega)G_{11}(\omega) - G_{12}(\omega)G_{13}(\omega) \\ G_{13}(\omega)G_{22}(\omega) - G_{12}(\omega)G_{23}(\omega) & G_{23}(\omega)G_{11}(\omega) - G_{12}(\omega)G_{13}(\omega) & G_{12}(\omega)^2 - G_{11}(\omega)G_{22}(\omega) \end{bmatrix} \tag{6.7}$$

with

$$\begin{aligned} det(\mathbf{G}(\omega)) = & -G_{33}(\omega)\, G_{12}(\omega)^2 + 2G_{12}(\omega)G_{13}(\omega)G_{23}(\omega) \\ & - G_{22}(\omega)\, G_{13}(\omega)^2 - G_{11}(\omega)\, G_{23}(\omega)^2 \\ & + G_{11}(\omega)G_{22}(\omega)G_{33}(\omega) \end{aligned} \tag{6.8}$$

The matrix $\mathbf{G}_{\mathrm{H}}(\omega)$ is then derived trough the inversion of the matrix $\left[\mathbf{G}(\omega)^{-\mathbf{1}} + \mathbf{H}\right]$ and can be defined as in Eq. (6.9).

$$\mathbf{G}_{\mathrm{H}}(\omega) = [\mathbf{G}(\omega)^{-1} + \mathbf{H}]^{-1} = \frac{\mathbf{N}}{den(\mathbf{G}_{\mathrm{H}}(\omega))} = \frac{1}{den(\mathbf{G}_{\mathrm{H}}(\omega))}\begin{bmatrix} N_{11}(\omega) & N_{12}(\omega) & N_{13}(\omega) \\ N_{21}(\omega) & N_{22}(\omega) & N_{23}(\omega) \\ N_{31}(\omega) & N_{32}(\omega) & N_{33}(\omega) \end{bmatrix} \tag{6.9}$$

Each term of Eq. (6.9) is defined in Eqs. (6.10)-(6.16).

$$\begin{aligned} den\big(\mathbf{G}_{\mathrm{H}}(\omega)\big) = 1 &+ G_{11}(\omega)H_1(\omega) + G_{22}(\omega)H_2(\omega) + G_{33}(\omega)H_3(\omega) + \cdots \\ &H_1(\omega)H_2(\omega)(G_{11}(\omega)G_{22}(\omega) - G_{12}(\omega)^2) \\ &+ H_1(\omega)H_3(\omega)(G_{11}(\omega)G_{33}(\omega) - G_{13}(\omega)^2) + \cdots \\ &H_2(\omega)H_3(\omega)(G_{22}(\omega)G_{33}(\omega) - G_{23}(\omega)^2) \\ &+ H_1(\omega)H_2(\omega)H_3(\omega)\Big(det\big(\mathbf{G}(\omega)\big)\Big) \end{aligned} \tag{6.10}$$

$$\begin{aligned} N_{11}(\omega) = G_{11}(\omega) &+ H_2(\omega)(G_{11}(\omega)G_{22}(\omega) - G_{12}(\omega)^2) \\ &+ H_3(\omega)(G_{11}(\omega)G_{33}(\omega) - G_{13}(\omega)^2) \\ &+ H_2(\omega)H_3(\omega)\Big(det\big(\mathbf{G}(\omega)\big)\Big) \end{aligned} \tag{6.11}$$

$$\begin{aligned} N_{22}(\omega) = G_{22}(\omega) &+ H_1(\omega)(G_{11}(\omega)G_{22}(\omega) - G_{12}(\omega)^2) \\ &+ H_3(\omega)(G_{22}(\omega)G_{33}(\omega) - G_{23}(\omega)^2) \\ &+ H_1(\omega)H_3(\omega)\Big(det\big(\mathbf{G}(\omega)\big)\Big) \end{aligned} \tag{6.12}$$

$$\begin{aligned} N_{33}(\omega) = G_{33}(\omega) &+ H_1(\omega)(G_{11}(\omega)G_{33}(\omega) - G_{13}(\omega)^2) \\ &+ H_2(\omega)(G_{22}(\omega)G_{33}(\omega) - G_{23}(\omega)^2) \\ &+ H_1(\omega)H_2(\omega)\Big(det\big(\mathbf{G}(\omega)\big)\Big) \end{aligned} \tag{6.13}$$

$$N_{12}(\omega) = N_{21}(\omega) = G_{12}(\omega) + H_3(\omega)\big(G_{12}(\omega)G_{33}(\omega) - G_{13}(\omega)G_{23}(\omega)\big) \tag{6.14}$$

$$N_{13}(\omega) = N_{31}(\omega) = G_{13}(\omega) + H_2(\omega)\big(G_{13}(\omega)G_{22}(\omega) - G_{12}(\omega)G_{23}(\omega)\big) \tag{6.15}$$

$$N_{23}(\omega) = N_{32}(\omega) = G_{23}(\omega) + H_1(\omega)\big(G_{23}(\omega)G_{11}(\omega) - G_{12}(\omega)G_{13}(\omega)\big) \tag{6.16}$$

The matrix $\mathbf{G}_{\mathrm{H}}(\omega)$ (Eq. (6.9)) defines the dynamic behaviour of the joint H-S system represented in Figure 6.1.

6.1.1 SDOF Structure

It is now considered the case of a SDOF structure. The modal parameters defining the dynamic behaviour of this structure are defined as in Eq. (6.17).

$$\Phi = [\varphi_1 \quad \varphi_2 \quad \varphi_3]^T, \omega_n , \zeta \tag{6.17}$$

The FRFs of the empty structure are defined as in Eq. (6.18).

$$\mathbf{G}(\omega) = \frac{1}{\omega_n^2 - \omega^2 + 2i\zeta\omega\omega_n}\begin{bmatrix} \varphi_1^2 & \varphi_1\varphi_2 & \varphi_1\varphi_3 \\ \varphi_1\varphi_2 & \varphi_2^2 & \varphi_2\varphi_3 \\ \varphi_1\varphi_3 & \varphi_2\varphi_3 & \varphi_3^2 \end{bmatrix} \tag{6.18}$$

To compute the matrix of the joint H-S system $\mathbf{G}_{\mathrm{H}}(\omega)$, the terms reported in Eqs. (6.10)-(6.16) are computed.

The considered structure is SDOF and the matrix $\mathbf{G}(\omega)$ has dimension 3x3. Therefore, the matrix $\mathbf{G}(\omega)$ is singular (dimension of $\mathbf{G}(\omega)$>number of DOFs) and its determinant, reported in Eq. (6.19), equals zero.

$$\begin{aligned} det\big(\mathbf{G}(\omega)\big) = \frac{1}{\omega_n^2 - \omega^2 + 2i\zeta\omega\omega_n}(&-\varphi_3^2(\varphi_1\varphi_2)^2 \\ &+ 2\varphi_1\varphi_2\varphi_1\varphi_3\varphi_2\varphi_3 - \varphi_2^2(\varphi_1\varphi_3)^2 - \varphi_1^2(\varphi_2\varphi_3)^2 \\ &+ \varphi_1^2\varphi_2^2\varphi_3^2) = 0 \end{aligned} \tag{6.19}$$

In the case of a SDOF structure, only the first four terms in Eq. (6.10) are non-zero, as proved in Eq. (6.20).

$$
\begin{aligned}
den\left(\mathbf{G}_{\mathrm{H}}(\omega)\right) &= 1 + G_{11}(\omega)H_1(\omega) + G_{22}(\omega)H_2(\omega) + G_{33}(\omega)H_3(\omega) \\
&+ \left(\frac{1}{\omega_n^2 - \omega^2 + 2\mathrm{i}\zeta\omega\omega_n}\right)^2 H_1(\omega)H_2(\omega)(\varphi_1^2\varphi_2^2 \\
&- \varphi_1\varphi_2\varphi_1\varphi_2) \\
&+ \left(\frac{1}{\omega_n^2 - \omega^2 + 2\mathrm{i}\zeta\omega\omega_n}\right)^2 H_1(\omega)H_3(\omega)(\varphi_1^2\varphi_3^2 \\
&- \varphi_1\varphi_3\varphi_1\varphi_3) \\
&+ \left(\frac{1}{\omega_n^2 - \omega^2 + 2\mathrm{i}\zeta\omega\omega_n}\right)^2 H_2(\omega)H_3(\omega)(\varphi_2^2\varphi_3^2 \\
&- \varphi_2\varphi_3\varphi_2\varphi_3) + H_1(\omega)H_2(\omega)H_3(\omega)\left(det\left(\boldsymbol{G}(\omega)\right)\right) \\
&= 1 + G_{11}(\omega)H_1(\omega) + G_{22}(\omega)H_2(\omega) + G_{33}(\omega)H_3(\omega)
\end{aligned}
\tag{6.20}
$$

The terms of the matrix $\mathbf{G}_{\mathrm{H}}(\omega)$ reported in Eqs. (6.11)-(6.16) can be simplified as in Eqs. (6.21)-(6.26).

$$
\begin{aligned}
&N_{11}(\omega) = G_{11}(\omega) + H_2(\omega)(\varphi_1^2\varphi_2^2 - \varphi_1\varphi_2\varphi_1\varphi_2) + H_3(\omega)(\varphi_1^2\varphi_3^2 - \\
&\varphi_1\varphi_3\varphi_1\varphi_3) + H_2(\omega)H_3(\omega)\left(det\left(\mathbf{G}(\omega)\right)\right) = G_{11}(\omega)
\end{aligned}
\tag{6.21}
$$

$$
\begin{aligned}
N_{22}(\omega) = G_{22}(\omega) &+ H_1(\omega)(\varphi_1^2\varphi_2^2 - \varphi_1\varphi_2\varphi_1\varphi_2) \\
&+ H_3(\omega)(\varphi_2^2\varphi_3^2 - \varphi_2\varphi_3\varphi_2\varphi_3) \\
&+ H_1(\omega)H_3(\omega)\left(det\left(\mathbf{G}(\omega)\right)\right) = G_{22}(\omega)
\end{aligned}
\tag{6.22}
$$

$$
\begin{aligned}
N_{33}(\omega) = G_{33}(\omega) &+ H_1(\omega)(\varphi_1^2\varphi_3^2 - \varphi_1\varphi_3\varphi_1\varphi_3) \\
&+ H_2(\omega)(\varphi_2^2\varphi_3^2 - \varphi_2\varphi_3\varphi_2\varphi_3) \\
&+ H_1(\omega)H_2(\omega)\left(det\left(\mathbf{G}(\omega)\right)\right) = G_{33}(\omega)
\end{aligned}
\tag{6.23}
$$

$$
N_{12}(\omega) = N_{21}(\omega) = G_{12}(\omega) + H_3(\omega)(\varphi_1\varphi_2\varphi_3^2 - \varphi_1\varphi_3\varphi_2\varphi_3) = G_{12}(\omega) \tag{6.24}
$$

$$
N_{13}(\omega) = N_{31}(\omega) = G_{13}(\omega) + H_2(\omega)(\varphi_1\varphi_3\varphi_2^2 - \varphi_1\varphi_2\varphi_2\varphi_3) = G_{13}(\omega) \tag{6.25}
$$

$$
N_{23}(\omega) = N_{32}(\omega) = G_{23}(\omega) + H_1(\omega)(\varphi_2\varphi_3\varphi_1^2 - \varphi_1\varphi_2\varphi_1\varphi_3) = G_{23}(\omega) \tag{6.26}
$$

By substituting the terms reported in Eqs. (6.20)- (6.26) in Eq. (6.9), Eq. (6.27) is obtained.

$$
\begin{aligned}
&\mathbf{G}_{\mathrm{H}}(\omega) \\
&= \frac{1}{1 + G_{11}(\omega)H_1(\omega) + G_{22}(\omega)H_2(\omega) + G_{33}(\omega)H_3(\omega)} \cdot \begin{bmatrix} G_{11}(\omega) & G_{12}(\omega) & G_{13}(\omega) \\ G_{21}(\omega) & G_{22}(\omega) & G_{23}(\omega) \\ G_{31}(\omega) & G_{32}(\omega) & G_{33}(\omega) \end{bmatrix} \\
&= \frac{1}{\left(\frac{1}{\omega_n^2 - \omega^2 + 2\mathrm{i}\zeta\omega\omega_n}\right)(H_1(\omega)\varphi_1^2 + H_2(\omega)\varphi_2^2 + H_3(\omega)\varphi_3^2 + \omega_n^2 - \omega^2 + 2\mathrm{i}\zeta\omega\omega_n)} \\
&\cdot \left(\frac{1}{\omega_n^2 - \omega^2 + 2\mathrm{i}\zeta\omega\omega_n}\right) \begin{bmatrix} \varphi_1^2 & \varphi_1\varphi_2 & \varphi_1\varphi_3 \\ \varphi_1\varphi_2 & \varphi_2^2 & \varphi_2\varphi_3 \\ \varphi_1\varphi_3 & \varphi_2\varphi_3 & \varphi_3^2 \end{bmatrix} \\
&= \frac{1}{(H_1(\omega)\varphi_1^2 + H_2(\omega)\varphi_2^2 + H_3(\omega)\varphi_3^2 + \omega_n^2 - \omega^2 + 2\mathrm{i}\zeta\omega\omega_n)} \begin{bmatrix} \varphi_1^2 & \varphi_1\varphi_2 & \varphi_1\varphi_3 \\ \varphi_1\varphi_2 & \varphi_2^2 & \varphi_2\varphi_3 \\ \varphi_1\varphi_3 & \varphi_2\varphi_3 & \varphi_3^2 \end{bmatrix}
\end{aligned}
\tag{6.27}
$$

Eq. (6.27) defines the dynamic behaviour of the joint H-S system for the case of a SDOF structure. Each term of Eq. (6.27) can be synthetically expressed as in Eq. (6.28).

$$
G_{H,ik}(\omega) = \frac{\varphi_i\varphi_k}{\left(\omega_n^2 - \omega^2 + 2\mathrm{i}\zeta\omega\omega_n + \sum_{s=1}^{n\_subjects} H_{\mathrm{s}}(\omega)\varphi_s^2\right)} \tag{6.28}
$$

Eq. (6.28) defines the generic term ik of the matrix of the joint H-S system.

For the sake of clarity, Eq. (6.28) was derived considering the case of a 3x3 $\mathbf{G}(\omega)$ but its validity can be extended to the case of a generic mxm $\mathbf{G}(\omega)$ matrix. Eq. (6.28) significantly simplifies the determination of $\mathbf{G}_{\mathrm{H}}(\omega)$. Indeed, this matrix can be directly determined by solving Eq. (6.28) instead of solving Eq. (6.4).

The properties of Eq. (6.28) will be discussed in Section 5.3.

In the next subsection the matrix $\mathbf{G}_{\mathrm{H}}(\omega)$ is derived considering the case of a 2 DOFs structure and is compared with the same matrix obtained via superposition of 2 SDOF systems.

6.1.2 2DOFs structure vs superposition of 2 SDOF systems

It is now considered the case of a 2DOFs structure. The modal parameters defining the dynamic behaviour of this structure are defined as in Eq. (6.29) .

$$
\boldsymbol{\Phi}_1 = [\varphi_{1,1} \quad \varphi_{2,1} \quad \varphi_{3,1}]^T, \boldsymbol{\Phi}_2 = [\varphi_{1,2} \quad \varphi_{2,2} \quad \varphi_{3,2}]^T, \omega_{n1}, \omega_{n2}, \zeta_1, \zeta_2 \tag{6.29}
$$

Accordingly, the matrix $\mathbf{G}(\omega)$ is expressed as in Eq. (6.30) or Eq. (6.31).

$$\mathbf{G}(\omega) = \frac{1}{\omega_{n1}^2 - \omega^2 + 2\mathrm{i}\zeta_1\omega\omega_{n1}} \begin{bmatrix} \varphi_{1,1}^2 & \varphi_{1,1}\varphi_{2,1} & \varphi_{1,1}\varphi_{3,1} \\ \varphi_{1,1}\varphi_{2,1} & \varphi_{2,1}^2 & \varphi_{2,1}\varphi_{3,1} \\ \varphi_{1,1}\varphi_{3,1} & \varphi_{2,1}\varphi_{3,1} & \varphi_{3,1}^2 \end{bmatrix} + \frac{1}{\omega_{n2}^2 - \omega^2 + 2\mathrm{i}\zeta_2\omega\omega_{n2}} \begin{bmatrix} \varphi_{1,2}^2 & \varphi_{1,2}\varphi_{2,2} & \varphi_{1,2}\varphi_{3,2} \\ \varphi_{1,2}\varphi_{2,2} & \varphi_{2,2}^2 & \varphi_{2,2}\varphi_{3,2} \\ \varphi_{1,2}\varphi_{3,2} & \varphi_{2,2}\varphi_{3,2} & \varphi_{3,2}^2 \end{bmatrix} \tag{6.30}$$

$$\mathbf{G}(\omega) = \begin{bmatrix} \frac{\varphi_{1,1}^2}{D_1} + \frac{\varphi_{1,2}^2}{D_2} & \frac{\varphi_{1,1}\varphi_{2,1}}{D_1} + \frac{\varphi_{1,2}\varphi_{2,2}}{D_2} & \frac{\varphi_{1,1}\varphi_{3,1}}{D_1} + \frac{\varphi_{1,2}\varphi_{3,2}}{D_2} \\ \frac{\varphi_{1,1}\varphi_{2,1}}{D_1} + \frac{\varphi_{1,2}\varphi_{2,2}}{D_2} & \frac{\varphi_{2,1}^2}{D_1} + \frac{\varphi_{2,2}^2}{D_2} & \frac{\varphi_{2,1}\varphi_{3,1}}{D_1} + \frac{\varphi_{2,2}\varphi_{3,2}}{D_2} \\ \frac{\varphi_{1,1}\varphi_{3,1}}{D_1} + \frac{\varphi_{1,2}\varphi_{3,2}}{D_2} & \frac{\varphi_{2,1}\varphi_{3,1}}{D_1} + \frac{\varphi_{2,2}\varphi_{3,2}}{D_2} & \frac{\varphi_{3,1}^2}{D_1} + \frac{\varphi_{3,2}^2}{D_2} \end{bmatrix} = \begin{bmatrix} G_{11}(\omega) & G_{12}(\omega) & G_{13}(\omega) \\ G_{21}(\omega) & G_{22}(\omega) & G_{23}(\omega) \\ G_{31}(\omega) & G_{32}(\omega) & G_{33}(\omega) \end{bmatrix} \tag{6.31}$$

The terms D_1 and D_2 are made explicit in Eqs. (6.32) and (6.33)

$$D_1 = \omega_{n1}^2 - \omega^2 + 2\mathrm{i}\zeta_1\omega\omega_{n1} \tag{6.32}$$

$$D_2 = \omega_{n2}^2 - \omega^2 + 2\mathrm{i}\zeta_2\omega\omega_{n2} \tag{6.33}$$

By substituting the terms of Eq. (6.31) in Eq. (6.8), Eq. (6.34) is obtained. Indeed, also in this case the dimension of $\mathbf{G}(\omega)$ is higher than the number of DOFs of the considered structure.

$$det\big(\mathbf{G}(\omega)\big) = 0 \tag{6.34}$$

In order to provide a clear comparison between the use of a complete model and the superposition of effects, the simplifying assumption given in Eq. (6.35) is considered and the term $G_{H,11}(\omega)$ is compared.

$$H_1 = H_2 = H\ ,\ H_3 = 0 \tag{6.35}$$

To compute the term $G_{H,11}(\omega)$ using the complete model, the non-zero terms of Eqs. (6.10) and (6.11) are made explicit in Eqs. (6.36)-(6.40).

$$G_{11}(\omega) = \frac{\varphi_{1,1}^2}{D_1} + \frac{\varphi_{1,2}^2}{D_2} = \frac{D_2\varphi_{1,1}^2 + D_1\varphi_{1,2}^2}{D_1 D_2} \tag{6.36}$$

$$G_{22}(\omega) = \frac{\varphi_{2,1}^2}{D_1} + \frac{\varphi_{2,2}^2}{D_2} = \frac{D_2\varphi_{2,1}^2 + D_1\varphi_{2,2}^2}{D_1 D_2} \tag{6.37}$$

$$G_{12}(\omega) = G_{21}(\omega) = \frac{\varphi_{1,1}\varphi_{2,1}}{D_1} + \frac{\varphi_{1,2}\varphi_{2,2}}{D_2} = \frac{D_2\varphi_{1,1}\varphi_{2,1} + D_1\varphi_{1,2}\varphi_{2,2}}{D_1 D_2} \tag{6.38}$$

$$\begin{aligned}
&(G_{11}(\omega)G_{22}(\omega) - G_{12}(\omega)^2) \\
&\quad = \frac{1}{(D_1 D_2)^2}\Big[\big(D_2\varphi_{1,1}^2 + D_1\varphi_{1,2}^2\big)\big(D_2\varphi_{2,1}^2 + D_1\varphi_{2,2}^2\big) \\
&\quad - \big(D_2\varphi_{1,1}\varphi_{2,1} + D_1\varphi_{1,2}\varphi_{2,2}\big)^2\Big] \\
&\quad = \frac{1}{(D_1 D_2)^2}\big[D_2^2\varphi_{1,1}^2\varphi_{2,1}^2 + D_1 D_2\varphi_{1,1}^2\varphi_{2,2}^2 + D_1 D_2\varphi_{2,1}^2\varphi_{1,2}^2 \\
&\quad + D_1^2\varphi_{1,2}^2\varphi_{2,2}^2 \\
&\quad - \big(D_2^2\varphi_{1,1}^2\varphi_{2,1}^2 + D_1^2\varphi_{1,2}^2\varphi_{2,2}^2 + 2\varphi_{1,1}\varphi_{2,1}\varphi_{1,2}\varphi_{2,2}\big)\big]
\end{aligned} \tag{6.39}$$

$$(G_{11}(\omega)G_{22}(\omega) - G_{12}(\omega)^2) = \frac{\varphi_{1,1}^2\varphi_{2,2}^2 + \varphi_{2,1}^2\varphi_{1,2}^2 - 2\varphi_{1,1}\varphi_{2,1}\varphi_{1,2}\varphi_{2,2}}{D_1 D_2} \tag{6.40}$$

By substituting Eqs. (6.36),(6.37) and (6.40) in (6.10), Eq. (6.41) is obtained.

$$\begin{aligned}
den\big(\mathbf{G}_{\mathrm{H}}(\omega)\big) &= 1 + \frac{D_2\varphi_{1,1}^2 + D_1\varphi_{1,2}^2}{D_1 D_2}H(\omega) + \frac{D_2\varphi_{2,1}^2 + D_1\varphi_{2,2}^2}{D_1 D_2}H(\omega) \\
&\quad + H^2(\omega)\frac{\varphi_{1,1}^2\varphi_{2,2}^2 + \varphi_{2,1}^2\varphi_{1,2}^2 - 2\varphi_{1,1}\varphi_{2,1}\varphi_{1,2}\varphi_{2,2}}{D_1 D_2} \\
&= \frac{1}{D_1 D_2}\Big[D_1 D_2 + \big(D_2\varphi_{1,1}^2 + D_1\varphi_{1,2}^2 + D_2\varphi_{2,1}^2 + D_1\varphi_{2,2}^2\big)H(\omega) \\
&\quad + \Big(\varphi_{1,1}^2\varphi_{2,2}^2 + \varphi_{2,1}^2\varphi_{1,2}^2 - 2\varphi_{1,1}\varphi_{2,1}\varphi_{1,2}\varphi_{2,2}\Big)H^2(\omega)\Big]
\end{aligned} \tag{6.41}$$

Similarly, by substituting Eqs. (6.36) and (6.40) in (6.11), Eq. (6.42) is obtained.

$$
\begin{aligned}
N_{11}(\omega) = & \frac{D_2\varphi_{1,1}^2 + D_1\varphi_{1,2}^2}{D_1 D_2} \\
& + H(\omega)\frac{\varphi_{1,1}^2\varphi_{2,2}^2 + \varphi_{2,1}^2\varphi_{1,2}^2 - 2\varphi_{1,1}\varphi_{2,1}\varphi_{1,2}\varphi_{2,2}}{D_1 D_2} \\
& = \frac{1}{D_1 D_2}\left[D_2\varphi_{1,1}^2 + D_1\varphi_{1,2}^2\right. \\
& \left. + \left(\varphi_{1,1}^2\varphi_{2,2}^2 + \varphi_{2,1}^2\varphi_{1,2}^2 - 2\varphi_{1,1}\varphi_{2,1}\varphi_{1,2}\varphi_{2,2}\right)H(\omega)\right]
\end{aligned}
\tag{6.42}
$$

Combining Eq. (6.41) and (6.42), Eq. (6.43) is obtained.

$$
\begin{aligned}
& G_{H,11}(\omega) = \frac{N_{11}(\omega)}{den\left(\mathbf{G}_{\mathrm{H}}(\omega)\right)} \\
& = \frac{D_2\varphi_{1,1}^2 + D_1\varphi_{1,2}^2 + \left(\varphi_{1,1}^2\varphi_{2,2}^2 + \varphi_{2,1}^2\varphi_{1,2}^2 - 2\varphi_{1,1}\varphi_{2,1}\varphi_{1,2}\varphi_{2,2}\right)H(\omega)}{D_1 D_2 + \left(D_2\varphi_{1,1}^2 + D_1\varphi_{1,2}^2 + D_2\varphi_{2,1}^2 + D_1\varphi_{2,2}^2\right)H(\omega) + \left(\varphi_{1,1}^2\varphi_{2,2}^2 + \varphi_{2,1}^2\varphi_{1,2}^2 - 2\varphi_{1,1}\varphi_{2,1}\varphi_{1,2}\varphi_{2,2}\right)H^2(\omega)}
\end{aligned}
\tag{6.43}
$$

Eq. (6.43) is the FRF obtained using the complete model of the joint H-S system as formulated in Eq. (6.4).

The same term can be obtained via superposition of effects from Eq. (6.28) by summing the contribution of two modes, and is computed in Eq. (6.44).

$$
\begin{aligned}
& G_{H,11}(\omega) = \frac{\varphi_{1,1}^2}{\left(D_1 + H(\omega)\left(\varphi_{1,1}^2 + \varphi_{2,1}^2\right)\right)} + \frac{\varphi_{1,2}^2}{\left(D_2 + H(\omega)\left(\varphi_{1,2}^2 + \varphi_{2,2}^2\right)\right)} \\
& = \frac{D_2\varphi_{1,1}^2 + D_1\varphi_{1,2}^2 + \left(\varphi_{1,1}^2\varphi_{2,2}^2 + \varphi_{2,1}^2\varphi_{1,2}^2 + 2\varphi_{1,1}^2\varphi_{1,2}^2\right)H(\omega)}{D_1 D_2 + \left(D_2\varphi_{1,1}^2 + D_1\varphi_{1,2}^2 + D_2\varphi_{2,1}^2 + D_1\varphi_{2,2}^2\right)H(\omega) + \left(\varphi_{1,1}^2\varphi_{2,2}^2 + \varphi_{2,1}^2\varphi_{1,2}^2 + \varphi_{1,1}^2\varphi_{1,2}^2 + \varphi_{2,1}^2\varphi_{2,2}^2\right)H^2(\omega)}
\end{aligned}
\tag{6.44}
$$

Comparing Eq. (6.43) with Eq. (6.44) it is immediate to note the difference in the results using the two approaches. Particularly, the equations differ for the evidenced terms. In the next subsection the difference between the two approaches is discussed with the support of numerical simulations.

6.1.2.1 Complete model vs SDOF model: numerical examples

The previous section proposed an analysis of the differences between the use of a complete model and the use of superposition of effects to describe the H-S phenomenon. The main advantage of using the superposition of effects is the high reduction of the computational cost. As an example, the time required to solve the complete model of a joint grandstand-human system (with the grandstand having 1150 people on it) is about 600 s. Conversely, the result via superposition of the effects can be obtained in less than 1 s.

A numerical example is used to analyze the differences between the two approaches. Particularly, the dynamic behavior of a structure with the first natural frequency equal to 5 Hz was simulated. The second natural frequency was varied in order to investigate the differences among the results. In all cases the damping ration value was set to 1% for both the vibration modes. The mode shapes of the considered structure are shown in Figure 6.2.

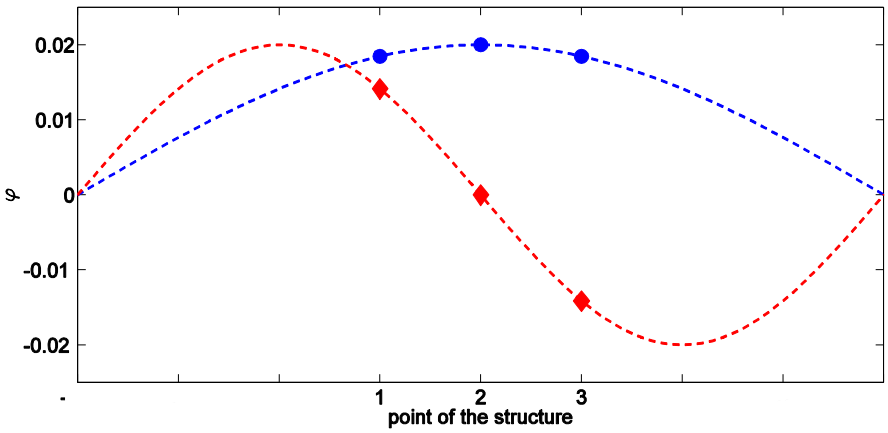

Figure 6.2: Mode shapes

Figure 6.3 reports the FRF for a structure with the second natural frequency equal to 6.5 Hz. In this case, as the two vibration modes have natural frequencies that are quite separate in frequency, the differences between the results obtained with the two approaches is low.

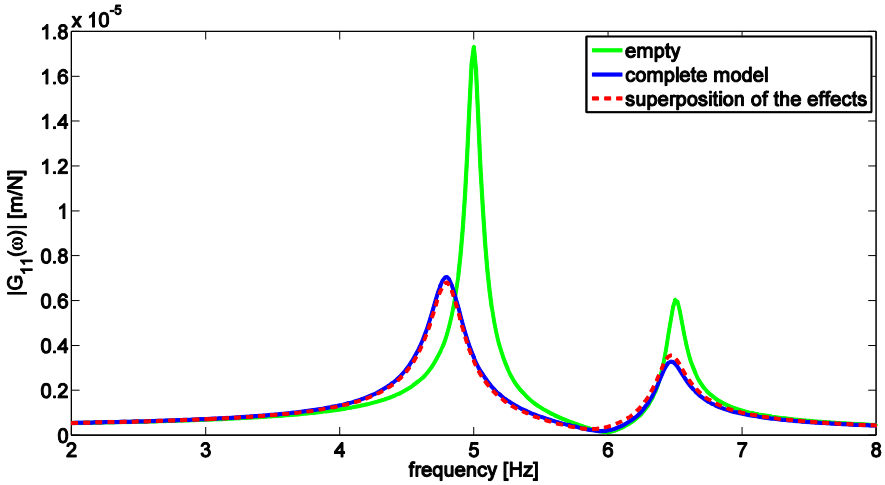

Figure 6.3: $\zeta_1=\zeta_2=1\%$, $f_{n1}=5$ Hz, $f_{n2}=6.5$ Hz

Figure 6.4 and Figure 6.5 report the FRF for a structure with the second natural frequency equal to 5.5 Hz and 5.1 Hz respectively. It is possible to notice that, as the distance between the two frequencies reduces, the differences between the FRFs obtained with the two approaches increase.

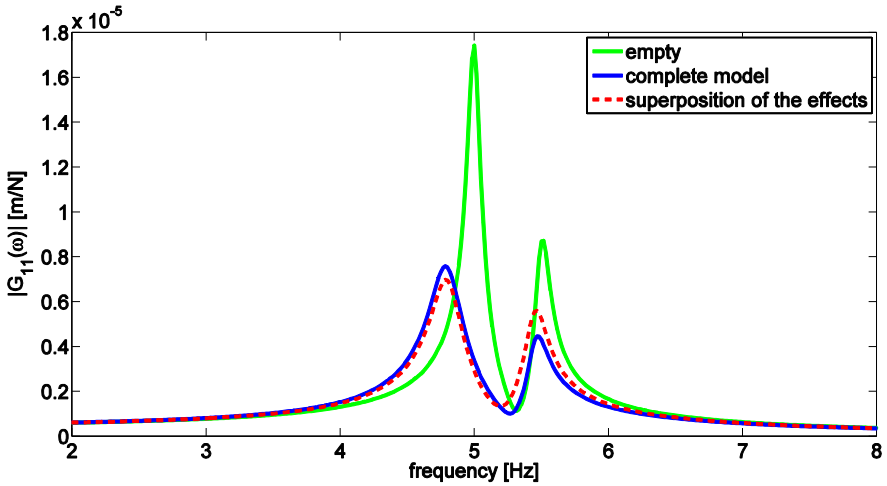

Figure 6.4: $\zeta_1=\zeta_2=1\%$, $f_{n1}=5$ Hz, $f_{n2}=5.5$ Hz

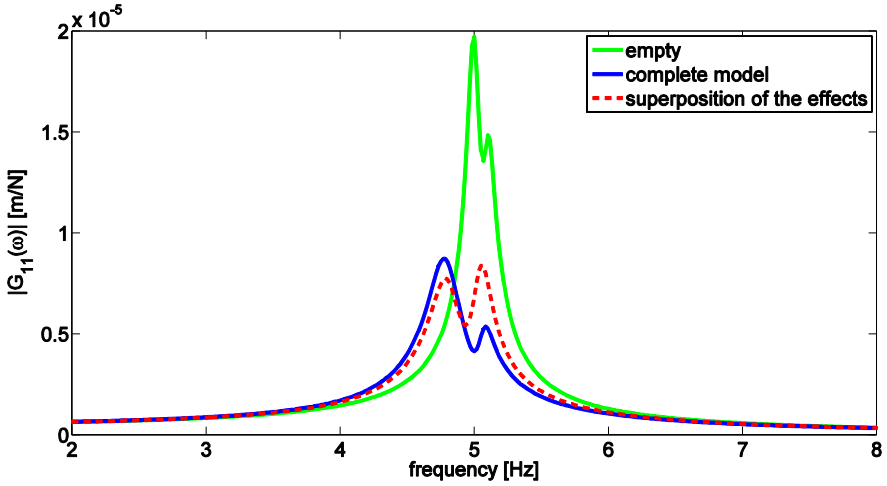

Figure 6.5: $\zeta_1=\zeta_2=1\%$, $f_{n1}=5$ Hz, $f_{n2}=5.1$ Hz

The numerical examples proposed in this Section aimed at showing that the use of superposition of the effects might be acceptable in some practical cases. However, it is suggested to verify the acceptability of such an assumption for any particular structure. If the superposition of effects can be applied without the results being significantly affected, the computational cost highly reduces. Indeed, the complete problem requires the solution of Eq. (6.4), whose cost depends on the

dimension of the matrices $\mathbf{G}(\omega)$ and $\mathbf{H}(\omega)$ (thus, on the number of people on the structure). Conversely, in case it is possible to assume the structure is 1DOF, the problem can be solved by using Eq. (6.28) with high reduction of computational cost.

An extensive analysis of the error introduced by the hypothesis of superposition of the effects is proposed in Section 6.3.1.

6.2 An approximate 1DOF approach

This section proposes a further simplification of the problem analyzed in the previous section under the hypothesis of SDOF structure. The purpose is to find a simple approach to understand the influence of people at a first approximation level from the direct analysis of the apparent mass curves.

It is supposed to have a structure occupied by an arbitrary number of subjects defined through the driving point FRF expressed in terms of the apparent mass as in Eq. (6.45)

$$H_{\mathrm{j}}(\omega) = H(\omega) = -\omega^2 M^*(\omega) = -\omega^2 \bar{M} m^*(\omega) \tag{6.45}$$

with $\bar{M}$ equal to the physical mass of the subject and $m^*(\omega)$ equal to the non-dimensional apparent mass.

Substituting Eq. (6.45) in Eq. (6.28), Eq. (6.46) is obtained.

$$\begin{aligned} G_{H,ik}(\omega) &= \frac{\varphi_i \varphi_k}{\left(\omega_n^2 - \omega^2 + 2\mathrm{i}\zeta\omega\omega_n + \sum_{j=1}^{n\_subjects} -\omega^2 M^*(\omega)\varphi_j^2\right)} = \\ &= \frac{\varphi_i \varphi_k}{\left(\omega_n^2 - \omega^2 + 2\mathrm{i}\zeta\omega\omega_n - \omega^2 M^*(\omega) \sum_{j=1}^{n\_subjects} \varphi_j^2\right)} \end{aligned} \tag{6.46}$$

By defining the apparent mass $M^*(\omega)$ as sum of its real and imaginary parts, as in Eq. (6.47)

$$M^*(\omega) = Re\{M^*(\omega)\} + \mathrm{i} \cdot Im\{M^*(\omega)\} \tag{6.47}$$

and defining the weighting coefficient β as in Eq. (6.48)

$$\beta = \bar{M} \cdot \sum_{j=1}^{n\_subjects} \varphi_j^2 \tag{6.48}$$

the FRF of the joint H-S system can be expressed as in Eq. (6.49)

$$G_{H,ik}(\omega) = \frac{\varphi_i \varphi_k}{\left(\omega_n^2 - \omega^2(1 + \beta \cdot Re\{m^*(\omega)\}) + \mathrm{i}\omega(2\zeta\omega_n - \omega\beta \cdot Im\{m^*(\omega)\})\right)} \tag{6.49}$$

The parameter β represents a mass ratio between:

- The physical mass of the subjects weighted for the square of the mode shapes
- The modal mass

As an example, the first mode of the structure investigated by Sachse (Chapter 3, Section 3.5) can be considered. For this structure, with modal mass 7040 kg and with the mode shape represented in Figure 3.30, a physical mass of subjects uniformly distributed equal to the modal mass would result in β=0.5, a physical mass of the subjects equal to 1/5 of the modal mass would result in β=0.1.

Assuming the resonance as the frequency at which the FRF reaches -90°, the denominator of Eq. (6.49) must respect the condition expressed in Eq. (6.50)

$$\omega_n^2 - \omega^2(1 + \beta \cdot Re\{m^*(\omega)\}) = 0 \tag{6.50}$$

Eq. (6.50) can be solved numerically and leads to the determination of a frequency $\bar{\omega}$ that respects the condition expressed in Eq. (6.51).

$$\frac{\omega_n^2}{(1 + \beta \cdot Re\{m^*(\bar{\omega})\})} = \bar{\omega}^2 \tag{6.51}$$

The graphical solution of Eq. (6.50) is shown through an example in Figure 6.6.

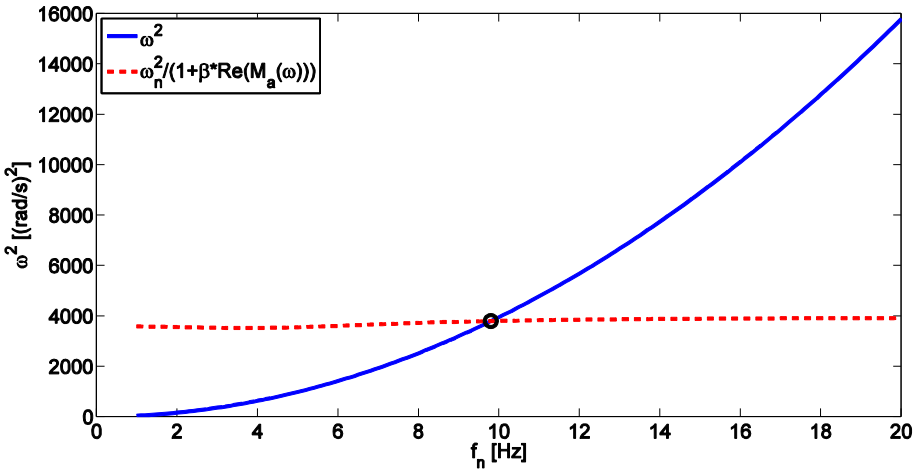

Figure 6.6: Approximate natural frequency (ζ=1%, f_{n1}=10 Hz)

Assuming the apparent mass $m^*(\omega)$ is constant and equal to the value that satisfied the condition stated in Eq. (6.51), FRF of the joint H-S system can be expressed as in Eq. (6.52)

$$\tilde{G}_{H,ik}(\omega) = \frac{\varphi_i \varphi_k}{\left(\omega_n^2 - \omega^2(1+\beta \cdot Re\{m^*(\overline{\omega})\}) + \mathrm{i}\omega(2\zeta\omega_n - \omega\beta \cdot Im\{m^*(\overline{\omega})\})\right)} \tag{6.52}$$

Eq. (6.52) can be rewritten in the form of (6.53)

$$\tilde{G}_{H,ik}(\omega) = \frac{\varphi_i \varphi_k/(1+\beta \cdot Re\{m^*(\overline{\omega})\})}{\left(\omega_n^2/(1+\beta \cdot Re\{m^*(\overline{\omega})\}) - \omega^2 + \mathrm{i}\omega\dfrac{(2\zeta\omega_n\overline{\omega}/\overline{\omega} - \omega\beta \cdot Im\{m^*(\overline{\omega})\})}{(1+\beta \cdot Re\{m^*(\overline{\omega})\})}\right)} \tag{6.53}$$

and the equivalent approximate modal parameters of the joint H-S can be expressed as in Eqs. (6.54) and (6.55).

$$\overline{\omega} = \sqrt{\omega_n^2/(1+\beta \cdot Re\{m^*(\overline{\omega})\})} \tag{6.54}$$

$$\overline{\zeta} = \frac{(2\zeta\omega_n/\overline{\omega} - \beta \cdot Im\{m^*(\overline{\omega})\})}{(1+\beta \cdot Re\{m^*(\overline{\omega})\})} \tag{6.55}$$

Eq. (6.52) allows to directly determine the effect of people in terms of changes of modal parameters.

As an example, Figure 6.7 and Figure 6.8 show a comparison between the results obtained with the complete model and the approximate solution for two structures with ζ=1% and f_n=4 Hz, f_n=8 Hz.

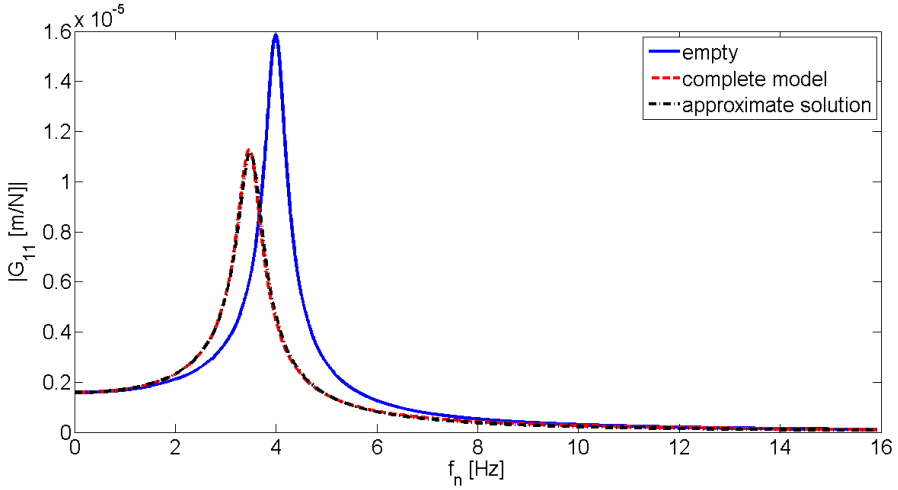

Figure 6.7: Approximate FRF (ζ=1%, f_n=4 Hz)

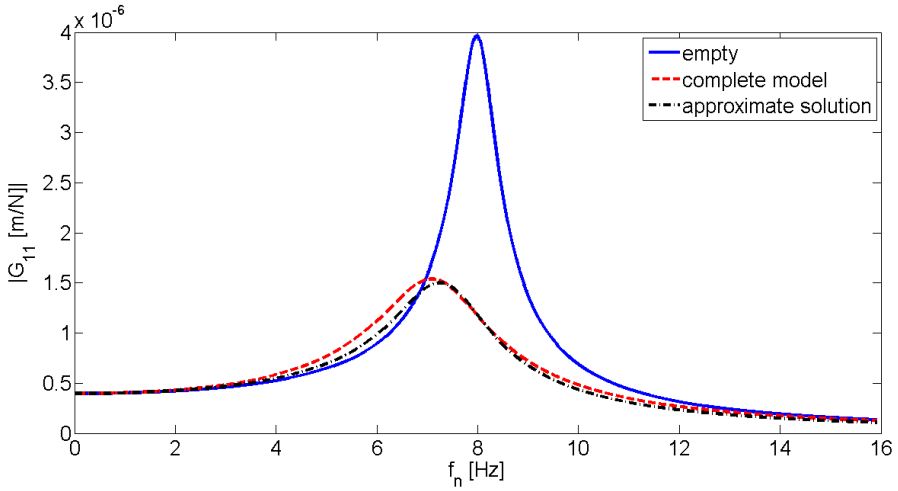

Figure 6.8: Approximate FRF (ζ=1%, f_n=8 Hz)

The quality of the approximation depends on the amount of the effect induced by people but results generally showed a good agreement between the approximate and the complete solution.

An extensive analysis of the error introduced by the hypothesis of superposition of the effects is proposed in Section 6.3.2.

6.3 Lumped parameters model and feedback approach

In order to propose an extensive investigation of the differences between using the complete model of H-S interaction and the superposition of the effects, the following simplifying hypothesis are assumed:

- Only one subject is standing on the structure at point 1. Therefore, the co-located FRF of point 1 ($G_{H,11}$) is analysed.
- The apparent mass of the subject is described through the 1DOF lumped parameters model proposed in [51] and named (1a) in [51] (Figure 2.1, Chapter 2). The corresponding normalised apparent mass curve is reported in Figure 6.9.

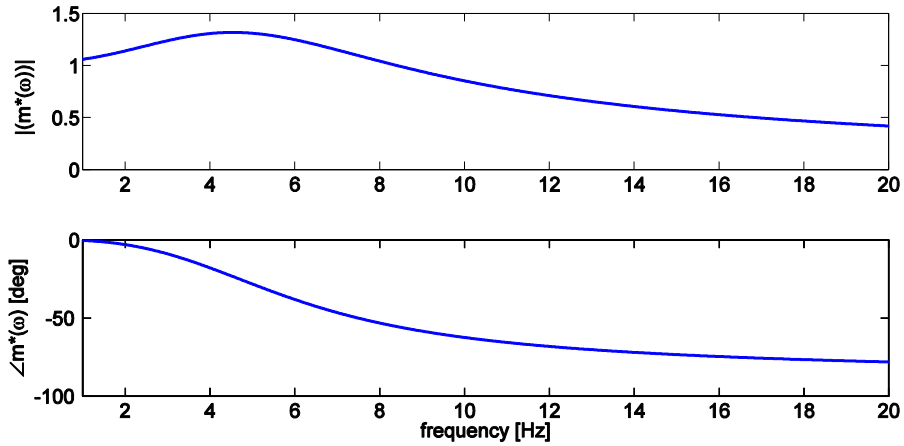

Figure 6.9: Apparent mass – standing subjects – model 1a

Under the second hypothesis (lumped parameters model), the apparent mass of the subject standing on the structure can be expressed (in the Laplace domain) as in Eq. (6.56)

$$H(s) = \bar{M} \cdot s^2 \frac{m_1 c_1 \cdot s + m_1 k_1}{m_1 \cdot s^2 + m_1 \cdot s + k_1} \tag{6.56}$$

The first hypothesis (i.e. $\mathbf{G}(\omega)$ is a 1x1 matrix) allows to easily express the FRF of the joint H-S system in the Laplace domain. Therefore, $G_{H,11}(s)$ can be derived from Eq. (6.4) and is expressed as in Eq. (6.57).

$$G_{H,11}(s) = \frac{1}{1/G_{11}(s) + H(s)} \tag{6.57}$$

It is noticed that Eq. (6.57) represents the solution of the Feedback system drawn in Figure 6.10.

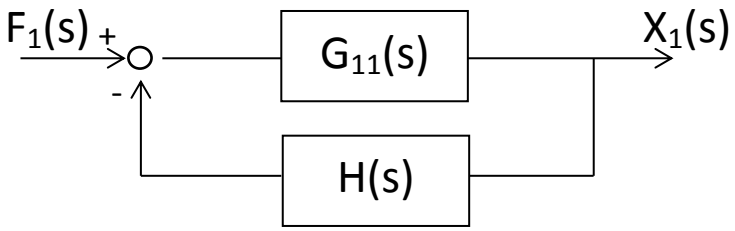

Figure 6.10: Feedback H-S system

Indeed, by solving the system represented in Figure 6.10, the FRF of the joint H-S system can be expressed from Eqs. (6.58)-(6.60)

$$X_1(s) = G_{11}(s)(F_1(s) - X_1(s)H(s)) \tag{6.58}$$

$$X_1(s)\big(1 + G_{11}(s)H(s)\big) = G_{11}(s)F_1(s) \tag{6.59}$$

$$G_{H,11}(s) = \frac{X_1(s)}{F(s)} = \frac{G_{11}(s)}{1 + H(s)G_{11}(s)} = \frac{1}{1/G_{11}(s) + H(s)} \tag{6.60}$$

The so-defined system was used to investigate the differences between the various approaches (complete model, superposition of effects, approximate solution).

Particularly, two analyses were performed. The results are reported in subparagraphs 6.3.1 and 6.3.2 respectively.

In 6.3.1 the results obtained with the complete model (Eqs. (6.61),(6.62))

$$G_{11}(s) = \frac{\varphi_{1,1}^2}{s^2 + 2\zeta_1\omega_{n1}s + \omega_{n1}^2} + \frac{\varphi_{1,2}^2}{s^2 + 2\zeta_2\omega_{n2}s + \omega_{n2}^2} \tag{6.61}$$

$$G_{H,11}(s) = \frac{1}{1/G_{11}(s) + H(s)} \tag{6.62}$$

are compared with the superposition of effects (Eqs. (6.63)-(6.65)) considering the case of a 2DOFs structure.

$$G_{11,1}(s) = \frac{\varphi_{1,1}^2}{s^2 + 2\zeta_1\omega_{n1}s + \omega_{n1}^2} \tag{6.63}$$

$$G_{11,2}(s) = \frac{\varphi_{1,2}^2}{s^2 + 2\zeta_2\omega_{n2}s + \omega_{n2}^2} \tag{6.64}$$

$$G_{H,11}(s) = \frac{1}{1/G_{11,1}(s) + H(s)} + \frac{1}{1/G_{11,2}(s) + H(s)} \tag{6.65}$$

In 5.3.2 the solution of the complete model (Eq. (6.62)) is compared with the approximate solution (Eq. (6.66)) considering the case of a SDOF structure.

$$G_{H,11}(s) = \frac{1}{1/G_{11,1}(s) + \widetilde{H}} \tag{6.66}$$

In Eq. (6.66) $\widetilde{H}$ is obtained with the constant value of apparent mass $m^*(\bar{\omega})$ that satisfies the condition expressed in Eq. (6.51), Figure 6.6.

In the analysis the structural parameters were varied. The results are shown in the next subsection.

6.3.1 Complete model vs superposition of the effects

In order to compare the results obtained with the complete model and the superposition of effects, many simulations were performed considering systems with different parameters. This section reports some of the obtained results, considered significant for the analysis.

All the reported results were obtained by fixing the damping ratio of the two modes of the empty structure (ζ_1, ζ_2), the natural frequency of the first mode (f_{n1}) and β_1, β_2. The natural frequency of the second mode was varied between 1 Hz and 20 Hz in order to cover a wide range of combinations of structural parameters.

The next subsections report a selection of the obtained results.

6.3.1.1 $\zeta_1=\zeta_2=1\%$, $\beta_1=\beta_2=0.1$, various f_{n1}

The first reported results refer to a structure with damping ratio of the two modes equal to 1% and $\beta_1=\beta_2=0.1$. These parameters are considered lifelike for a structure in operating conditions. Figure 6.11 and Figure 6.12 reports the natural frequencies and damping ratios obtained with the complete model and via superposition of the effects for the case $f_{n1}=2$ Hz. Figure 6.13, Figure 6.14 refer to the case of $f_{n1}=6$ Hz and Figure 6.15, Figure 6.16 refer to the case of $f_{n1}=16$ Hz. The 4 curves reported in the Figures represent the modal parameters of the two modes obtained with the complete model and the superposition of the effects.

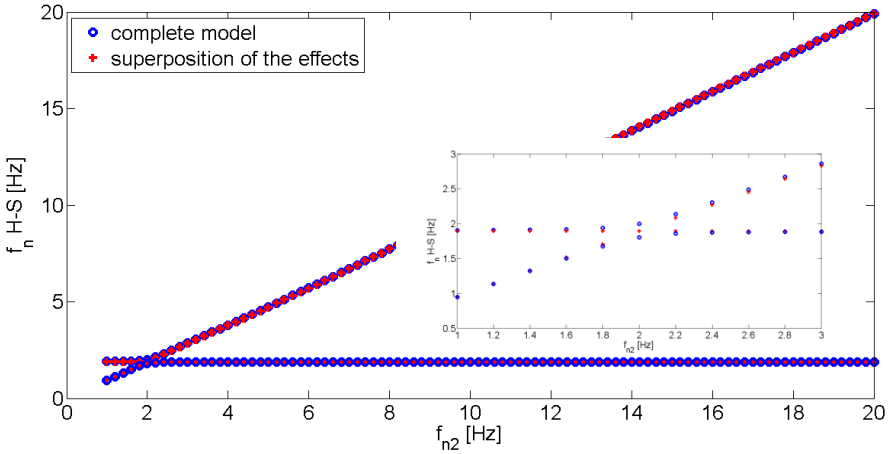

Figure 6.11: Natural frequencies: $\beta_1=\beta_2=0.1$, $\zeta_1=\zeta_2=1\%$, $f_{n1}=2$ Hz

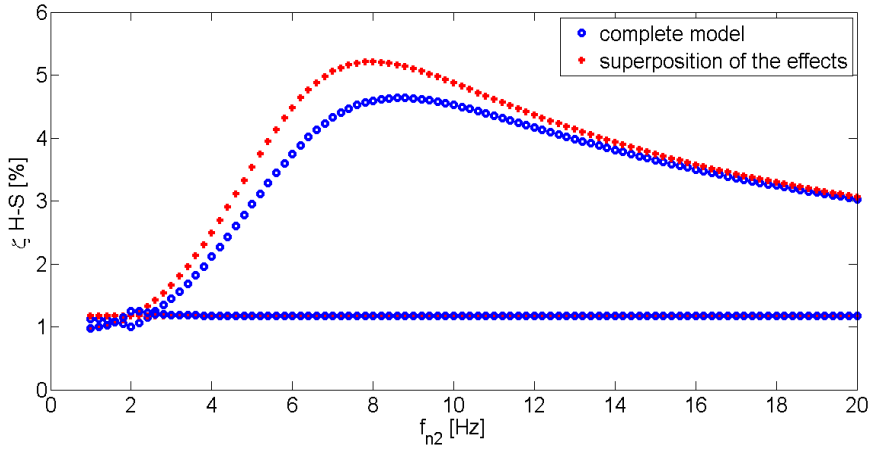

Figure 6.12: Damping ratios: $\beta_1=\beta_2=0.1$, $\zeta_1=\zeta_2=1\%$, $f_{n1}=2$ Hz

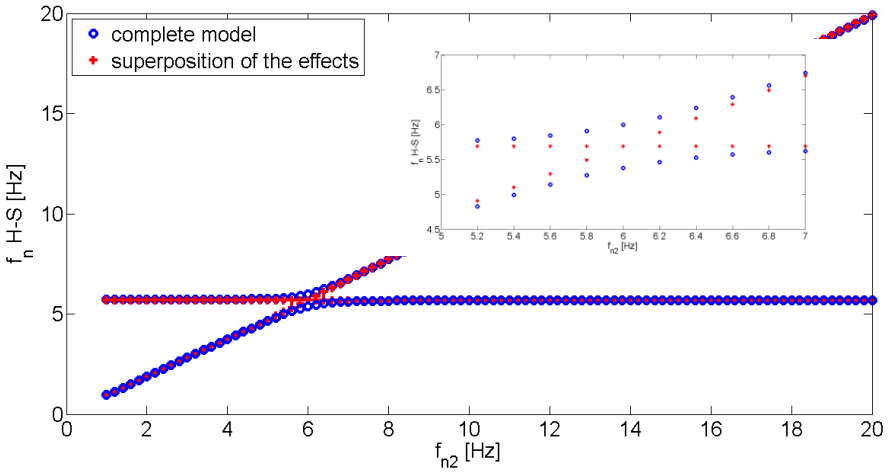

Figure 6.13: Natural frequencies: $\beta_1=\beta_2=0.1$, $\zeta_1=\zeta_2=1\%$, $f_{n1}=6$ Hz

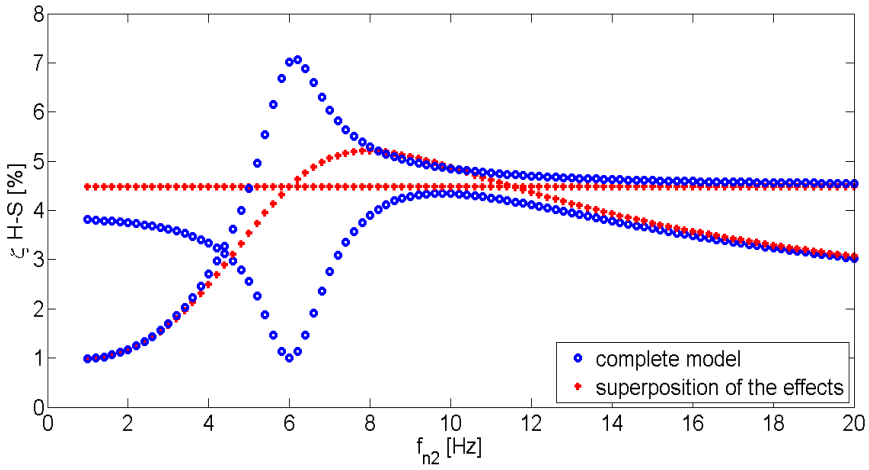

Figure 6.14: Damping ratios: $\beta_1=\beta_2=0.1$, $\zeta_1=\zeta_2=1\%$, $f_{n1}=6$ Hz

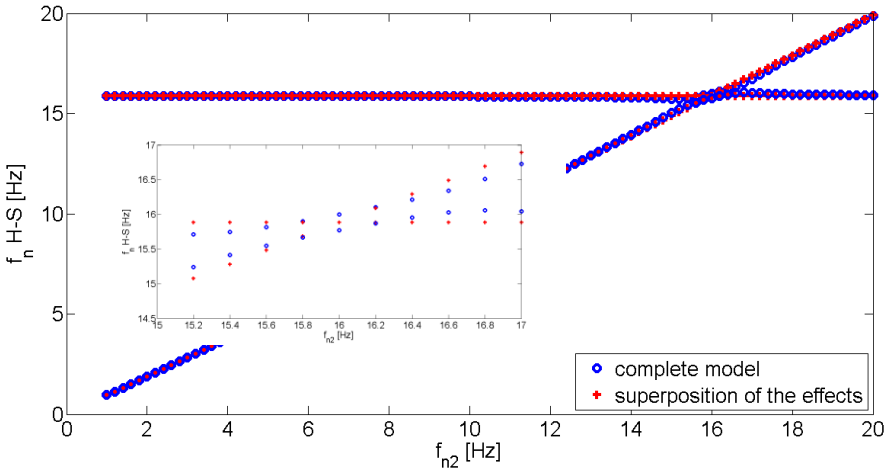

Figure 6.15: Natural frequencies: $\beta_1=\beta_2=0.1$, $\zeta_1=\zeta_2=1\%$, $f_{n1}=16$ Hz

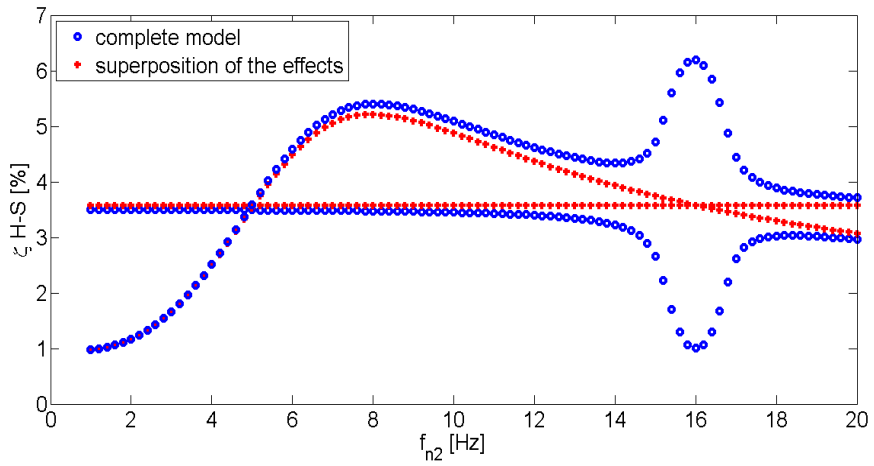

Figure 6.16: Damping ratios: $\beta_1=\beta_2=0.1$, $\zeta_1=\zeta_2=1\%$, $f_{n1}=16$ Hz

Several considerations can be drawn from the analysis of the reported results:

- a good agreement between the complete model and the superposition of the effects is generally found only if $f_{n2} << f_{n1}$ or $f_{n2} >> f_{n1}$
- For a wide range of frequencies the results obtained with the two approaches are very different, especially as for the damping ratio.
- The amount of the approximation introduced by the use of the superposition of the effects depends on the natural frequency of the first mode. As an example, the difference between the two approaches is lower for the case of f_{n1} = 2 Hz than in the other cases. Indeed, the

influence of humans highly depends on the natural frequency of the empty structure as it depends on the apparent mass which has frequency dependent values

6.3.1.2 $\zeta_1=\zeta_2=5\%$, $\beta_1=\beta_2=0.1$, $f_{n1}=6$ Hz

In order to investigate the influence of the damping ratio of the empty structure on the results, the dynamics of structure with parameters $\zeta_1=\zeta_2=5\%$, $f_{n1}=6$ Hz, $\beta_1=\beta_2=0.1$ was simulated. Figure 6.17 and Figure 6.18 show the obtained results.

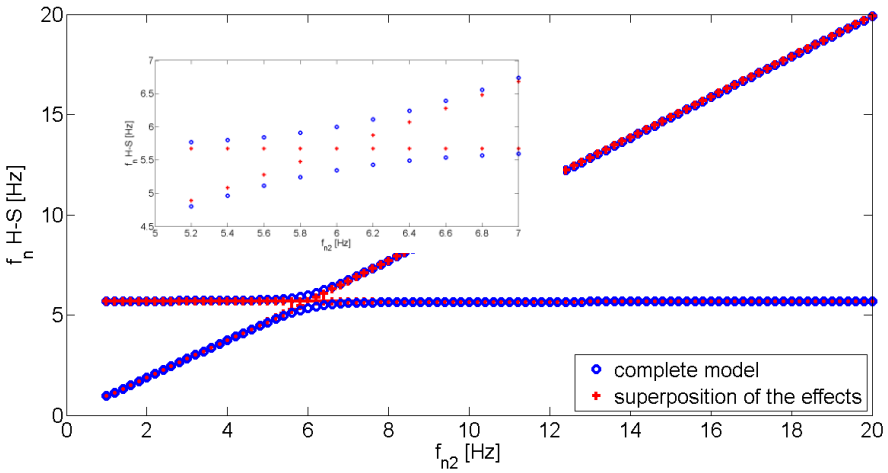

Figure 6.17: Natural frequencies: $\beta_1=\beta_2=0.1$, $\zeta_1=\zeta_2=5\%$, $f_{n1}=6$ Hz

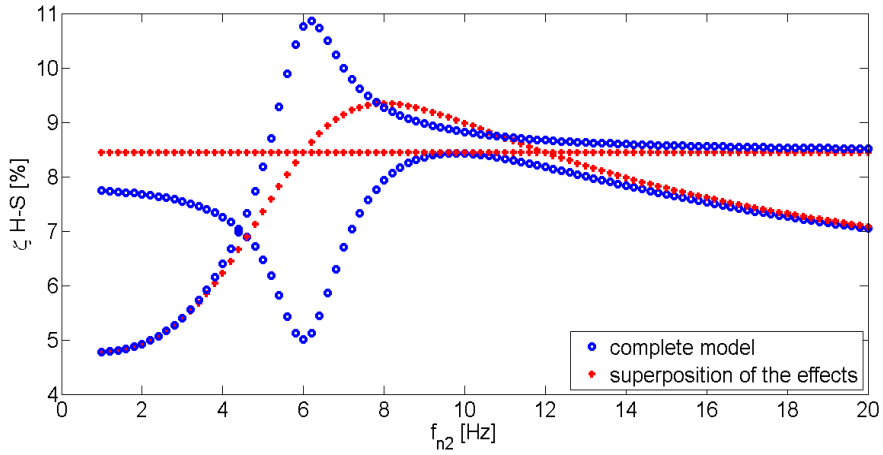

Figure 6.18: Damping ratios: $\beta_1=\beta_2=0.1$, $\zeta_1=\zeta_2=5\%$, $f_{n1}=6$ Hz

From the analysis of the results reported in Figure 6.17 and Figure 6.18 it can be concluded that:

- The results are slightly influenced by the damping ratio of the empty structure. Indeed, the identified modal parameters show a trend close to those reported in Figure 6.13 and Figure 6.14 (i.e. $\zeta_1=\zeta_2=1\%$). Particularly, the damping ratio nearly assumes the same trend shown in Figure 6.18 scaled by the difference between the initial values.

6.3.1.3 $\zeta_1=\zeta_2=1\%$, $f_{n1}=6$ Hz, various β

The influence of the amount of the physical mass of the subject on the structure was investigated by varying the parameter β and considering a structure with parameters $\zeta_1=\zeta_2=1\%$, $f_{n1}=6$ Hz. Figure 6.19 and Figure 6.20 report the results for the case of $\beta=0.05$. Figure 6.21 and Figure 6.22 refer to the case of $\beta=0.25$.

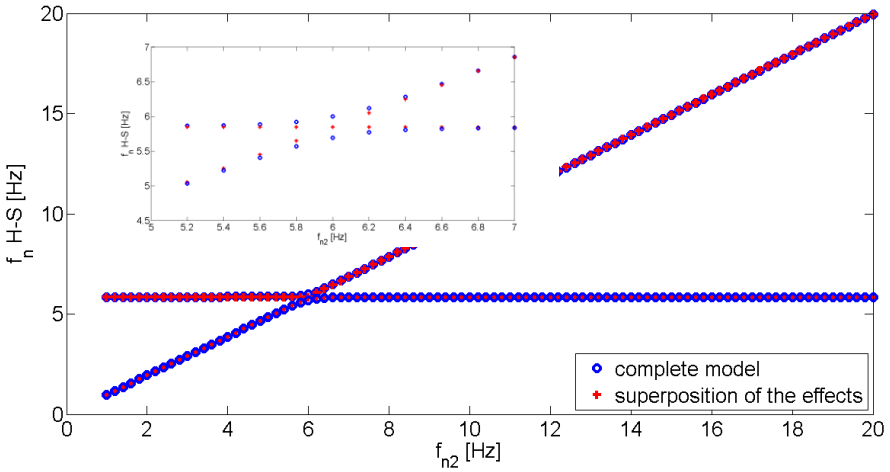

Figure 6.19: Natural frequencies: $\beta_1=\beta_2=0.05$, $\zeta_1=\zeta_2=1\%$, $f_{n1}=6$ Hz

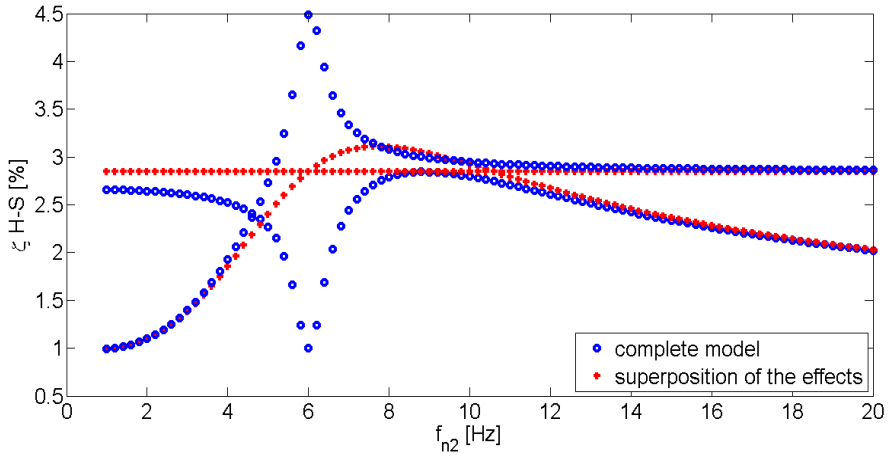

Figure 6.20: Damping ratios: $\beta_1=\beta_2=0.05$, $\zeta_1=\zeta_2=1\%$, $f_{n1}=6$ Hz

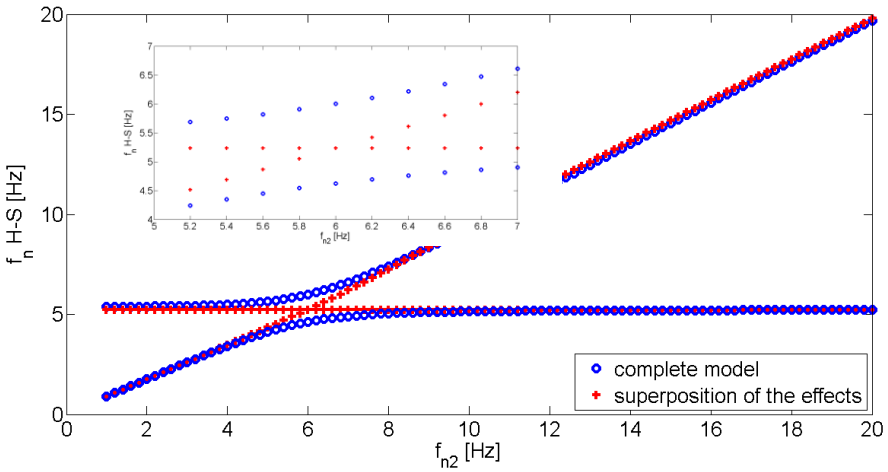

Figure 6.21: Natural frequencies: $\beta_1=\beta_2=0.25$, $\zeta_1=\zeta_2=1\%$, $f_{n1}=6$ Hz

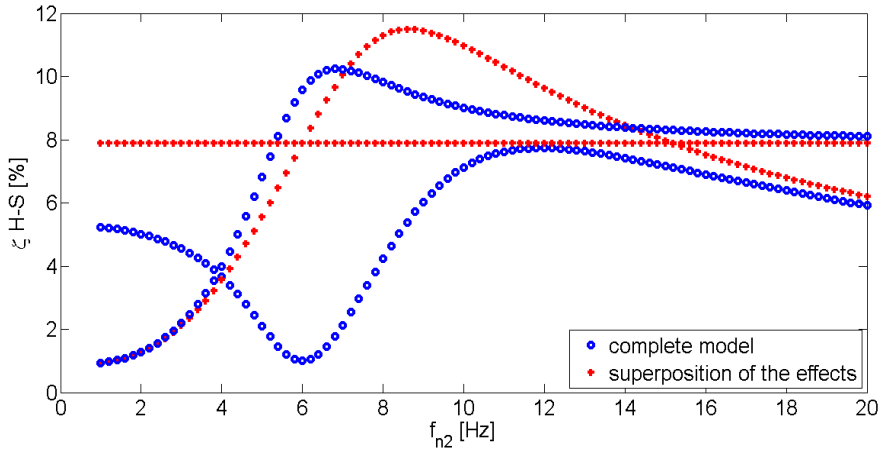

Figure 6.22: Damping ratios: $\beta_1=\beta_2=0.25$, $\zeta_1=\zeta_2=1\%$, $f_{n1}=6$ Hz

From the analysis of the above reported results it is possible to conclude that:

- As expected, the differences between the results of the two methods reduces with the influence of people. However, in the range where the two natural frequencies are very close, the difference between the results remains high.
- Increasing the amount of physical mass, the differences between the results obtained by using the two approaches increase as well.
- The trend of the identified modal parameters highly depends on the mass ratio β.

The reported results show that the use of superposition of effects to simulate the dynamic response of joint H-S systems might lead to erroneous estimations for a wide range of structures. Indeed, it could be assumed that the superposition of the effects could be applied with good results only if the vibration modes have natural frequencies that are well separated.

Therefore, even though the superposition of effects presents undoubted advantages, it is advisable to check if this can be applied the particular case, without introducing non acceptable errors.

6.3.2 Complete model vs approximate solution

The previous sections showed that the applicability of the superposition of the effects should be verified in each particular case. However, it was generally seen that the superposition of the effects introduces small errors when the modes are well separated. In this case the approximate solution proposed in Section 6.3 might be applied too. Thus, this subsection proposes an analysis of the differences

between the complete model and the approximate solution for a SDOF structure. All the reported results were obtained by fixing the damping ratio of the empty structure (ζ) and β. Also in this case the natural frequency (f_n) of the empty structure was varied in the analysis between 1 Hz and 20 Hz. The next subsections report some of the obtained results.

6.3.2.1 Low mass ratio (β=0.05)

Figure 6.23 reports the differences between the natural frequencies estimated with the complete model (f_n H-S compl) and the approximate model (f_n H-S approx) for the case of a structure with ζ=1%, ζ=2% and ζ=5%, β=0.05.

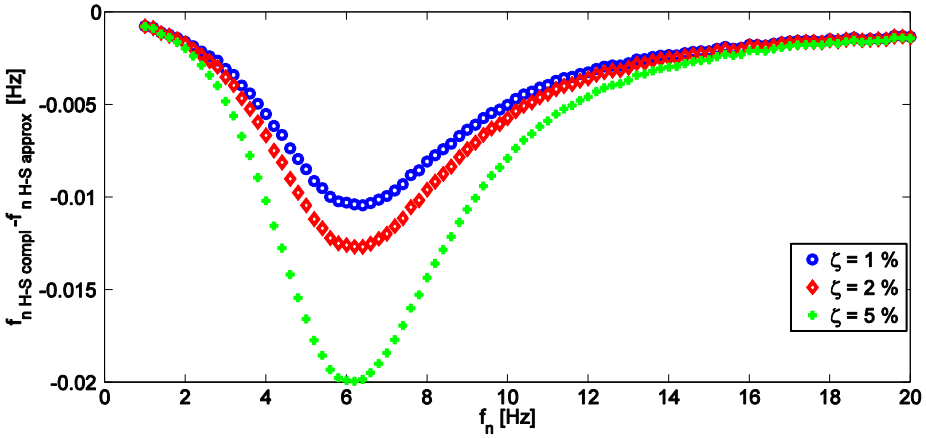

Figure 6.23: Natural frequency: β=0.05

Figure 6.24 and Figure 6.25 report the absolute and relative error between the damping ratios estimated with the complete model and the approximate model.

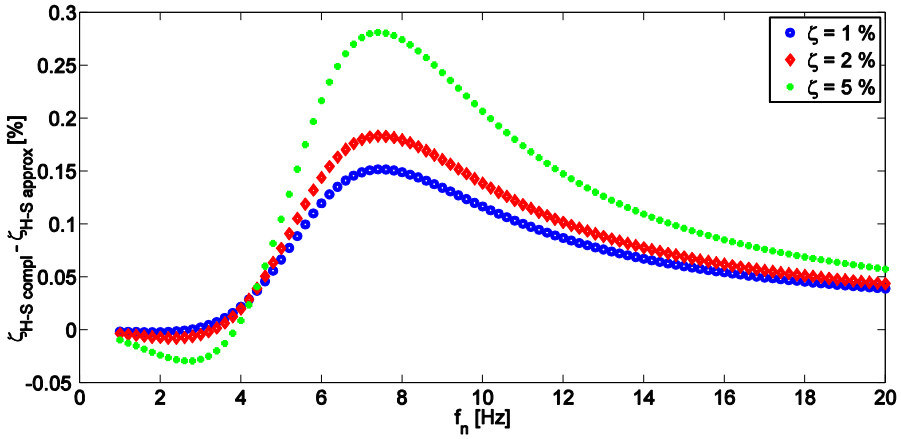

Figure 6.24: Damping ratio: β=0.05 – absolute error

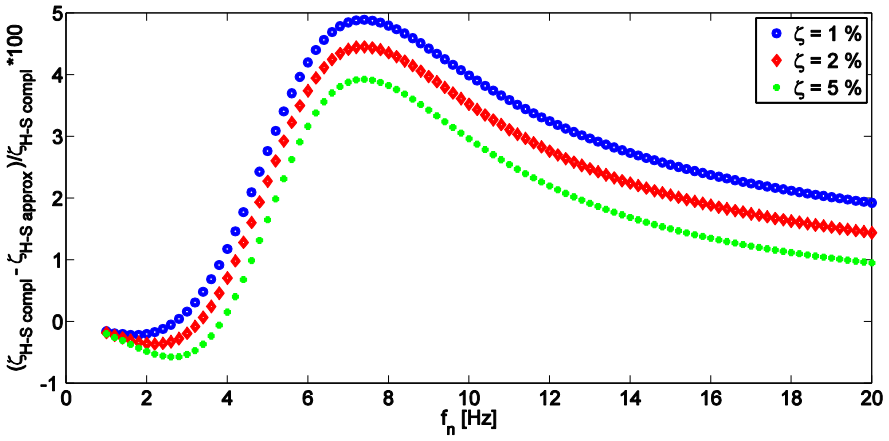

Figure 6.25: Damping ratio: β=0.05 – relative error

Results show that:

- The damping ratio of the empty structure influences the approximation.
- the difference between the natural frequency identified with the approximate and the complete solution can be considered small (with maximum value of about 1/100 Hz for the case of ζ=1% and a maximum value of about 2/100 Hz for the case of ζ=5%).
- The approximation introduces a small error in the identified damping ratio.
- The maximum differences are reached in the range of frequencies were the influence of humans on the modal parameters is higher (see Figure 6.9).

6.3.2.2 High mass ratio (β=0.25)

Figure 6.26, Figure 6.27 and Figure 6.28 reports the results obtained from simulations with β=0.25.

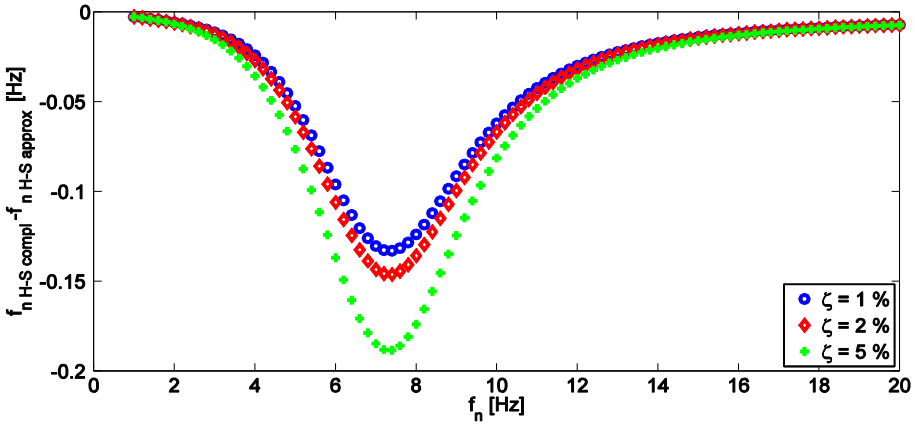

Figure 6.26: Natural frequency: β=0.25

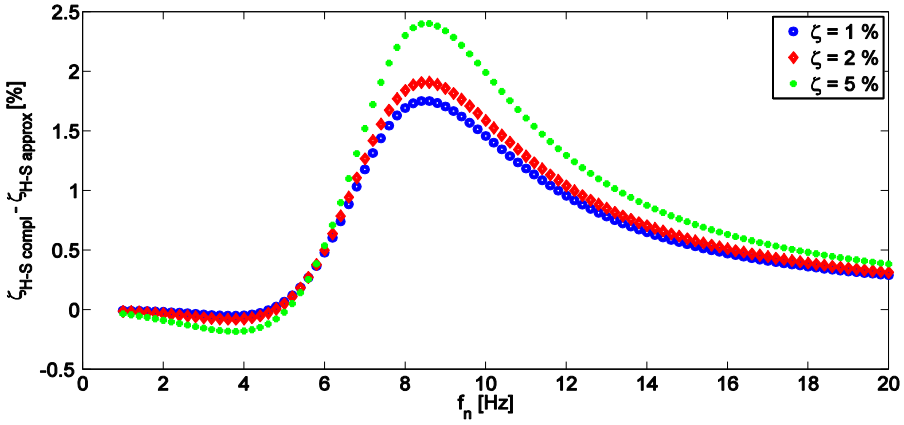

Figure 6.27: Damping ratio: β=0.25 – absolute error

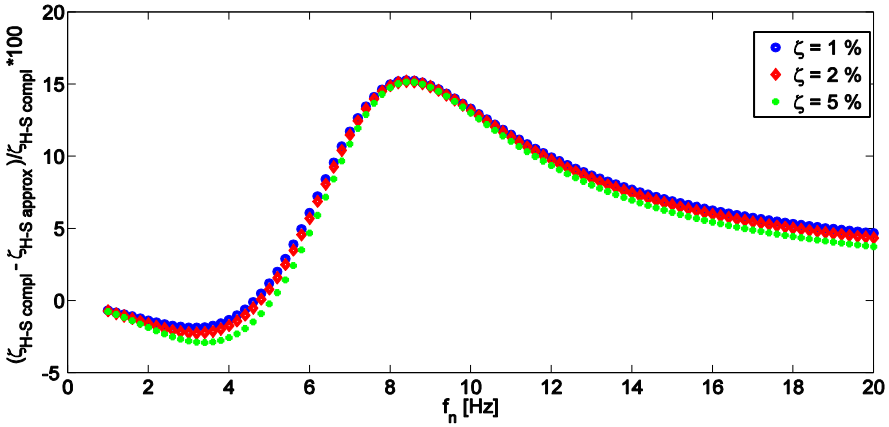

Figure 6.28: Damping ratio: β=0.25 – relative error

Results show that:

- The absolute differences between the results obtained with the complete model and the approximate solution increases with the amount of people.
- the relative error seems to be little influenced by the damping ratio of the empty structure.
- even with a high amount of mass on the structure, the error obtained with the approximate solution remains limited and could be considered acceptable in many practical applications.

In conclusion, the approximate solution proposed in Section 6.2 could provide a good approximation of the complete model in many practical cases. However, the application of the approximation requires the applicability of the superposition of the effects. The main advantage of the approximation is the possibility of identifying the type of effect of human subjects (i.e. increasing or decreasing of natural frequency and damping ratio) from the direct analysis of the apparent mass curves.

The next section proposes an analysis of the influence of different apparent mass curves on the dynamic properties of joint H-S systems.

6.4 Analysis of different apparent mass curves

As discussed in the previous chapters of this work, the GRFs exerted by passive people on a structure (modelled here through the apparent masses) are highly influenced by the postures assumed by the subject on the structure. Thus, the effect of human presence on the modal parameters of the joint H-S system varies with the posture of the subjects.

In this section the possible effects are analysed considering various apparent mass curves.

6.4.1 Vertical direction

The influence of subjects standing on structures vibrating in the vertical direction was first analysed.

This influence has already been partially treated in chapters 2-4 as the experimental cases studied in this work dealt with the analysis of structures exposed to vertical vibrations.

As for vertical vibrations, it is known that people generally introduce additional damping and reduce the natural frequencies with respect to the empty structure.

Figure 6.29 reports the real and imaginary parts of the average apparent masses named 2a in [51] for standing and on one leg subjects. The non-dimensional values of the apparent mass were multiplied by a physical mass $\bar{M}=100$ kg.

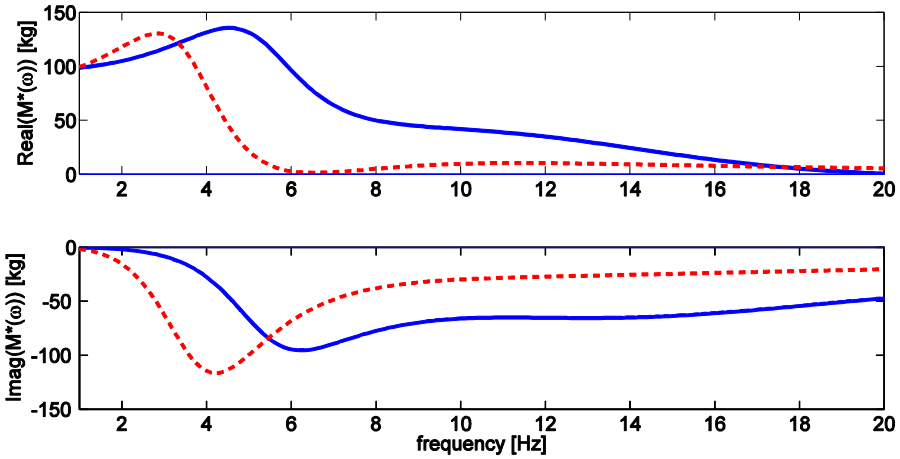

Figure 6.29: Apparent mass – model 2a (solid: standing, dashed: one leg)- Real and Imaginary parts

According to the apparent mass values reported in Figure 6.29, as the real part of the apparent mass is positive in the frequency range 1-20 Hz, it is expected that the natural frequency of the joint H-S system decreases (Eq. (6.54)). Conversely, as the imaginary part is always negative, it is expected an increase of the damping ratio. However, for low frequencies, as the imaginary part of the apparent mass is small, according to Eq. (6.55) the damping ratio could experience a small decrease.

The state of the art reports some cases of increase of natural frequencies when dealing with vertical vibrations. The experimental case treated in Chapter 3 of this work reported a similar case, as the mode with natural frequencies at 16.8 Hz showed an increase of such value due to people's presence. In literature this increase is generally reported for structures with natural frequencies higher than 14 Hz. The average value of apparent mass reported in [51], Figure 6.29, cannot explain such a behaviour. However, this result can be explained using the measured values of the apparent mass reported in Chapter 3, Figure 3.4.

Figure 6.30 reports the real and imaginary parts of these masses.

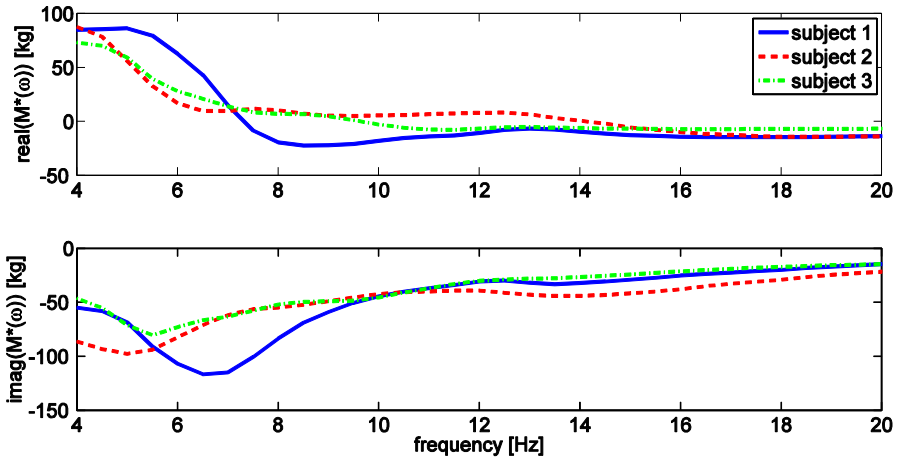

Figure 6.30: Measured apparent masses – Standing subjects - Real and Imaginary parts

Figure 6.30 shows that the real part of the apparent mass of standing subjects decreases with the frequency and can reach negative values. If this happens, the natural frequencies of the joint H-S system can increase due to people's presence, as reported in literature or as shown in Chapter 2.

Figure 6.31 and Figure 6.32 show the average apparent mass (model 2a [51]) for subjects in a bent legs posture.

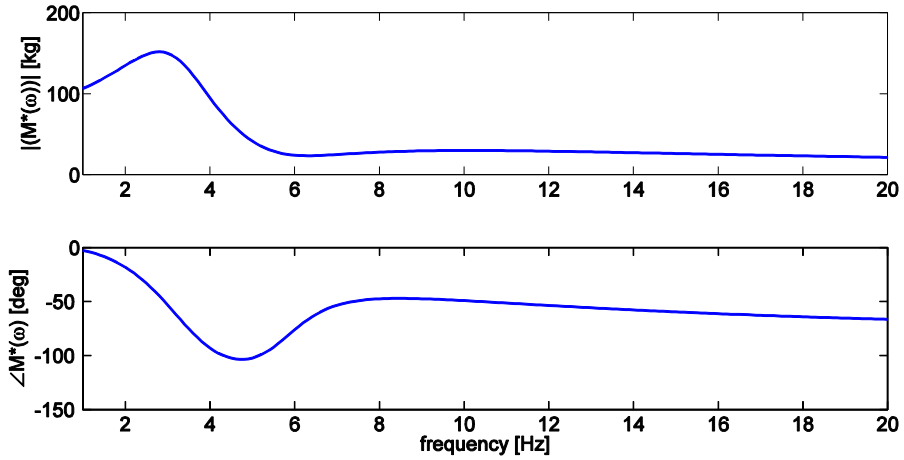

Figure 6.31: Apparent mass (bent legs)- Amplitude and phase

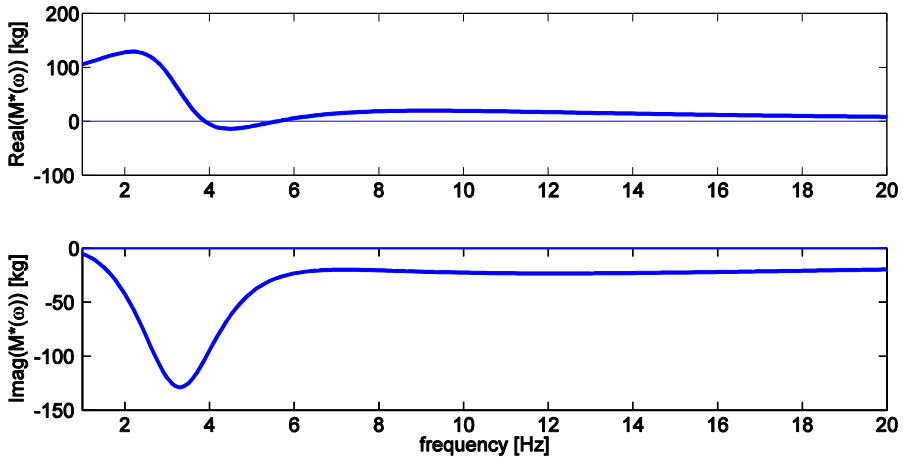

Figure 6.32: Apparent mass (bent legs)- Real and Imaginary parts

Also in this case it is possible to observe that there is a small range of frequencies where the real part of the apparent mass becomes negative. Therefore, around this range of frequencies the natural frequencies of the joint H-S system could increase.

6.4.2 Horizontal direction

In this work the proposed model was validated considering the case of structures vibrating in the vertical direction. However, some considerations regarding structures vibrating in the horizontal direction are proposed in this Section.

To the purpose of investigating the dynamic behavior of joint H.S systems in the horizontal direction, the work by Matsumoto and Griffin [120] was used.

In their work the authors propose an extensive analysis of the apparent mass of subjects exposed to vibrations in the lateral and fore-and-aft direction.

As for the apparent mass in the lateral direction the authors investigate the influence of the distance between the two feet on the apparent mass values.

Figure 6.33 reports the apparent mass values for a distance of 0.3 m and 0.45 m between the feet. These values were extracted from the figures reported in [120].

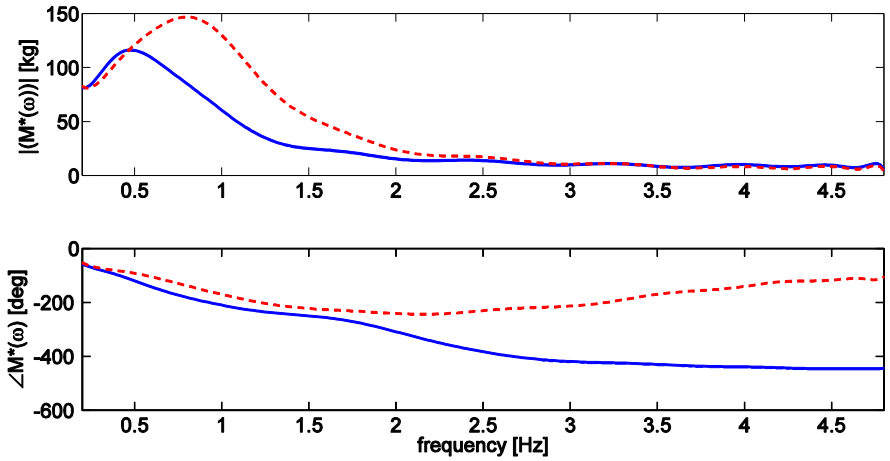

Figure 6.33: Apparent mass – lateral direction (solid: 0.3 m, dashed: 0.45 m)- Amplitude and phase

Figure 6.34 reports the same apparent masses in terms of real and imaginary parts.

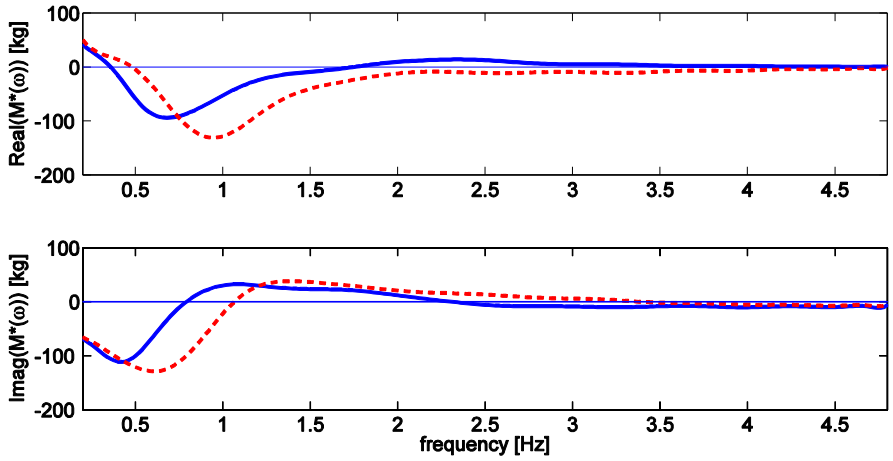

Figure 6.34: Apparent mass – lateral direction (solid: 0.3 m, dashed: 0.45 m)- Real and Imaginary parts

From an analysis of the apparent mass curves reported in Figure 6.34 it is possible to see that there is a wide range of frequencies where the real part of the apparent mass is negative and a range of frequencies where the imaginary part of the apparent mass is positive. Therefore, it is expected that people interacting with a structure vibrating in the lateral direction could both reduce or increase the natural frequency and increase or reduce the damping ratio of the structure.

As an example Figure 6.35 reports a comparison between the lateral FRF of an empty structure with ζ=1 %, f_n=1.5 Hz and the FRF of the same structure occupied by one subject.

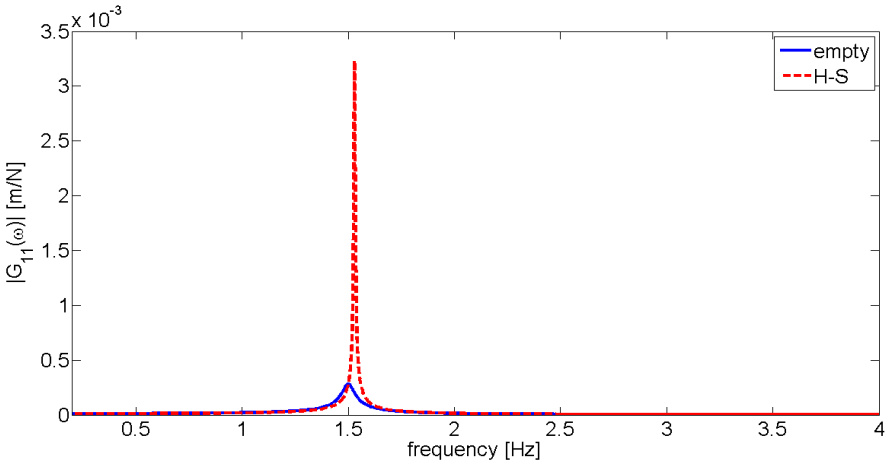

Figure 6.35: H-S system – lateral direction - ζ=2%, f_n=1.5 Hz

From Figure 6.35 it is possible to see that the subject's presence modifies the FRF of the structure increasing the natural frequency and decreasing the damping ratio. Thus, in this case people would cause an amplification of the peak of the FRF, with a negative effect on the amplitudes of the vibrations.

Figure 6.36 reports a comparison between the lateral FRF of an empty structure with ζ=2 %, f_n=0.5 Hz and the FRF of the same structure occupied by one subject. Opposite to the case reported in Figure 6.35, in this case it is possible to notice an increase in the damping ratio of the joint H-S system.

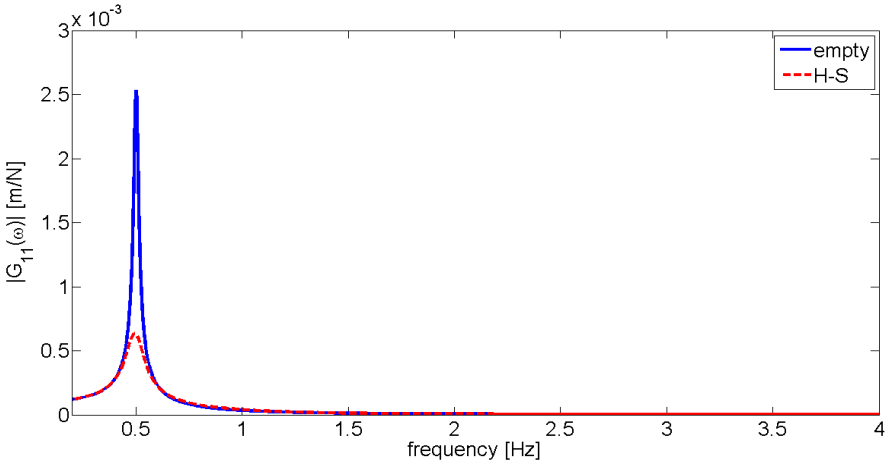

Figure 6.36: H-S system – lateral direction - ζ=2%, f_n=0.5 Hz

The results reported in Figure 6.35 and Figure 6.36 evidence that people's presence can both increase or reduce the damping of a structure subject to lateral vibrations and, in the latter case, produce an amplification of vibration levels.

Figure 6.37 reports the apparent mass value for the case of fore-and-aft vibrations. Also these values were extracted from the figures reported in [120].

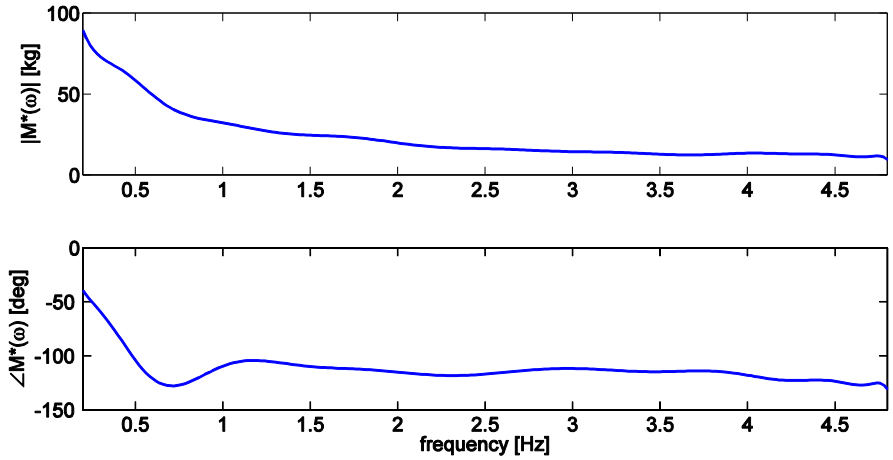

Figure 6.37: Apparent mass – fore and aft direction - Amplitude and phase

Figure 6.38 reports the same apparent masses in terms of real and imaginary parts.

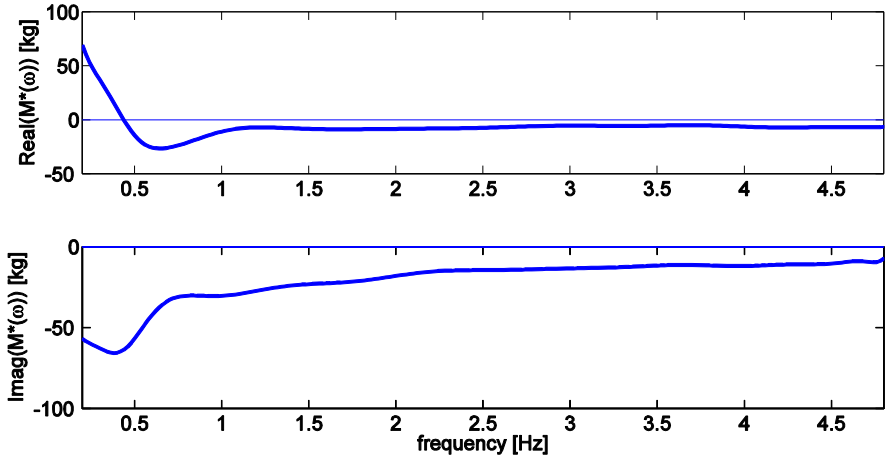

Figure 6.38: Apparent mass – fore and aft direction - Real and Imaginary parts

Also in this case, as for the case of vertical vibrations, the imaginary part of the apparent mass is negative in the available frequency range. Therefore, the imaginary parts of the apparent mass contributes to the parameters of the joint H-

S system increasing the damping ratio. Conversely, the real part of the apparent mass assumes negative values above a frequency of about 0.4 Hz. Therefore the changes of natural frequencies (increase or decrease) depends on the natural frequency of the empty structure.

The analysis of different apparent mass curves allowed verifying that people can influence the modal parameters of a structure in various ways. Particularly, people can increase or decrease the damping ratio and the natural frequency of a structure. The modification of the modal parameters depend on the characteristics of the apparent mass of the subject in contact with the structure and, therefore, on the characteristics and posture of the subject.

6.5 Summary

This chapter proposed a theoretical analysis of the dynamic behavior of joint H-S systems.

The H-S interaction was first investigated by analyzing the properties of the matrix $\mathbf{G}_{\mathrm{H}}(\omega)$, i.e. the matrix of the joint H-S system. The observation of the analytical form of this matrix allowed to evidence the differences between the use of the complete model proposed in this work and the superposition of the effects to predict the dynamic behavior of MDOFs structures occupied by people. Furthermore, the analysis of the matrix $\mathbf{G}_{\mathrm{H}}(\omega)$ allowed obtaining a simplified expression for such matrix under the hypothesis of SDOF structures.

An approximate approach based on the analysis of the apparent mass curves was proposed to predict the type of influence due to people's presence on the modal parameters of the joint H-S system.

The differences between the various possible solutions (complete model, superposition of the effects, approximate solution) were extensively investigated considering the case of a structure occupied by a single subject with apparent mass defined with a lumped parameters model. This assumption allowed to define the poles of the joint H-S system analytically. Results showed that under the hypothesis of SDOF structure the approximate solution introduces small errors with respect to the complete model. Conversely, the use of the superposition of the effects for MDOFs structure can introduce high errors if the modes are not well separated.

The last part of the Chapter proposed an analysis of the effect of people in different postures and for different directions of vibration through the analysis of various apparent mass curves. Results showed that people can both increase and decrease the natural frequency and damping ratio of a structure.

Chapter 7

A case study: San Siro Stadium

This Chapter proposes an analysis of the effects of people's presence on a grandstand of the San Siro stadium. The influence of people was first quantified during some football matches. The effects were analysed in terms of changes in modal parameters and were compared with predictions obtained with the model proposed in Chapter 3. Then, a numerical analysis is proposed to investigate the influence of crowd's distribution on the modal parameters of the joint H-S systems. Finally, the results obtained by using the superposition of the effects (Chapter 6, Section 6.1.2) are compared with those obtained by solving the complete model (Chapter 3).

In the previous Chapters a model to predict the dynamic behaviour of joint H-S systems was proposed and validated considering slender staircases as test structures. In addition, several theoretical considerations were proposed. In this Chapter some of the problems faced in the former are reviewed considering a stadium grandstand as a test case structure. Such a structure is very different from the aforementioned. Indeed, the considered grandstand cannot be considered as a slender structure and the occupancy (up to 2330 people) is much higher than those expected on a staircase. Therefore, the proposed approach was applied also in this case in order to verify its effectiveness on a structure quite different from those previously treated. To this purpose the effect of people during some football matches was analysed and some theoretical analyses were performed. As for stadia grandstands, many works available in literature dealt with the analysis of the dynamic behaviour of grandstands [45],[17],[18],[20]. Thus, the approach proposed in this work offers a new tool to investigates the dynamics of this kind of structures as well.

7.1 The structure

The analysis proposed in this Chapter focuses on a portion of grandstand located on the third level (commonly called "ring") of the San Siro stadium. The construction of the third ring started in 1990, on the occasion of the World Cup played in Italy. For such an occasion the Milan City Council began a deep change and renewal of the stadium. The project consisted in placing independent backings for the new level all around the existing stadium. Eleven cylindrical towers of reinforced concrete were built for this purpose. Seven towers are 30 m tall, while the four corner towers are 51 m tall as they also provide support for the roof of the stadium. The 3rd level is then composed of 10 grandstands supported by 11 concrete towers. Every grandstand, about 50 m long, consists of a pre-compressed box beam sustained by 4 bearings and every grandstand is structurally separated from the contiguous ones. Thus, each grandstand of the 3rd ring is totally independent from the other stadium structures. This work focuses on the analysis of vibrations of the portion of grandstand located between tower 5 and tower 6 (Figure 7.1 and Figure 7.2).

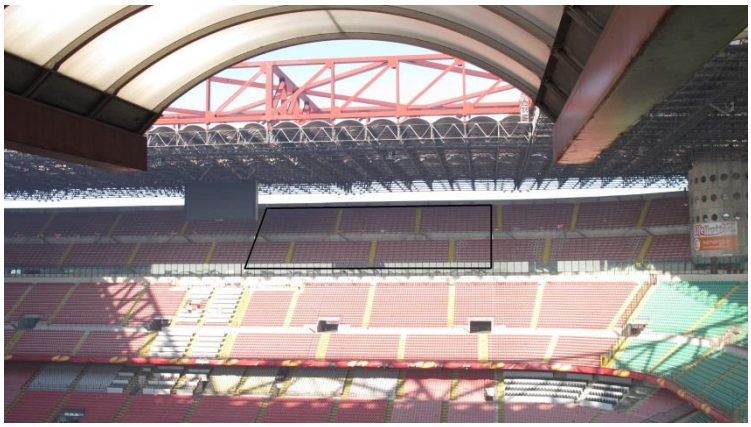

Figure 7.1: Grandstand section

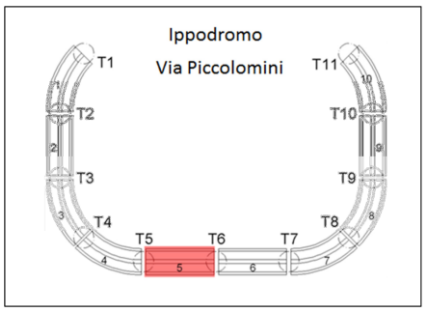

Figure 7.2: Grandstand section - plan

During previous tests campaigns, the structure was tested in order to obtain its experimental FRFs in several points. These data had been used to update a FE model that was exploited in this work. To the purpose of the work the structure was also instrumented with accelerometers during some football matches. The next sections report the measurement setup for such tests.

7.2 Experimental setup

In order to derive the dynamic response of the grandstand, sensors were positioned in such a way not to disturb the normal operating conditions. Particularly, accelerometers were placed at the lower edge of the grandstand in a non-accessible position. Such a choice allowed to measure the accelerations in operating conditions. High sensitivity seismic piezo-accelerometers were used to measure the accelerations in selected points of the grandstand. The selected sensors have proven to be adequate for ambient vibration testing, having a very low noise floor and an adequate full scale value.

During the football matches 11 accelerometers were available on the

grandstand. Seven accelerometers measured the vibrations in the vertical direction and the remaining four accelerometers measured the vibrations in the horizontal direction. Figure 7.3 shows the experimental configuration.

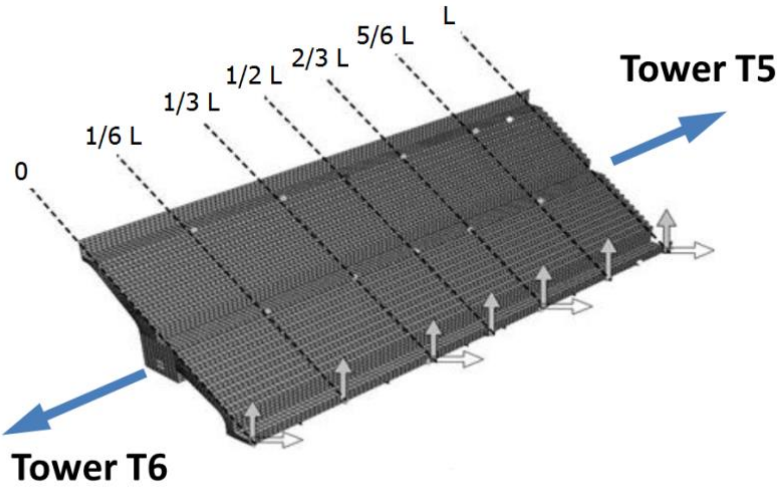

Figure 7.3: Setup of the accelerometers

7.3 Structure dynamics and data analysis

The collected data were analysed by means of OMA techniques [118],[119] in order to obtain the structure modal parameters. Both ambient vibration data (empty grandstand) and football matches were analysed.

7.3.1 Ambient vibration testing

The analysis of ambient vibration testing (empty structure) allowed extracting the modal parameters of the first four vibration modes. Reference values of such parameters are reported in Table 7.1.

	f_n [Hz]	ζ [%]
Mode 1	3.15	1.30
Mode 2	3.29	1.42
Mode 3	5.44	1.35
Mode 4	5.73	1.47

Table 7.1: Ambient vibration testing – modal parameters

7.3.2 Football matches

The analysis of four football matches is proposed in this work. The considered football matches are:

1. Milan – Parma (February 15, 2013)
2. Milan – Barcelona (February 20, 2013)
3. Inter – Milan (February 24, 2013)
4. Milan – Lazio (March 2, 2013)

During the first match (Milan - Parma) the grandstand occupancy was scarce, approximately 14% of the total capacity. During the last match (Milan - Lazio) the occupancy was about 31%. Conversely, during the second and third considered matches the grandstand was almost full.

The results related to the analysis of the first half of all the considered matches are proposed. Indeed, the first half is the part of the match where people sit on the grandstand for most of the time. During the other parts of the events, such as the entrance or the interval and the last part of the second half, people often move on the structure. This causes at least two problems: a) the dynamic behaviour of the structure changes in time; b) people introduce a force that may contain dominant harmonic components. These two aspects make the analysis of such data less reliable.

Figure 7.4 shows an example of PSD of the grandstand.

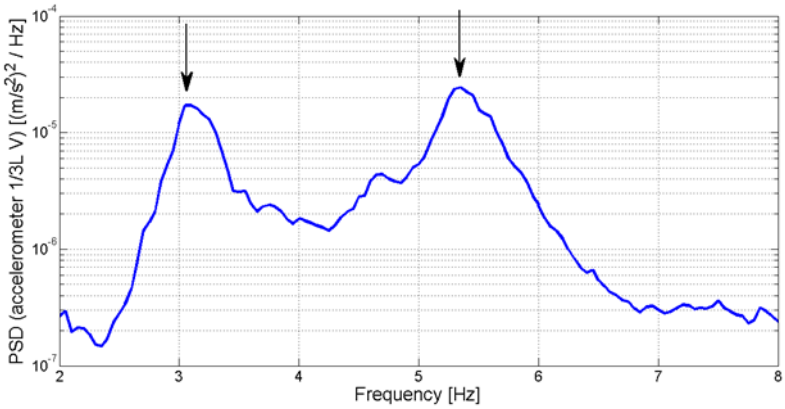

Figure 7.4: Inter – Milan: Example of PSD (accelerometer 1/3L V)

As for the football matches, the identification was considered reliable only for the two dominant modes around 3.30 Hz (mode 1) and 5.40 Hz (mode 3). Table 7.2 and Table 7.3 reports the obtained natural frequencies and damping ratios.

Match	f_n [Hz]	ζ [%]
Milan – Parma	3.29	2.18
Milan – Barcelona	3.18	3.83
Inter – Milan	3.10	4.45
Milan – Lazio	3.21	2.90

Table 7.2: Football matches – modal parameters – mode 1

Match	f_n [Hz]	ζ [%]
Milan – Parma	5.46	1.84
Milan – Barcelona	5.33	3.20
Inter – Milan	5.37	2.78
Milan – Lazio	5.41	2.13

Table 7.3: Football matches – modal parameters – mode 3

The results show that people generally cause a decrease of the natural frequencies and an increase of the damping ratios. The obtained changes are increase with the number of people on the grandstand. In addition, experimental results show that the influence of people is higher for the first mode.

7.4 Modal parameters prediction using the H-S model

In order to obtain a prevision of the changes in modal parameters due to people's presence the method proposed in Chapter 3 is used. The approach proposed in Chapter 3 was validated analysing the experimental Frequency Response Functions (FRFs) of the staircase plus passive subjects. Thus, the modal parameters of the joint human-structure system could be accurately estimated. As regards real-life structures, such as the stadia grandstand considered in this work, the actual force exerted on the structure in unknown. Thus, the experimental data were analysed by means of Operational Modal Analysis [118],[119] (OMA) techniques to extract the modal parameters. Therefore, the results obtained from the OMA of the football matches were compared with those predicted with the H-S model.

The application of the method proposed in Chapter 3 requires the knowledge of:

- the modal model of the empty structure. To this purpose a FE model of the grandstand was employed. However, the available FE model of the

grandstand could not provide an accurate description of the modes 1 and 2. Therefore, only the modes 3 and 4 were analysed when modelling the dynamic behaviour of the joint Human-Structure system.

Thus, the dynamics of the structure was simulated using the two modes at 5.40 Hz and 5.73 Hz. The mode at 5.73 Hz was included in the simulations since it could influence the overall results (refer to Chapter 6, Section 6.1.2). However only the modal parameters of the mode at 5.40 Hz where compared to the experimental values because this was the only mode that could be correctly identified from the experimental data. The modal parameters of the FE model are reported in Table 7.4. It is possible to notice that these parameters slightly differ from those obtained from the analysis of the ambient vibration data (Table 7.3). The associated mode shapes are reported in Figure 7.5, Figure 7.6, Figure 7.7 and Figure 7.8.

	f_n [Hz]	ζ [%]
Mode 3	5.40	1.94
Mode 4	5.73	1.78

Table 7.4: Modal parameters – FEM

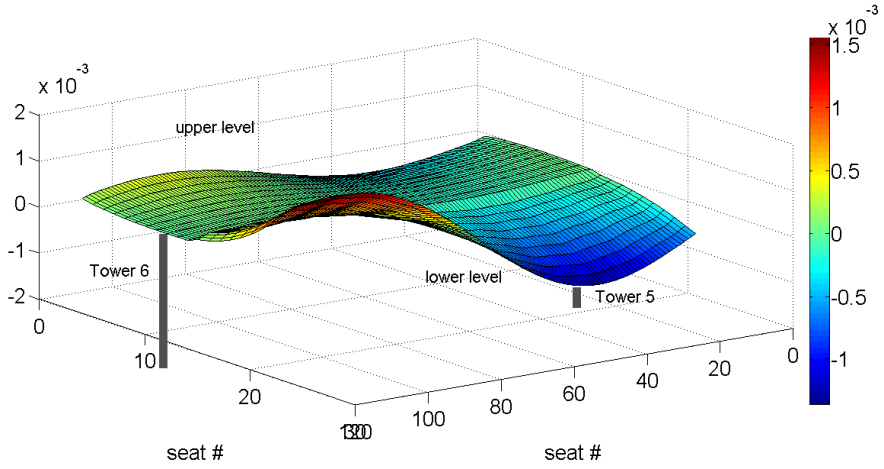

Figure 7.5: Mode 3 – vertical direction

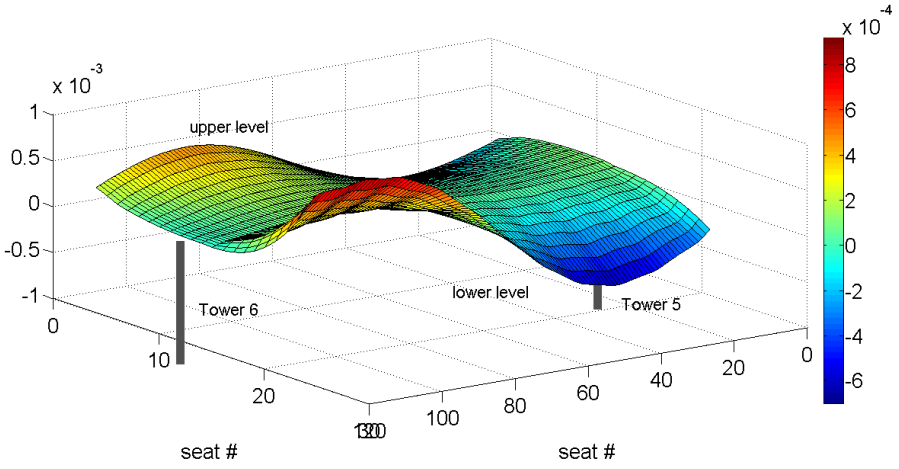

Figure 7.6: Mode 3 – horizontal (fore and aft) direction

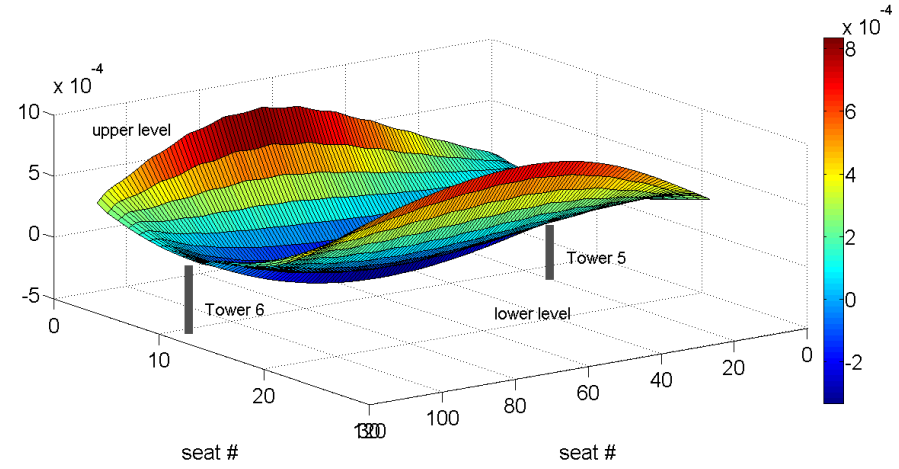

Figure 7.7: Mode 4 – vertical direction

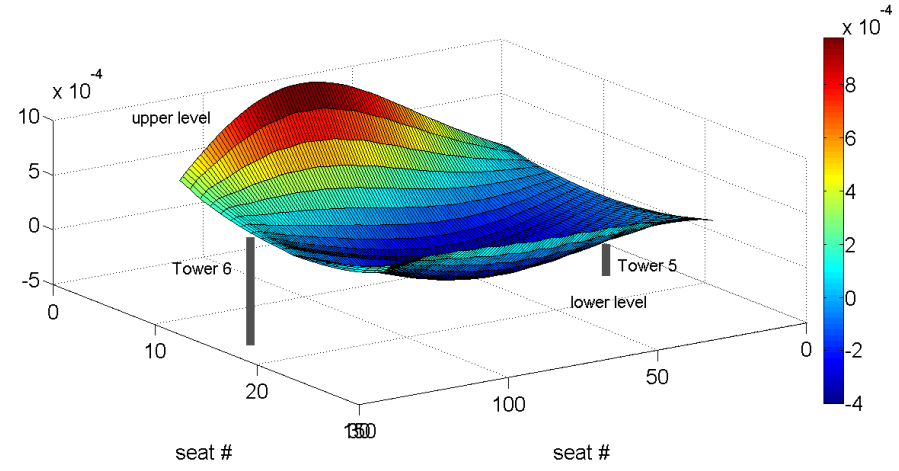

Figure 7.8: Mode 4 – horizontal (fore and aft) direction

- the driving point FRF (apparent mass) of each subject on the structure. As for a stadium grandstand, during football matches people are expected to sit for most of the time. Many works regarding the dynamic behaviour of the seated human body are proposed in literature. Some of these works [78],[121],[122], considered suitable to represent the dynamic behaviour of humans sitting on a stadium seat, were employed.

The FRFs of the joint H-S system are obtained combining the model of the empty structure and the apparent mass of seated subject. The modal parameters extracted from the analysis of these FRFs are compared with those obtained experimentally. The next subsections report the obtained results.

7.4.1 Milan – Barcelona and Inter - Milan

As for the matches Milan – Barcelona and Inter – Milan, the grandstand was almost full. Hence, the grandstand was supposed to be full when modelling the joint H-S system. Therefore, the results are identical for the two matches. Figure 7.9 shows, as an example, the grandstand occupancy for the match Milan – Barcelona.

Figure 7.9: Milan – Barcelona – Grandstand occupancy

For these two matches, two kinds of model available in literature for the apparent mass of seated human body were used and compared. Particularly, apparent masses with [78],[121] and without seat backrest [122] were used. Table 7.5 shows the obtained results.

	f_n [Hz]	ζ [%]
Full - With Backrest	5.30	3.23
Full - Without Backrest	5.32	3.45

Table 7.5: H-S predicted modal parameters – full grandstand - mode 3

It is possible to notice that the choice of the model to represent the dynamic behaviour of the seated human body (with or without backrest) slightly influences the result.

The results obtained with the model of the joint H-S system (Table 7.5) can be compared with those obtained experimentally (Table 7.3). The results show that the predicted damping ratios are slightly higher than those obtained from the analysis of the experimental data. However, the damping ratio used in the FE model is slightly higher than the damping ratio obtained from the analysis of the ambient vibration data as well. Therefore, the experimental and predicted results are compatible in terms of increase in damping ratio. The same considerations apply to the decrease of the natural frequency.

7.4.2 Milan – Lazio

During the football match Milan – Lazio the grandstand occupancy was scarce, approximately 26%. Pictures of the grandstand were taken before and during the match. Therefore, from the analysis of the pictures it was possible to know the approximate location of the spectators during the match. Figure 7.10 shows a frame of the grandstand occupancy.

Figure 7.10: Milan – Lazio – Grandstand occupancy

One of the main advantages of the approach proposed in Chapter 3 is the possibility of introducing the subjects locally on the structure. This allowed to simulate accurately people's distribution on the structure. Table 7.6 reports the obtained results.

	f_n [Hz]	ζ [%]
Milan - Lazio	5.36	2.54

Table 7.6: H-S predicted modal parameters – Milan – Lazio – mode 3

The results obtained with the H-S model are consistent with the experimental values (Table 7.3), both in terms of increase in damping ratio and decrease in natural frequency.

7.4.3 Milan – Parma

Like the football match Milan – Lazio, the analysis of the football match Milan – Parma was performed introducing people locally on the structure to simulate the FRFs of the joint H-S system. Also in this case pictures of the grandstand were used in order to gather information about crowd's distribution. The obtained results are reported in Table 7.7.

	f_n [Hz]	ζ [%]
Milan - Parma	5.39	2.11

Table 7.7: H-S predicted modal parameters – Milan – Parma – mode 3

Also in this case the obtained damping ratio is consistent with the value obtained from the analysis of the experimental data (Table 7.3). As for the natural frequency, results confirmed a small variation of its value.

7.5 Effect of different people's distribution

In order to assess the possible effect of different crowd distribution on the grandstand several simulations were carried out.

To this purpose, the dynamics of the structure was simulated considering the vibration modes reported in Table 7.4, Figure 7.5, Figure 7.6, Figure 7.7 and Figure 7.8.

Different occupancy rates were considered, i.e. 10%, 30% and 50%.

In addition, three possible probability distributions of the crowd were simulated. The three considered probability distribution are named random, central and lateral configurations in the following. In the random configuration the

crowd's distribution was simulated using a uniform random probability distribution. The central configuration was intended to simulate the distribution of a grandstand located in the centre of one side of the football field. In this case, people tend to be more concentrated at the lower levels. An example of such a distribution is reported in Figure 7.11 (50 % occupancy).

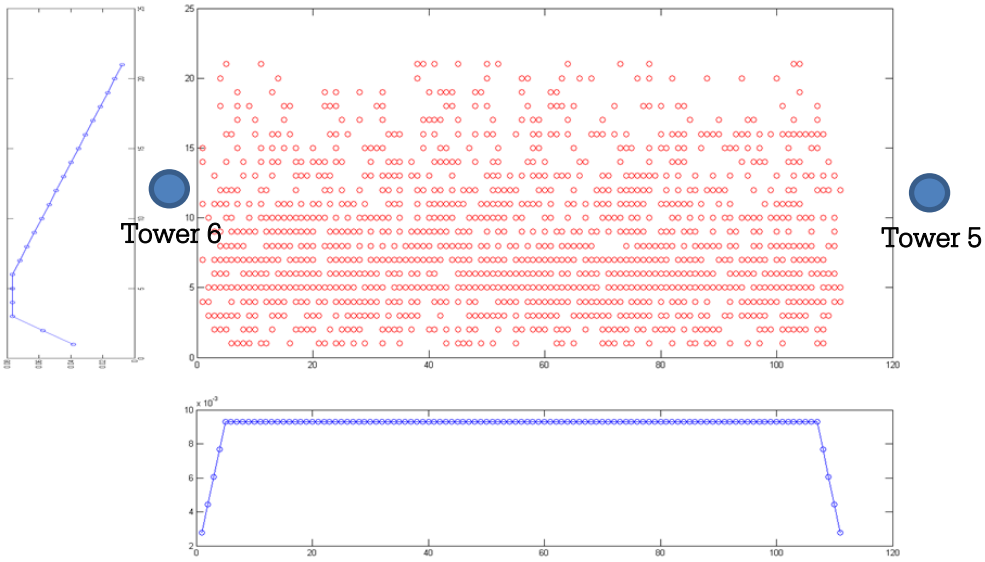

Figure 7.11: Probability distribution: central

The lateral configuration was intended to simulate the distribution of a grandstand located close to one edge of the football field. In this case, people tend to be more concentrated in the side of the grandstand that is closer to the centre of the field. An example of such a distribution is reported in Figure 7.12 (50% occupancy).

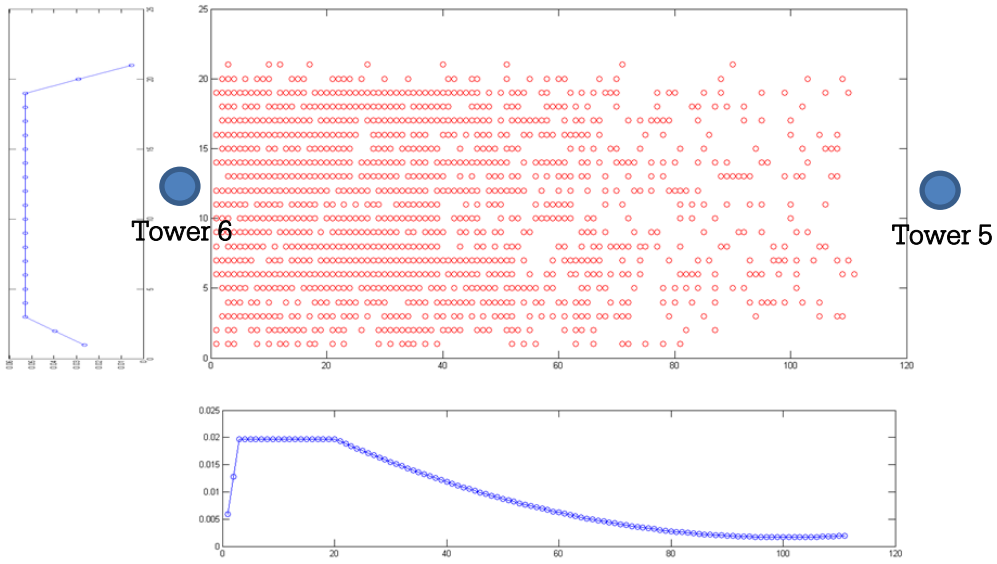

Figure 7.12: Probability distribution: lateral

For each of the 3 probability distribution and for each of the 3 occupancy rates, 300 simulations were performed.

For a given distribution, results show a general increase of people's effect with the occupancy rate. As an example, Figure 7.13, Figure 7.14, Figure 7.15 and Figure 7.16 show the natural frequencies and damping ratios of the grandstand occupied by people randomly distributed and with different occupancy rates.

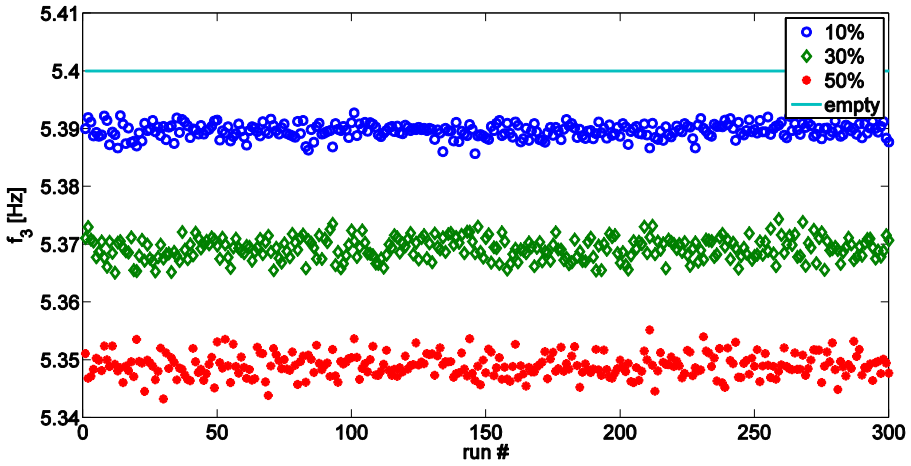

Figure 7.13: Random distribution – Natural frequency – mode 3

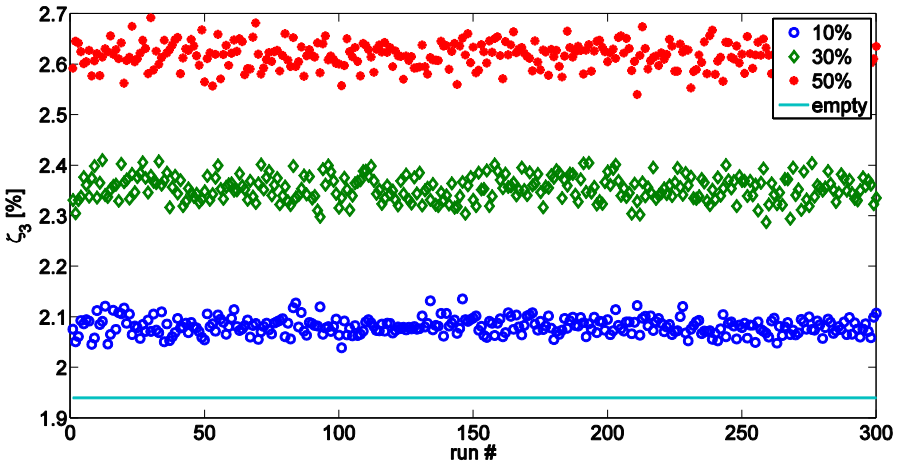

Figure 7.14: Random distribution – Damping ratio – mode 3

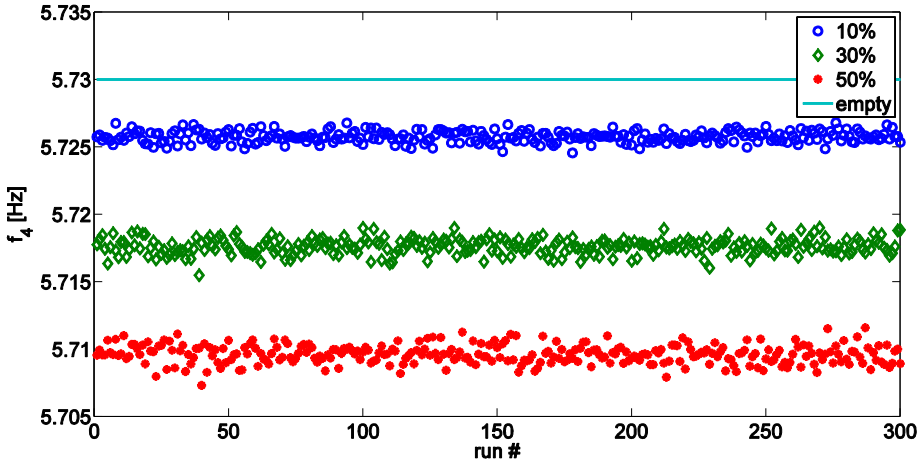

Figure 7.15: Random distribution – Natural frequency – mode 4

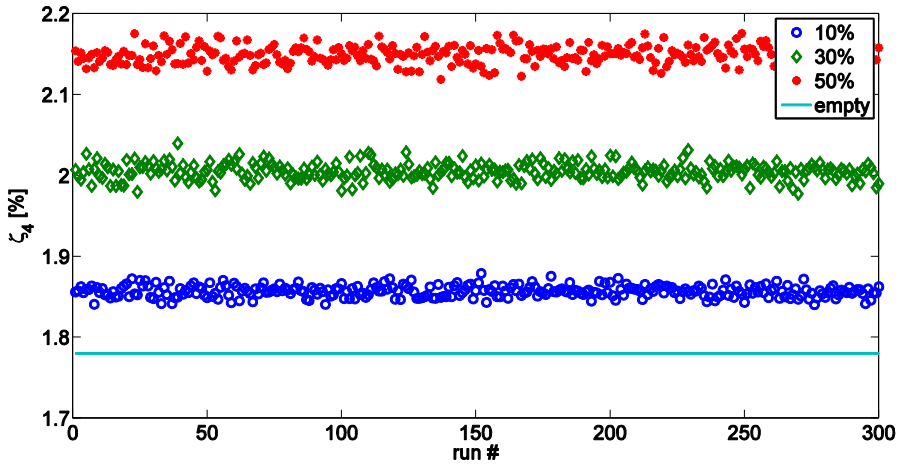

Figure 7.16: Random distribution – Natural frequency – mode 4

Results show that people decrease the natural frequencies of the structure and increase the damping ratios. Furthermore, it is possible to notice that people's effect linearly increase with the occupancy rate.

Since people's effect is proportional to the amplitude of the vibration mode where the subject is located, it is possible to notice that the type of distribution highly influences the changes of modal parameters. As an example, Figure 7.17 and Figure 7.18 show the natural frequency and damping ratio of mode 4 with 50% occupancy rate and different distributions.

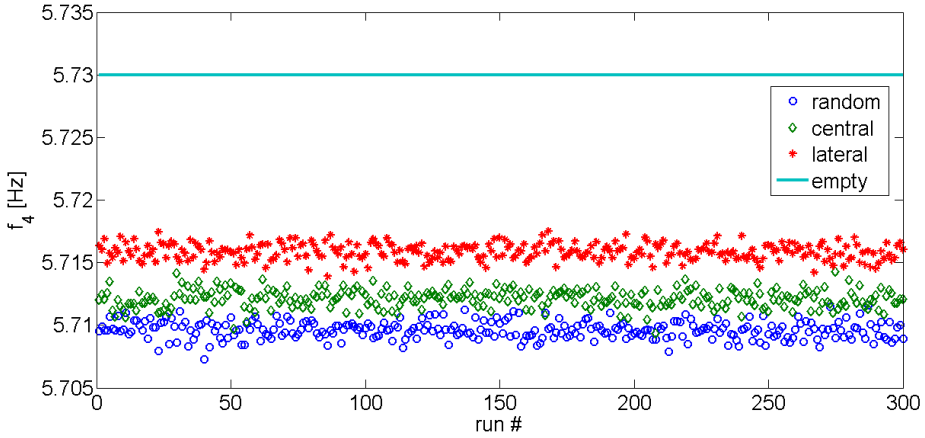

Figure 7.17: 50 % occupancy – various distributions – Natural frequency – mode 4

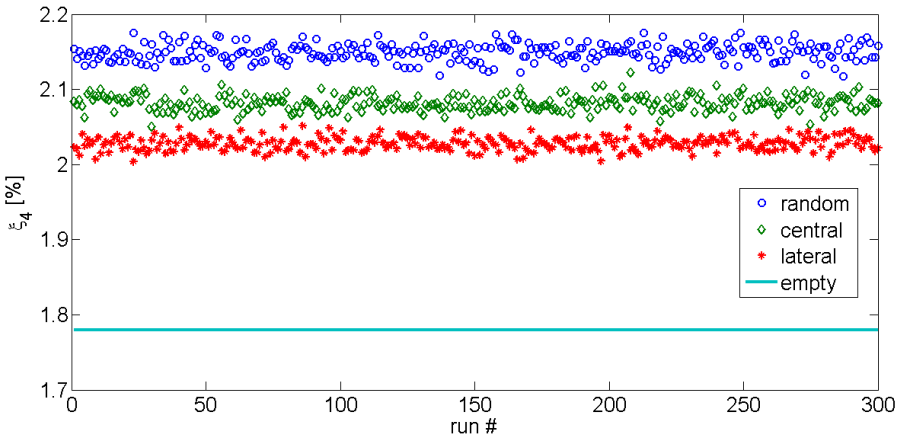

Figure 7.18: 50 % occupancy – various distributions – Damping ratio – mode 4

It is possible to notice that the same amount of people can have different effects on the modal parameters of the joint H-S system.

This implies that different occupancy rates could lead to similar modifications of structural modal parameters if the crowd's distribution changes. This is exemplified in Figure 7.19 and Figure 7.20.

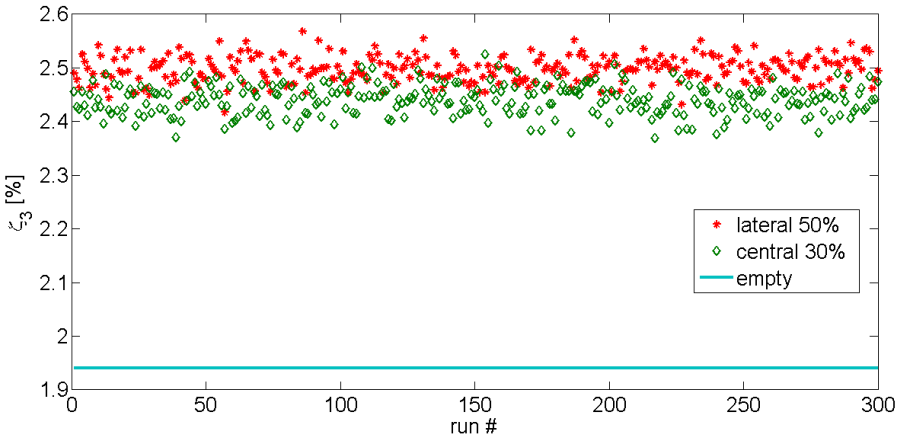

Figure 7.19: Damping ratio – mode 3 – different distribution and occupancy rates

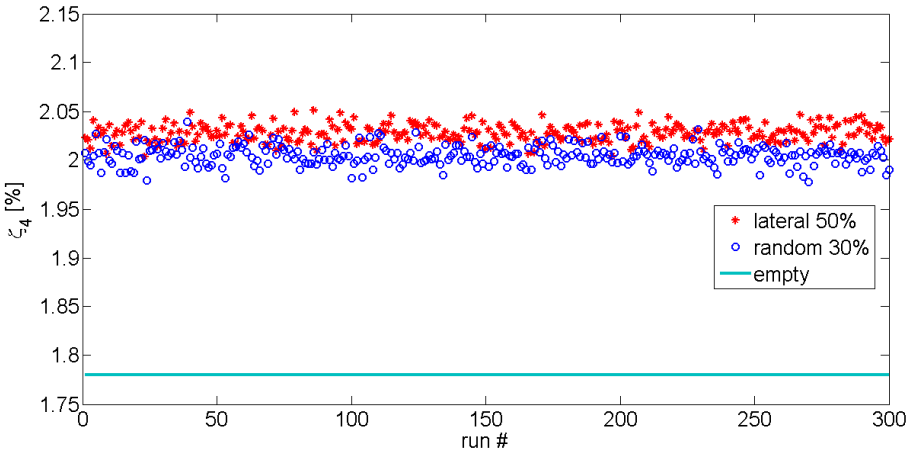

Figure 7.20: Damping ratio – mode 4 – different distribution and occupancy rates

Results show that a lower number of subjects on the structure can have the same effect of a higher number of subjects distributed in a different way.

7.6 Comparison between the complete H-S model and the superposition of the effects

The simulations described in Section 7.5 were compared with those performed using the same crowd's distributions and the superposition of the effects (Chapter 6, Section 6.3.2).

As an example, Figure 7.21, Figure 7.22, Figure 7.23 and Figure 7.24 show the results obtained for the case of random configuration with 50% occupancy rate. The results are shown in terms of difference between the parameters obtained with the superposition of the effects (app) and the complete model (compl). The results are compared with the difference between the modal parameters of the complete model and the modal parameters of the empty structure (empty).

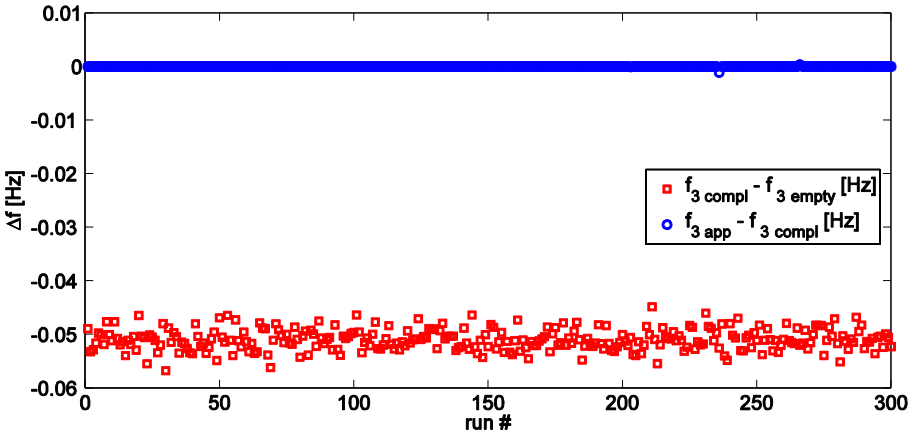

Figure 7.21: Natural frequency – mode 3 – complete model vs superposition of the effects

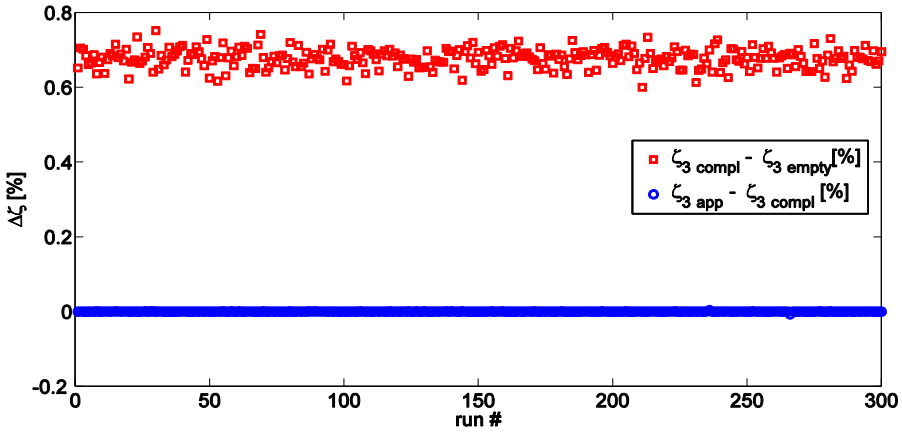

Figure 7.22: Damping ratio – mode 3 – complete model vs superposition of the effects

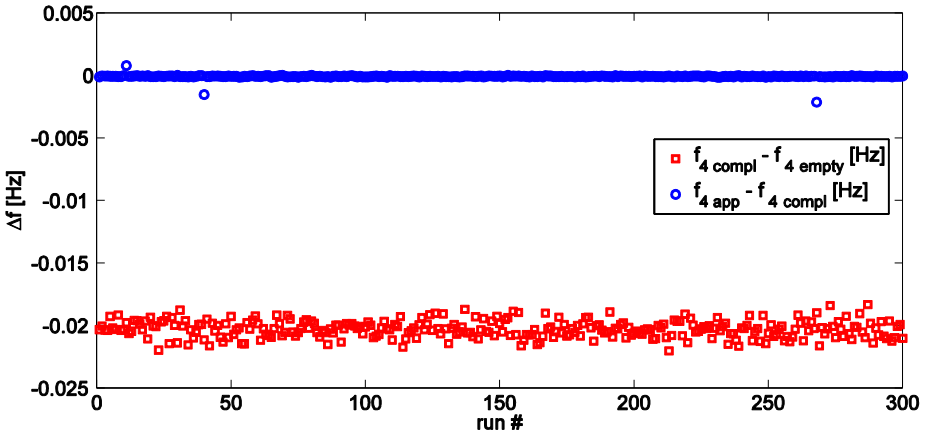

Figure 7.23: Natural frequency – mode 4 – complete model vs superposition of the effects

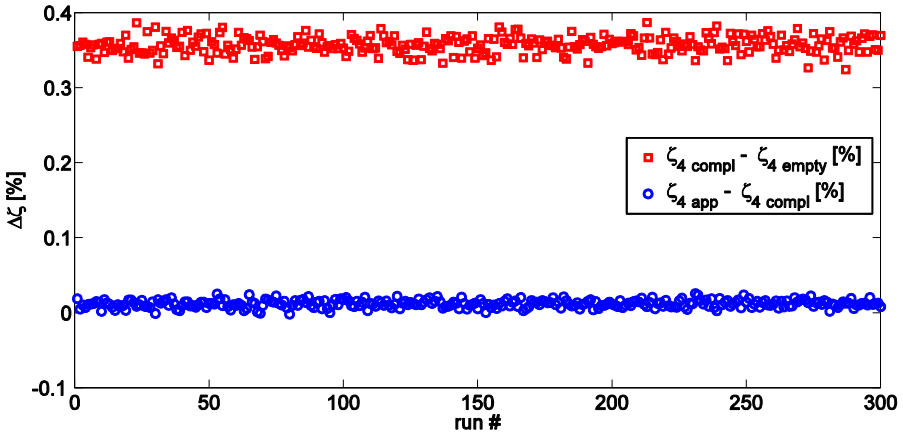

Figure 7.24: Damping ratio – mode 4 – complete model vs superposition of the effects

Results show that, for the structure under analysis, the use of the superposition of the effects introduces errors on the estimated modal parameters that are much lower that the differences between the parameters of the empty structure and those of the joint H-S system. Thus, for such a structure the superposition of the effects could be applied without introducing a significant modification in the obtained results.

7.7 Summary

This Chapter dealt with the analysis of the vibrations of a grandstand of the San Siro Stadium. Particularly, some data related to football matches were analysed.

The analysis of the football matches by means of OMA techniques showed the influence of people on the modal parameters of the structure. Particularly, damping ratios increases and natural frequencies decreases were recorded. The experimental results were compared with those obtained with a model to predict changes of modal parameters due to people's presence. The results of the model were consistent with the experimental evidence.

The effect of different people's distribution was evaluated by means of numerical simulations. Results showed that the effect of people on the modal parameters increase with the occupation rate. However, it was also proved that the modification of modal parameters is highly influenced by people's distribution. Indeed, people in a certain configuration can produce a modification of modal parameters similar to that produced by a lower number of people in a different configuration.

Finally, the differences between the use of the complete model of H-S interaction (Chapter 3) and the superposition of the effects (Chapter 6) were investigated. For the particular structure, the use of the superposition of the effects was proved to have little influence on the modal parameters of the joint H-S system.

Chapter 8

Conclusions

This chapter proposes a summary of the main contents of this work. The relevance of the proposed methods is highlighted and the main results are reviewed.

This work proposed a model to include the effect of people's presence when simulating the dynamic behaviour of joint H-S systems.

At first the influence of passive people was considered. An appropriate analytical model was proposed to include the effect of people's presence. The method only requires the knowledge of the modal model of the empty structure as an input. Each subject is then added locally on the structure by means of his/her apparent mass. With respect to other methods currently available from literature, the proposed approach places no constraints on the number of structural degrees of freedom taken into consideration. Two slender staircases and data available in literature were used to validate this approach. Passive people's presence could produce a significant increase of damping ratios. Conversely, natural frequencies and mode shapes were slightly modified. Initially, in order to simulate the dynamics of the joint H-S system people were included in the modal model of the empty structure using their measured apparent mass to verify the method. In this case, the results obtained were very close to the experimental data. This provided actual evidence of the effectiveness of the proposed approach. Then, people's presence was simulated by employing average values of the apparent mass found in literature in order to extend the results to real-life applications. Satisfactory results were obtained also in this case in terms of identification of changes of modal parameters due to people's presence.

The method was then extended with the purpose of accurately quantifying the in-service vibration amplitudes of a slender structure due to people's presence. The methodology is based on the superposition of two contributions produced by people acting on a structure. Particularly, people's effect is decoupled in passive Ground Reaction Forces (GRFs) and active forces. The GRFs are used to find an appropriate equivalent model to represent the dynamics of a structure occupied by moving people. The active force is then introduced on this modified model to obtain a prediction of the structural vibrations.

First, tests under controlled conditions were performed to validate the proposed approach. One subject was asked to march on a force plate, while a second subject was standing still on the structure. The actual force induced by a single subject and the structural response were measured at the same time. Results show that the use of the model of the empty structure to simulate the structural response causes an overestimation of the vibration amplitudes. Conversely, the use of the proposed methodology leads to results compatible with the experimental measurements. To represent the dynamic behaviour of moving subjects both

experimental data and models of the apparent mass were used. Good results were obtained in both cases.

The proposed approach was then extended to the case of normal operating conditions. To this purpose two main problems were investigated in the work. The first issue regards the identification of GRFs representative of the average influence of moving people in terms of changes of modal parameters. To this purpose a set of apparent masses, representative of various postures taken by people during motion, was measured. Thus, an average apparent mass was obtained and used to assess people's influence. The second issue regards the identification of appropriate active forces. As in normal operating conditions the actual force exerted by people could not be measured, an appropriate set of possible forces was measured. Thus, a statistical approach was used to simulate the structural response. An appropriate simulation procedure was used to obtain predictions of the structural vibrations. The results show that by using the modal model of the empty structure the obtained amplitudes overestimate the actual structural response. Conversely, by using the approach proposed in this work, results are compatible with the experimental measurements.

The analytical matrix of the joint H-S system was then analyzed in order to highlight its properties. The observation of the analytical form of this matrix allowed to evidence the differences between the use of the complete model proposed in this work and the superposition of the effects to predict the dynamic behavior of MDOFs structures occupied by passive people. Furthermore, the analysis of the joint H-S matrix allowed obtaining a simplified expression for such matrix under the hypothesis of SDOF structures. An approximate approach based on the analysis of the apparent mass curves was proposed to predict the type of influence due to people's presence on the modal parameters of the joint H-S system. The differences between the various possible solutions (complete model, superposition of the effects, approximate solution) were extensively investigated considering then case of a structure occupied by a single subject with apparent mass defined with a lumped parameters model. This assumption allowed to define the poles of the joint H-S system analytically. Results showed that under the hypothesis of SDOF structure the approximate solution introduces small errors with respect to the complete model. Conversely, the use of the superposition of the effects for MDOFs structure can introduce errors that can hardly quantified a-priori if the modes are not well separated. An analysis of the effect of people in different postures and for different directions of vibration through the analysis of various apparent mass curves was also proposed. Results showed that people can both increase and decrease the natural frequencies and damping ratios of a structure.

In the last Chapter of the work, some of the problems investigated in the previous Chapters were reviewed considering a stadium grandstand as test case structure. Such a structure is very different from the aforementioned. Indeed, the considered grandstand cannot be considered as a slender structure and the occupancy (up to 2330 people) is much higher than those expected on a staircase. Therefore, the proposed approach was applied also in this case in order to verify its effectiveness on a structure very different from those previously treated. To this purpose the effect of people during some football matches was analysed and some theoretical analyses were performed. Thus, an extension of the model to a different and more complex case was proposed. The impact of the number of people on the structure on its dynamic behaviour was analysed and the effect of different people's distribution was evaluated by means of simulations. Results showed that the effect of people on the modal parameters increase with the occupation rate. However, it was also proved that the modification of modal parameters is highly influenced by people's distribution. Indeed, people in a certain configuration can produce a modification of modal parameters similar to that produced by a lower number of people in a different configuration.

In summary, this study proposed and validated a method to describe the dynamic behaviour of joint H-S systems, which could be used to obtain reliable predictions of such a behaviour.

Annex A

Experimental mode shapes

This annex reports the experimental mode shapes identified from the analysis of the FRFs of the empty staircases reported in Chapter 3. As an example, the mode shapes identified from the analysis of the FRFs of the joint people-Campus Bicocca staircase system are also reported and compared to those of the empty structure.

A.1 Campus Bovisa Staircase – Empty structure

Point #	Mode 1 (7.85 Hz)	Mode 2 (8.86 Hz)	Mode 3 (16.80 Hz)
1	0.000831	0.000497	0.000660
2	0.000884	0.000089	-0.000249
3	0.009448	0.011446	0.007678
4	0.015723	-0.006885	-0.007703
5	0.014241	0.015218	0.007531
6	0.018798	0.003307	-0.000589
7	0.020766	-0.009982	-0.008367
8	0.017048	0.020344	0.006112
9	0.024554	-0.012473	-0.005921
10	0.016365	0.022071	0.002965
11	0.021119	0.004559	0.000700
12	0.024197	-0.013447	-0.002115
13	0.011429	0.019677	-0.001913
14	0.018169	-0.012996	0.003163
15	0.000734	0.009112	-0.007432
16	-0.001201	0.002951	-0.005887
17	0.000045	-0.002928	0.004596
18	-0.000600	0.000637	-0.001897

Table A. 1: Campus Bovisa staircase - Unit modal mass scaled mode shape vectors – Empty structure

A.2 Campus Bicocca Staircase – Empty Structure

Point #	Mode 1 (6.70 Hz)	Mode 2 (9.55 Hz)	Mode 3 (10.75 Hz)	Mode 4 (11.21 Hz)
1	0.003160	0.001827	0.000942	0.001686
2	0.007133	0.005532	0.001773	0.004064
3	0.010940	0.008795	0.002709	0.006386
4	0.012941	0.011287	0.003437	0.008016
5	0.012604	0.011464	0.003586	0.008553
6	0.010290	0.009056	0.003054	0.007239
7	0.006724	0.005800	0.001984	0.004968
8	0.002629	0.001913	0.000750	0.001969
9	0.004102	-0.000336	0.000871	-0.000477
10	0.008747	0.000259	0.001619	-0.000508
11	0.011813	0.000553	0.002230	-0.000182
12	0.014116	0.000718	0.003002	-0.000098
13	0.013996	0.001324	0.003213	0.000778
14	0.012076	0.000983	0.002700	0.000440
15	0.007789	0.001056	0.001752	0.000802
16	0.003076	0.000372	0.000556	0.000285
17	0.004263	-0.002341	0.000537	-0.002382
18	0.008952	-0.005334	0.001051	-0.004825
19	0.012665	-0.008135	0.001657	-0.006717
20	0.014646	-0.008911	0.002149	-0.007283
21	0.014799	-0.008848	0.002256	-0.007182
22	0.011746	-0.006552	0.001674	-0.005743
23	0.007626	-0.004221	0.000922	-0.003799
24	0.003211	-0.001255	0.000250	-0.001672

Table A. 2: Campus Bicocca staircase - Unit modal mass scaled mode shape vectors – empty structure

A.3 Campus Bicocca Staircase – Passive people

Point #	Mode 1 (6.61 Hz)	Mode 2 (9.55 Hz)	Mode 3 (10.75 Hz)	Mode 4 (11.21 Hz)
1	0.003068	0.001820	0.000797	0.001703
2	0.006948	0.005631	0.001637	0.004118
3	0.010356	0.008862	0.002585	0.006342
4	0.013017	0.011726	0.003343	0.008265
5	0.012994	0.012105	0.003484	0.008952
6	0.010832	0.009667	0.002946	0.007668
7	0.007168	0.006257	0.001880	0.005305
8	0.002828	0.002090	0.000679	0.002111
9	0.004166	-0.000435	0.000843	-0.000567
10	0.008892	0.000125	0.001666	-0.000650
11	0.011524	0.000248	0.002192	-0.000553
12	0.014861	0.000700	0.003075	-0.000253
13	0.014832	0.001587	0.003274	0.000889
14	0.013027	0.001193	0.002802	0.000545
15	0.008431	0.001317	0.001809	0.000988
16	0.003338	0.000484	0.000589	0.000379
17	0.004459	-0.002509	0.000627	-0.002520
18	0.009405	-0.005667	0.001234	-0.005123
19	0.013302	-0.008615	0.001838	-0.007163
20	0.015677	-0.009356	0.002361	-0.007696
21	0.015875	-0.009210	0.002476	-0.007548
22	0.012702	-0.006776	0.001900	-0.005967
23	0.008245	-0.004326	0.001088	-0.003916
24	0.003462	-0.001255	0.000342	-0.001689

Table A. 3: Campus Bicocca staircase - Unit modal mass scaled mode shape vectors – 3 people

Point #	Mode 1 (6.57 Hz)	Mode 2 (9.52 Hz)	Mode 3 (10.75 Hz)	Mode 4 (11.20 Hz)
1	0.003148	0.001812	0.000795	0.001700
2	0.007128	0.005662	0.001600	0.004073
3	0.010597	0.008923	0.002512	0.006254
4	0.013457	0.011840	0.003278	0.008198
5	0.013515	0.012288	0.003441	0.008946
6	0.011337	0.009802	0.002936	0.007665
7	0.007527	0.006359	0.001883	0.005320
8	0.002971	0.002130	0.000683	0.002124
9	0.004309	-0.000491	0.000795	-0.000586
10	0.009074	0.000051	0.001596	-0.000696
11	0.011750	0.000202	0.002114	-0.000675
12	0.015207	0.000653	0.002994	-0.000273
13	0.015289	0.001561	0.003186	0.000876
14	0.013511	0.001169	0.002743	0.000534
15	0.008766	0.001325	0.001777	0.001008
16	0.003471	0.000490	0.000576	0.000391
17	0.004536	-0.002579	0.000585	-0.002536
18	0.009561	-0.005818	0.001157	-0.005155
19	0.013525	-0.008817	0.001745	-0.007205
20	0.015960	-0.009561	0.002260	-0.007727
21	0.016221	-0.009414	0.002369	-0.007572
22	0.013020	-0.006933	0.001816	-0.005988
23	0.008459	-0.004423	0.001037	-0.003924
24	0.003557	-0.001287	0.000319	-0.001694

Table A. 4: Campus Bicocca staircase - Unit modal mass scaled mode shape vectors – 5 people

Point #	Mode 1 (6.53 Hz)	Mode 2 (9.48 Hz)	Mode 3 (10.74 Hz)	Mode 4 (11.20 Hz)
1	0.003118	0.001814	0.000894	0.001705
2	0.007080	0.005656	0.001707	0.003983
3	0.010495	0.008951	0.002777	0.006079
4	0.013364	0.011815	0.003310	0.007892
5	0.013522	0.012313	0.003337	0.008643
6	0.011439	0.009859	0.002720	0.007429
7	0.007551	0.006405	0.001686	0.005165
8	0.002997	0.002133	0.000578	0.002060
9	0.004289	-0.000535	0.001060	-0.000690
10	0.009132	0.000341	0.001812	-0.000926
11	0.011563	0.000585	0.002545	-0.000908
12	0.015082	0.000715	0.003221	-0.000687
13	0.015420	0.001527	0.003339	0.000678
14	0.013807	0.001251	0.002618	0.000572
15	0.008754	0.001351	0.001687	0.000930
16	0.003563	0.000463	0.000493	0.000359
17	0.004486	-0.002590	0.000789	-0.002489
18	0.009472	-0.005830	0.001476	-0.005092
19	0.013339	-0.008819	0.002160	-0.007118
20	0.015765	-0.009599	0.002641	-0.007711
21	0.016076	-0.009391	0.002688	-0.007499
22	0.012908	-0.006924	0.001978	-0.005935
23	0.008380	-0.004412	0.001137	-0.003886
24	0.003526	-0.001284	0.000366	-0.001672

Table A. 5: Campus Bicocca staircase - Unit modal mass scaled mode shape vectors – 10 people

A.4 Campus Bicocca Staircase – Comparison among mode shapes

Figure A.1, Figure A.2, Figure A.3 and Figure A.4 show a graphical comparison among the mode shapes of the empty structure and the mode shapes of the joint Passive people – structure systems. Results show that the presence of people has a small effect on the identified mode shapes.

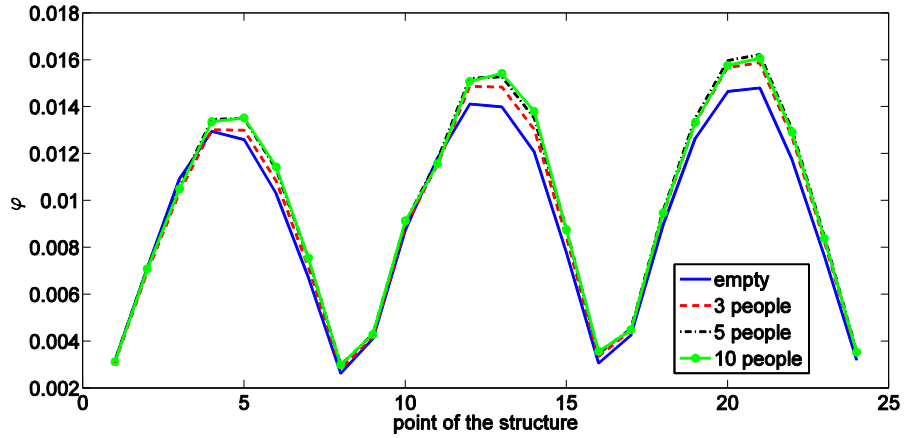

Figure A. 1: Campus Bicocca staircase – experimental mode shapes – mode 1

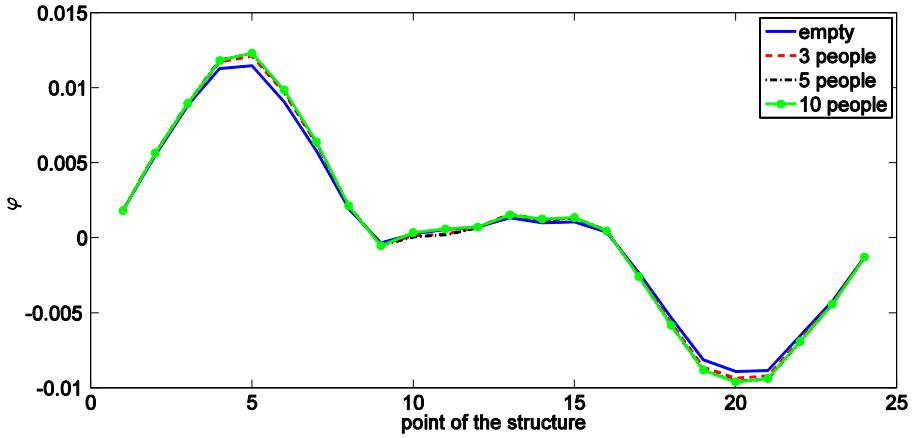

Figure A. 2: Campus Bicocca staircase – experimental mode shapes – mode 2

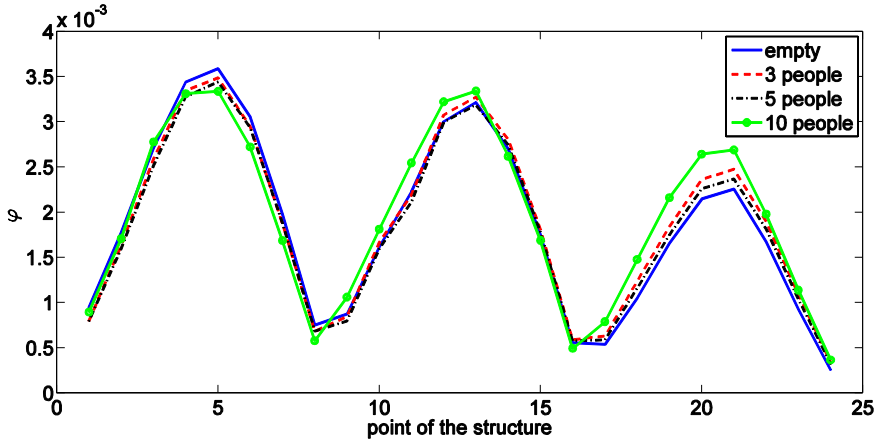

Figure A. 3: Campus Bicocca staircase – experimental mode shapes – mode 3

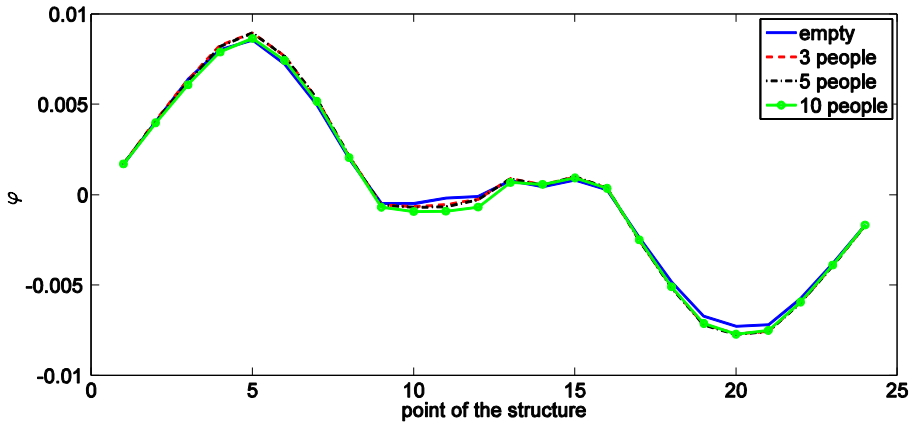

Figure A. 4: Campus Bicocca staircase – experimental mode shapes – mode 4

References

[1] R. Sachse, A. Pavic, P. Reynolds, Human-structure dynamic interaction in civil engineering dynamics: A literature review, Shock and Vibration Digest, 35 (1) (2003) 3-18

[2] S. Živanović, A. Pavic, P. Reynolds, Vibration serviceability of footbridges under human-induced excitation: a literature review, Journal of Sound and Vibration, Volume 279, Issues 1–2, 6 January 2005, Pages 1-74, ISSN 0022-460X, http://dx.doi.org/10.1016/j.jsv.2004.01.019.

[3] Pavic, A.; Reynolds, P.; Vibration serviceability of long-span concrete building floors. Part 1: Review of background information, Shock and Vibration Digest, v 34, n 3, p 191-211, May 2002

[4] Pavic, A.; Reynolds, P.; Vibration serviceability of long-span concrete building floors. Part 2: Review of mathematical modelling approaches, Shock and Vibration Digest, v 34, n 4, p 279-297, July 2002

[5] Jones, C.A.; Reynolds, P.; Pavic, A.; Vibration serviceability of stadia structures subjected to dynamic crowd loads: A literature review, Journal of Sound and Vibration, v 330, n 8, p 1531-1566, April 11, 2011

[6] J.M.W. Brownjohn, A. Pavic, Human-induced vibrations on footbridges, 3rd International Conference on Bridge Maintenance, Safety and Management - Bridge Maintenance, Safety, Management, Life-Cycle Performance and Cost, July 16, 2006 - July 19, 2006

[7] J.G.S. da Silva, P.C.G. da S. Vellasco, S.A.L. de Andrade, L.R.O. de Lima, F.P. Figueiredo, Vibration analysis of footbridges due to vertical human loads, Computers and Structures, v 85, n 21-22, p 1693-1703, November 2007

[8] J.F.S. Rodrigues, P.A.O. Almeida, Statistical treatment of vibrations induced by spectators on Brazilian football stadium, Conference Proceedings of the Society for Experimental Mechanics Series, 2006, IMAC-XXIV

[9] S.P. Nhleko, M.S. Williams, A. Blakeborough, Vibration perception and comfort levels for an audience occupying a grandstand with perceivable motion, Conference Proceedings of the Society for Experimental Mechanics Series, 2009, IMAC-XXVII

[10] M. Setareh, Vibrations due to walking in a long-cantilevered office building structure, Journal of Performance of Constructed Facilities, v 26, n 3, p 255-270, June 2012S. Zivanovic, A. Pavic, P. Reynolds,

[11] EN 1990 - Eurocode, Basis of structural design, 2002.

[12] International Organization for Standardization ISO 10137, Bases for design of structures - Serviceability of buildings and walkways against vibration, 2007

[13] Sètra, Technical Guide - Assessment of vibrational behaviour of footbridges under pedestrian loading, Service d'Etudes techniques des routes et autoroutes, Paris, 2006

[14] R. Sachse, The influence of human occupants on the dynamic properties of slender structure, PhD Thesis, The University of Sheffield, UK, April 2002

[15] R. Sachse, Modelling effects of human occupants on modal properties of slender structures, The Structural Engineer, 80(5) (2002)

[16] R. Sachse, A. Pavic, P. Reynolds, Parametric study of modal properties of damped two-degree-of-freedom crowd–structure dynamic systems, Journal of Sound and Vibration, Volume 274, Issues 3–5, 22 July 2004, Pages 461-480

[17] J.H.H. Sim, Human-Structure Interaction in Cantilever Grandstands, PhD Thesis, The University of Oxford, UK, 2006

[18] J. Sim, A. Blakeborough, M. Williams, Modelling effects of passive crowds on grandstand vibration, Proceedings of the Institution of Civil Engineers: Structures and Buildings, 159(5) (2006) 261-272

[19] J. Sim, A. Blakeborough, M. Williams, Modelling of joint crowd-structure system using equivalent reduced-DOF system, Shock and Vibration, 14(4) (2007) 261-270

[20] Institution of Structural Engineers (2008), "Dynamic performance requirements for permanent grandstands subject to crowd action: Recommendations for management, design and assessment", London.

[21] M. Setareh, Evaluation and assessment of vibrations owing to human activity, Proceedings of the Institution of Civil Engineers: Structures and Buildings, v 165, n 5, p 219-231, May 2012

[22] V. Racic, J.M.W. Brownjohn, A. Pavic, Human walking and running forces: Novel experimental characterization and application in civil engineering dynamics, Conference Proceedings of the Society for Experimental Mechanics Series, 2008, IMAC-XXVI: Conference and Exposition on Structural Dynamics - Technologies for Civil Structures

[23] V. Racic, A. Pavic, J.M.W. Brownjohn, Experimental identification and analytical modelling of human walking forces: Literature review, Journal of Sound and Vibration, v 326, n 1-2, p 1-49, September 25, 2009

[24] S.C. Kerr, N.W.M. Bishop, Human induced loading on flexible staircases, Engineering Structures, v 23, n 1, p 37-45, Jan 2001

[25] N.W.M. Bishop, M. Willford, R. Pumphrey, Human induced loading of flexible staircases, Safety Science, v 18, n 4, p 261-276, Feb 1995

[26] C.M. Casado, I.M. Díaz, J. De Sebastián, A.V. Poncela, A. Lorenzana, Implementation of passive and active vibration control on an in-service footbridge, Structural Control and Health Monitoring, v 20, n 1, p 70-87, January 2013

[27] M. Hudson, P. Reynolds, Potential benefits of incorporating active vibration control in floor structures, Structural Engineer, v 91, n 2, p 46-48, February 2013

[28] D. Nyawako, P. Reynolds, Technologies for mitigation of human-induced vibrations iin civil engineering structures, Shock and Vibration Digest, v 39, n 6, p 465-493, November 2007

[29] P. Reynolds, A framework for advanced methods of control of human-induced vibrations, Proceedings of SPIE - The International Society for Optical Engineering, v 8345, 2012, Sensors and Smart Structures Technologies for Civil, Mechanical, and Aerospace Systems 2012

[30] J.M.W. Brownjohn, Energy dissipation from vibrating floor slabs due to human-structure interaction, Shock and Vibration 8(6): 315-23, 2001.

[31] J.M.W. Brownjohn, X. Zheng, The effects of human postures on energy dissipation from vibrating floors, in Chau, F.S. and Quan, C. (eds). Second International Conference on Experimental Mechanics. Proceedings of SPIE, Vol. 4317: 489-93. 2001.

[32] P. Reynolds, A. Pavic, Z. Ibrahim, Changes of modal properties of a stadium structure occupied by a crowd, Proceedings of XXII International Modal Analysis Conference, Orlando, Fl, USA, 2004.

[33] C.A. Jones, A. Pavic, P. Reynolds, R.E. Harrison, Verification of equivalent mass-spring-damper models for crowd-structure vibration response prediction, Canadian Journal of Civil Engineering, v 38, n 10, p 1122-1135, October 2011

[34] G. Busca, A. Cappellini, S. Manzoni, M. Vanali, M. Tarabini, Quantification of changes of modal parameters due to the presence of passive people on a slender structure, Journal of Sound and Vibration, 10/2014; 333(21):5641–5652

[35] L. Pedersen, Damping Effect of Humans, Proceedings of XXX International Modal Analysis Conference, Jacksonville, FL USA, 2012

[36] B.R. Ellis, T. Ji, Human-structure interaction in vertical vibrations, Proceedings of the ICE: Structures and Buildings 122(1) 1997, pp. 1-9.

[37] B.R. Ellis, T. Ji, J.D. Littler, Crowd actions and grandstands, in Symposium: Places of Assembly and Long-Span Building Structures, Birmingham, UK, 7-9 September, 1994. Zürich, Switzerland: IABSE. Report 71: 277-82, 1994.

[38] B.R. Ellis, T. Ji, J.D. Littler, The response of grandstands to dynamic forces induced by crowds, Australasian Structural Engineering Conference, Sydney, Australia, 1994.

[39] J.M.V. Brownjohn, Energy dissipation in one-way slabs with human participation, Proceedings of the Asia-Pacific Vibration Conference '99, Nanyang Technological University, Singapore, Vol. 1 1999,: pp. 155-60.

[40] S. Falati, The contribution of non-structural components to the overall dynamic behaviour of concrete floor slabs. PhD Thesis, University of Oxford, Oxford, UK 1999.

[41] Salyards, Kelly A., Robert J. Human-structure interaction: Effects of crowd characteristics Source: Conference Proceedings of the Society for Experimental Mechanics Series, v 4, p 247-254, 2011, Civil Engineering Topics - Proceedings of the 29th IMAC, a Conference on Structural Dynamics, 2011

[42] R.L.Pimentel; Vibration performance of pedestrian bridges due to human-induced loads; Thesis (PhD) University of Sheffield, Sheffield, UK; 1997

[43] S.V.Ohlsson; Floor vibration and human discomfort; Thesis (PhD) Chalmers University of Technology, Göteborg, Sweden; 1982

[44] S. Zivanovic, A. Pavic, E.T. Ingòlfsson, Modeling spatially unrestricted pedestrian traffic on footbridges, Journal of Structural Engineering, v 136, n 10, p 1296-1308, October 2010

[45] S. Zivanovic, I.M. Dìaz, A. Pavic, Influence of walking and standing crowds on structural dynamic properties, Conference Proceedings of the Society for Experimental Mechanics Series, 2009, IMAC-XXVII: Conference and Exposition on Structural Dynamics - Model Verification and Validation

[46] F. Walley, St James's Park Bridge, Proceedings of the ICE 12 1959, pp. 217-22

[47] D.E. Allen, J.H. Rainer, Floor vibration, NRCC. Canadian Building Digest (CBD) 173 (1975).

[48] A: Ebrahimpour, R.L. Sack, P.D. van Kleek, Computing crowd loads using a nonlinear equation of motion, in Proceeding of the 4th International Conference on Civil and Structural Engineering 1989, pp. 47-52.

[49] J.H. Rainer, G. Pernica, Vibration characteristics of a floor sample. Ottawa, Canada: NRCC, Division of Building Research. NRCC-24298 1985.

[50] R.O. Foschi, A. Gupta, Reliability of floors under impact vibration, Canadian Journal of Civil Engineering 14(5) (1997) 683-9.

[51] Y. Matsumoto, M.J. Griffin, Mathematical models for the apparent masses of standing subjects exposed to vertical whole-body vibration. Journal of Sound and Vibration 260 (2003) 431-451.

[52] T. E. Fairley, M. J. Griffin, The apparent mass of the seated human body: Vertical vibration, Journal of Biomechanics, Volume 22, Issue 2, 1989, Pages 81-94

[53] L. Wei, M.J. Griffin, Mathematical models for the apparent mass of the seated human body exposed to vertical vibration, Journal of Sound and Vibration, Volume 212, Issue 5, 21 May 1998, Pages 855-874

[54] Y. Matsumoto, M.J. Griffin, Dynamic response of the standing human body exposed to vertical vibration: influence of posture eand vibration magnitude, Journal of Sound and Vibration, Volume 212, Issue 1, 23 April 1998, Pages 85-107

[55] N.A. Alexander, Theoretical treatment of crowd-structure interaction dynamics, Structures and Buildings, Vol. 159 (6), 12.2006, p. 329 - 338.

[56] A. Pavic, P. Reynolds, Experimental verification of novel 3DOF model for grandstand crowd-structure dynamic interaction, Proceedings of the 26th International Modal Analysis Conference (IMAC XXVI), 2008.

[57] Z. Ibrahim, The Effects of Crowds on Dynamic Characteristics of Stadia Structures, PhD Thesis, Department of Civil and Structural Engineering, University of Sheffield, UK, 2006.

[58] J.W. Qin, S.S. Law, Q.S. Yang, N. Yang, Pedestrian-bridge dynamic interaction, including human participation, Journal of Sound and Vibration, v 332, n 4, p 1107-1124, February 18, 2013

[59] E. Shahabpoor, A. Pavic, V. Racic, Using MSD model to simulate human-structure interaction during walking, Topics in Dynamics of Civil Structures - Proceedings of the 31st IMAC, A Conference on Structural Dynamics, 2013, p 357-364, 2013,

[60] H. Bachmann, A.J. Pretlove, H. Rainer, Dynamic forces from rhythmical human body motions, Vibration Problems in Structures: Practical Guidelines, Birkhäuser, Basel, 1995,

[61] Racic, Vitomir; Pavic, Aleksandar; Brownjohn, James Mark William, Modern facilities for experimental measurement of dynamic loads induced by humans: A literature review, Shock and Vibration, v 20, n 1, p 53-67, 2013; ISSN: 10709622; DOI: 10.3233/SAV-2012-0727;

[62] F. Dierick, M. Penta, D. Renaut, C. Detrembleur, A force measuring treadmill in clinical gait analysis, Gait and Posture 20 (2004) 299–303.

[63] R. Kram, Force Treadmill for measuring vertical and horizontal ground reaction forces, Journal of Applied Physiology 85 (1998) 764–769.

[64] A. Forner Cordero, H.J.F. Koopman, F.C.T. van der Helm, Use of pressure insoles to calculate the complete ground reaction forces, Journal of Biomechanics 37 (2004) 1427–1432.

[65] H.H. Savelberg, A.L. de Lange, Assessment of the horizontal, fore-aft component of the ground reaction force from insole pressure patterns by using artificial neural networks, Clinical Biomechanics 14 (1999) 585–592.

[66] M. Lord, Spatial resolution in plantar pressure measurement, Medical Engineering and Physics 19 (1997) 140–144.

[67] N.W.M. Bishop, M. Willford, R. Pumphrey, Human induced loading of flexible staircases, Safety Science, v 18, n 4, p 261-276, Feb 1995

[68] M. Kasperski, B. Czwikla; A refined model for human induced loads on stairs; Conference Proceedings of the Society for Experimental Mechanics Series 2012, Volume 1, pp 27-39

[69] H. Bachmann, Vibration Problems in Structures, Birkhauser, Basel, Boston, Berlin, 1995

[70] Racic, Vitomir, Brownjohn, James Mark William, Stochastic model of near-periodic vertical loads due to humans walking, Advanced Engineering Informatics, v 25, n 2, p 259-275, April 2011; ISSN: 14740346; DOI:10.1016/j.aei.2010.07.004

[71] Racic, Vitomir; Brownjohn, James M.W.; Pavic, Aleksandar, Random model of vertical walking force signals, Proceedings of the 30th IMAC, A Conference on Structural Dynamics, 2012; ISSN: 21915644, E-ISSN: 21915652; ISBN-13: 9781461424123; DOI:10.1007/978-1-4614-2413-0_8

[72] Racic, V.; Brownjohn, J.M.W.; Pavic, A., Stochastic model of continuously measured vertical pedestrian loads, Proceedings of the Sixth International

Conference on Bridge Maintenance, Safety and Management, p 3701-3708, 2012, ISBN-13: 9780415621243

[73] Racic, Vitomir; Brownjohn, James M.W.; Pavic Aleksandar, Novel experimental characterisation of human-induced loading, Proceedings of the Society for Experimental Mechanics Series, 2009, IMAC-XXVII: Conference and Exposition on Structural Dynamics - Model Verification and Validation; ISSN: 21915644, E-ISSN: 21915652; ISBN-13: 9781605609614

[74] Racic, Vitomir; Brownjohn, James M.W.; Pavic, Aleksandar, Human walking and running forces: Novel experimental characterization and application in civil engineering dynamics, Conference Proceedings of the Society for Experimental Mechanics Series, 2008, IMAC-XXVI: Conference and Exposition on Structural Dynamics - Technologies for Civil Structures; ISSN: 21915644, E-ISSN: 21915652; ISBN-13: 9781605600666;

[75] Subashi, G.H.M.J.; Matsumoto, Y.; Griffin, M.J., Modelling resonances of the standing body exposed to vertical whole-body vibration: Effects of posture, Journal of Sound and Vibration, v 317, n 1-2, p 400-418, October 21, 2008

[76] Matsumoto, Y.; Griffin, M.J., Comparison of biodynamic responses in standing and seated human bodies, Journal of Sound and Vibration, v 238, n 4, p 691-704, December 7, 2000

[77] Toward, Martin G.R.; Griffin, Michael J., Apparent mass of the human body in the vertical direction: Inter-subject variability, Journal of Sound and Vibration, v 330, n 4, p 827-841, February 14, 2011

[78] Toward, Martin G.R.; Griffin, Michael J., Apparent mass of the human body in the vertical direction: Effect of seat backrest, Journal of Sound and Vibration, v 327, n 3-5, p 657-669, November 13, 2009

[79] E.T. Ingòlfsson, C.T. Georgakis, J. Jonsson, Pedestrian-induced lateral vibrations of footbridges: A literature review, Engineering Structures, v 45, p 21-52, December 2012

[80] Danbon F, Grillaud G. Dynamic behaviour of a steel footbridge. Characterisation and modelling of the dynamic loading induced by a nmoving crowd on the Solferino footbridge in Paris. In: Proceedings of Footbridge 2005, second international conference, Venice, 2005.

[81] Dallard P, Fitzpatrick AJ, Flint A, Le Bourva S, Low A, Smith RMR, et al. The London Millennium Footbridge. Struct Eng 2001; 79(22):17–33

[82] Rönnquist A, Strømmen E, Wollebæk L. Dynamic properties from full scale recordings and FE-modelling of a slender footbridge with flexible connections. Struct Eng Int 2008;4:421–6.

[83] Da Fonseca A, Balmond C, Conceptual design of the new Coimbra fotbridge. In: Proceedings of Footbridge 2005, second international conference, Venice, 2005

[84] Macdonald JHG. Pedestrian-induced vibrations of the Clifton Suspension Bridge, UK. Proc ICE: Bridge Eng 2008;161(BE2):69–77. http://dx.doi.org/10.1680/bren.2008.161.2.69.

[85] Roberts TM. Lateral pedestrian excitation of footbridges. J Bridge Eng 2005;10(1):107–12.

[86] Roberts TM, Synchronised pedestrian lateral excitation of footbridges. In: Proceedings of the 6th international conference on structural dynamics, Paris, 2005

[87] Johnson R. A mathematical modelling of the pedestrian induced lateral vibrations of the Millennium Bridge. MSc thesis, University of Bristol, 2005.

[88] Venuti, Fiammetta; Bruno, Luca; Bellomo, Nicola; Crowd dynamics on a moving platform: Mathematical modelling and application to lively footbridges, Mathematical and Computer Modelling, v 45, n 3-4, p 252-269, February 2007

[89] Venuti F., Bruno L. Crowd-structure interaction in lively footbridges under synchronous lateral excitation: a literature review. Phys Life Rev 2009;6:176–206. http://dx.doi.org/10.1016/j.plrev.2009.07.001.

[90] Reynolds, Paul, A framework for advanced methods of control of human-induced vibrations, Proceedings of SPIE - The International Society for Optical Engineering, v 8345, 2012, Sensors and Smart Structures Technologies for Civil, Mechanical, and Aerospace Systems 2012

[91] Varela, Wendell D.; Battista, Ronaldo C., Control of vibrations induced by people walking on large span composite floor decks, Engineering Structures, v 33, n 9, p 2485-2494, September 2011

[92] Chen, Xin; Ding, Youliang; Li, Ai-qun; Zhang, Zhiqiang; Sun, Peng; Investigations on serviceability control of long-span structures under human-induced excitation, Earthquake Engineering and Engineering Vibration, v 11, n 1, p 57-71, March 2012

[93] Qi, Manyi; Zhang, Zhiqiang; Ma, Fei; Li, Aiqun; Vibration control analysis of high-rise cantilevered floors under pedestrian walking loads, Applied Mechanics and Materials, v 94-96, p 1110-1114, 2011, Advances in Structural Engineering

[94] Venuti, Fiammetta; Bruno, Luca; Mitigation of human-induced lateral vibrations on footbridges through walkway shaping, Engineering Structures, v 56, p 95-104, November 2013

[95] Philp, R.; Reynolds, P.; Nyawako, D.S.; Semi-active control of staircase vibration under human excitation, Conference Proceedings of the Society for Experimental Mechanics Series, v 4, p 263-272, 2011, Civil Engineering Topics - Proceedings of the 29th IMAC, a Conference on Structural Dynamics, 2011

[96] Hudson, M.J. ; Reynolds, P., Implementation considerations for active vibration control in the design of floor structures, Engineering Structures, v 44, p 334-358, November 2012; ISSN: 01410296; DOI: 10.1016/j.engstruct.2012.05.034

[97] Shahabpoor, Erfan; Reynolds, Paul; Nyawako, Donald; A comparison of direct velocity, direct and compensated acceleration feed-back control systems in mitigation of low-frequency floor vibrations, Conference Proceedings of the Society for Experimental Mechanics Series, v 4, p 177-187, 2011, Dynamics of Civil Structures - Proceedings of the 28th IMAC, A Conference on Structural Dynamics, 2010

[98] Dìaz, Ivàn M.; Reynolds, Paul; Acceleration feedback control of human-induced floor vibrations, Engineering Structures, v 32, n 1, p 163-173, January 2010

[99] Díaz, Iván M. ; Reynolds, Paul, On-off nonlinear active control of floor vibrations, Mechanical Systems and Signal Processing, 2010; ISSN: 08883270, E-ISSN: 10961216; DOI: 10.1016/j.ymssp.2010.02.011

[100] Reynolds, Paul; Dìaz, Ivàn M.; Nyawako, Donald S.; Vibration testing and active control of an office floor, Conference Proceedings of the Society for Experimental Mechanics Series, 2009, IMAC-XXVII: Conference and Exposition on Structural Dynamics - Model Verification and Validation

[101] Nyawako, D.; Reynolds, P.; Response-dependent velocity feedback control for mitigation of human-induced floor vibrations, Smart Materials and Structures, v 18, n 7, 2009

[102] Dìaz, Ivàn M.; Pereira, Emiliano; Reynolds, Paul; Integral resonant control scheme for cancelling human-induced vibrations in light-weight pedestrian structures, Structural Control and Health Monitoring, v 19, n 1, p 55-69, February 2012

[103] Hudson, Malcolm J. ; Reynolds, Paul ; Nyawako, Donald S., Comparison of passive and active mass dampers for control of floor vibrations, Proceedings

of SPIE - The International Society for Optical Engineering, v 8345, 2012, Sensors and Smart Structures Technologies for Civil, Mechanical, and Aerospace Systems 2012; ISSN: 0277786X, ISBN-13: 9780819490025; DOI: 10.1117/12.915956

[104] Noormohammadi, Nima; Reynolds, Paul; Employing hybrid tuned mass damper to solve off-tuning problems for controlling human induced vibration in Stadia, Topics in Dynamics of Civil Structures - Proceedings of the 31st IMAC, A Conference on Structural Dynamics, 2013, p 71-78, 2013, Topics in Dynamics of Civil Structures - Proceedings of the 31st IMAC, A Conference on Structural Dynamics, 2013

[105] Noormohammadi, Nima; Reynolds, Paul; Experimental investigation of dynamic performance of a prototype hybrid tuned mass damper under human excitation, Proceedings of SPIE - The International Society for Optical Engineering, v 8688, 2013, Active and Passive Smart Structures and Integrated Systems 2013

[106] National Building Code of Canada 2010

[107] BS 6399-1: 1996

[108] D. J. Ewins, Modal testing: theory, practice and application, 2nd Ed., Taylor and Francis Group, London, 2001

[109] S. Krenk, Lectures presented at 'Semi–Active Vibration Suppression – The Best from Active and Passive Technologies', CISM, Udine, October 1–5, 2007

[110] M. A. Woodbury, Inverting modified matrices, Statistical Research Group, Memo. Rep. no. 42, Princeton University, Princeton, N. J., 1950

[111] B. Peeters, H. Van der Auweraer, P. Guillaume, J. Leuridan, The PolyMAX frequency-domain method: a new standard for modal parameter estimation?, Shock and Vibration 11(3-4) (2004) 395-409

[112] J. Bendat, A.G. Piersol, Random data: analysis and measurement procedures, John Wiley & Sons, 1993

[113] Peeters, Bart; Vecchio, Antonio; Van Der Auweraer, Herman, PolyMAX modal parameter estimation from operational data, Proceedings of the 2004 International Conference on Noise and Vibration Engineering, ISMA, p 1049-1063, 2004, Proceedings of the 2004 International Conference on Noise and Vibration Engineering, ISMA

[114] B. Peeters, F. Vanhollebeke, and H. Van Der Auweraer, "Operational PolyMAX for estimating the dynamic properties of a stadium structure during a football game," in Proceedings of the XXIII IMAC, 2005, no. 1

[115] M. A. Woodbury, Inverting modified matrices, Statistical Research Group, Memo. Rep. no. 42, Princeton University, Princeton, N. J., 1950

[116] B. Peeters, H. Van der Auweraer, P. Guillaume, J. Leuridan, The PolyMAX frequency-domain method: a new standard for modal parameter estimation?, Shock and Vibration 11(3-4) (2004) 395-409

[117] J. Bendat, A.G. Piersol, Random data: analysis and measurement procedures, John Wiley & Sons, 1993

[118] Peeters, Bart; Vecchio, Antonio; Van Der Auweraer, Herman, PolyMAX modal parameter estimation from operational data, Proceedings of the 2004 International Conference on Noise and Vibration Engineering, ISMA, p 1049-1063, 2004, Proceedings of the 2004 International Conference on Noise and Vibration Engineering, ISMA

[119] B. Peeters, F. Vanhollebeke, and H. Van Der Auweraer, "Operational PolyMAX for estimating the dynamic properties of a stadium structure during a football game," in Proceedings of the XXIII IMAC, 2005, no. 1

[120] Matsumoto, Y.; Griffin, M.J.; The horizontal apparent mass of the standing human body, Journal of Sound and Vibration, v 330, n 13, p 3284-3297, June 20, 2011

[121] Qiu,Y., Griffin,M.J. (2011) Modelling the fore-and-aft apparent mass of the human body and the transmissibility of seat backrests. Vehicle Systems Dynamics 49(5), 703-72.

[122] Ki-Sun Kim, Jongwan Kim, Kwang-joon Kim, Dynamic modeling of seated human body based on measurements of apparent inertia matrix for fore-and-aft/vertical/pitch motion, Journal of Sound and Vibration, Volume 330, Issue 23, 7 November 2011, Pages 5716-5735

Abbreviations

DOF	Degree Of Freedom
FRF	Frequency Response Function
GRF	Ground Reaction Force
H-S	Human-Structure
HSI	Human Structure Interaction
IRF	Impulse Response Function
MDOF	Multi Degrees Of Freedom
MSD	Mass-Spring-Damper
rms	Root mean square
SDOF	Single Degree Of Freedom
TMD	Tuned Mass Damper
TP	Test Point
TS	Test Subject

Nomenclature

Vectors and matrices variables are in bold

Scalars variables are in italics

c_1	Matsumoto and Griffin Lumped parameters model – damping of the first DOF
c_2	Matsumoto and Griffin Lumped parameters model – damping of the second DOF
D_j	Denominator of the matrix $\mathbf{G}(\omega)$ (j^{th} mode)
$\mathbf{f}(\omega)$	Generic force vector
$\mathbf{f}^{\mathrm{ACTIVE}}(\omega)$	Active forces vector
$\mathbf{f}^{\mathrm{GR}}(\omega)$	Ground Reaction Forces vector– moving subject
f^{Human}	Ground Reaction Force
$\mathbf{f}^{\mathrm{Human}}(\omega)$	Ground Reaction Forces vector
f_n	Natural frequency [Hz]
$F_1(s)$	Force applied to point 1- Laplace domain
$\mathbf{G}(\omega)$	FRF matrix – Empty structure
$G_{ik}(\omega)$	Element i,k of the matrix $\mathbf{G}(\omega)$
$G_{ik}(s)$	Element i,k of the matrix $\mathbf{G}(\mathrm{s})$ – Laplace domain
$\mathbf{G}_{\mathrm{H}}(\omega)$	FRF matrix – H-S system
$G_{H,ik}(\omega)$	Element i,k of the matrix $\mathbf{G}_{\mathrm{H}}(\omega)$
$G_{H,ik}(s)$	Element i,k of the matrix $\mathbf{G}_{\mathrm{H}}(\mathrm{s})$ – Laplace domain
$\tilde{G}_{H,ik}(\omega)$	Approximate FRF in point i,k of the joint H-S system
$H_k(\omega)$	Transfer function of the subject located at point k
$\mathbf{H}(\omega)$	Matrix of subjects' transfer functions
$H_{\mathrm{i}}(\omega)$	Element i,i of the matrix $\mathbf{H}(\omega)$
$H(s)$	Subject's transfer function – Laplace domain
$\widetilde{H}(s)$	Approximate subject's transfer function – Laplace domain
i	Imaginary unit

k	Generic point of the structure
k_1	Matsumoto and Griffin Lumped parameters model – stiffness of the first DOF
k_2	Matsumoto and Griffin Lumped parameters model – stiffness of the second DOF
$\mathrm{K_p}$	Number of structural discretization points
m	Number of passive subjects on the structure
m_0	Matsumoto and Griffin Lumped parameters model – mass of the supporting structure
m_1	Matsumoto and Griffin Lumped parameters model – mass of the first DOF
m_2	Matsumoto and Griffin Lumped parameters model – mass of the second DOF
$m^*(\omega)$	Normalized apparent mass
$\bar{M}$	Physical mass of the subject
$M^*(\omega)$	Generic apparent mass
$M_{\mathrm{a}}{}^*(\omega)$	Apparent mass representative of the generic a^{th} posture
$M_{\mathrm{eq}}{}^*(\omega)$	Equivalent apparent mass of moving people
M^*_{fr}	Fraction of apparent mass associated to each $\mathrm{K_p}$ point
n	Number of modes
n_p	Number of people moving on the structure
$n\_subjects$	Number of subjects on the structure
$\mathbf{N}(\omega)$	Numerator of the matrix $\mathbf{G}_{\mathrm{H}}(\omega)$
$N_{\mathrm{ik}}(\omega)$	Element i,k of the matrix $\mathbf{N}(\omega)$
P	Number of postures considered to determine the equivalent apparent mass of the joint Structure-moving people system
$\mathbf{w}_k$	Vector defining the spatial distribution of a subject located at point k of the structure
$\mathbf{W}$	Matrix of spatial distribution of all the subjects on the structure
x	Displacement
$\dot{x}$	Velocity
$\ddot{x}$	Acceleration
$\mathbf{x}(\omega)$	Full displacement vector (frequency domain)
$X_1(s)$	Displacement of point 1 – Laplace domain

α_{a}	Apparent mass weighting coefficient
β	Weighted mass ratio
β_j	Weighted mass ratio – j$^{\mathrm{th}}$ mode
ζ	Non-dimensional damping ratio
ζ_j	Non-dimensional damping ratio of the j$^{\mathrm{th}}$ mode
$\bar{\zeta}$	Approximate damping ratio of the joint H-S system
σ	Standard deviation
φ_i	Modal constants in the i^{th} point (SDOF system)
$\varphi_{i,j}$	Modal constants of the j^{th} vibration mode in the i^{th} point
$\varphi_{k,j}$	Modal constants of the j^{th} vibration mode in the k$^{\mathrm{th}}$ point
$\boldsymbol{\phi}$	Mode shape vector (SDOF system)
$\boldsymbol{\phi_j}$	Mode shape vector of the j$^{\mathrm{th}}$ mode
$\bar{\omega}$	Approximate natural frequency of the joint H-S system
ω_{n}	Natural frequency [rad/s]
ω_{nj}	Natural frequency of the j$^{\mathrm{th}}$ mode

List of Figures

List of Tables